INFORMATION TO USERS

This manuscript has been reproduced from the microfilm master. UMI films the text directly from the original or copy submitted. Thus, some thesis and dissertation copies are in typewriter face, while others may be from any type of computer printer.

The quality of this reproduction is dependent upon the quality of the copy submitted. Broken or indistinct print, colored or poor quality illustrations and photographs, print bleedthrough, substandard margins, and improper alignment can adversely affect reproduction.

In the unlikely event that the author did not send UMI a complete manuscript and there are missing pages, these will be noted. Also, if unauthorized copyright material had to be removed, a note will indicate the deletion.

Oversize materials (e.g., maps, drawings, charts) are reproduced by sectioning the original, beginning at the upper left-hand corner and continuing from left to right in equal sections with small overlaps.

Photographs included in the original manuscript have been reproduced xerographically in this copy. Higher quality 6" x 9" black and white photographic prints are available for any photographs or illustrations appearing in this copy for an additional charge. Contact UMI directly to order.

ProQuest Information and Learning
300 North Zeeb Road, Ann Arbor, MI 48106-1346 USA
800-521-0600

METABOLIC AND INHIBITORY DIFFERENCES BETWEEN CYTOCHROMES P450 3A4 AND 3A5

by

Donavon J. McConn II

A dissertation submitted in partial fulfillment of the requirements for the degree of

Doctor of Philosophy

University of Washington

2001

Program Authorized to Offer Degree: Pharmaceutics

UMI Number: 3036505

UMI Microform 3036505

ProQuest Information and Learning Company
300 North Zeeb Road
P.O. Box 1346
Ann Arbor, MI 48106-1346

Doctoral Dissertation

In presenting this dissertation in partial fulfillment of the requirements for the Doctoral degree at the University of Washington, I agree that the Library shall make its copies freely available for inspection. I further agree that extensive copying of this dissertation is allowable only for scholarly purposes, consistent with "fair use" as prescribed in the U.S. Copyright Law. Requests for copying or reproduction of this dissertation may be referred Bell and Howell Information and Learning, 300 North Zeeb Road, Ann Arbor, MI 48106-1346, to whom the author has granted "the right to reproduce and sell (a) copies of the manuscript in microform and/or (b) printed copies of the manuscript made from microform."

Signature 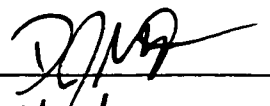

Date 9/25/09

University of Washington
Graduate School

This is to certify that I have examined a copy of a doctoral dissertation by

Donavon J. McConn II

and have found that it is complete and satisfactory in all respects,
and that any and all revisions required by the final
examining committee have been made

Chair of Supervisory Committee:

Kenneth E. Thummel

Reading Committee:

Kenneth E. Thummel

René H. Levy

Kent L. Kunze

Date: 9/25/01

University of Washington

Abstract

METABOLIC AND INHIBITORY DIFFERENCES BETWEEN CYTOCHROMES P450 3A4 AND 3A5

by Donavon J. McConn II

Chairperson of the Supervisory Committee:
Professor Kenneth E. Thummel
Department of Pharmaceutics

Cytochrome P450 (CYP) 3A4 and 3A5 constitute the dominant drug metabolizing enzymes in the liver and small intestine, and the content and activity of these enzymes is widely variable. Accurate knowledge of *in vivo* CYP3A activity is vital to predicting potential drug-drug interactions that may occur. Furthermore, any inhibitory differences between the two CYP3A isoforms would further complicate the accurate prediction of *in vivo* interactions. The purpose of this dissertation was to evaluate the excretory profile and regioselective metabolism of midazolam, an *in vivo* probe of CYP3A activity, in order to better understand its disposition and metabolic characteristics. Moreover, the inhibitory capability of a series of compounds was tested with CYP3A4 and CYP3A5.

Initial work focused on the variable urinary recovery and potential biliary secretion of midazolam *in vivo*. Biliary samples were analyzed to determine if secretion into bile could explain the variable urinary recovery of midazolam. Although midazolam metabolites were detectable in bile at relatively high levels, fecal analysis suggested the

biliary compounds were reabsorbed, and that biliary secretion is an unlikely mechanism to describe variable urinary recovery.

Midazolam 4-hydroxylation is a secondary metabolic pathway mediated by CYP3A, and its chemical instability *in vivo* may also contribute to variable urinary recovery. To address this, midazolam metabolism was examined in a panel of 60 human liver microsomes, and the relative importance of 1'- and 4-hydroxylation was determined at three different substrate concentrations.

Midazolam metabolism was also examined in intestinal samples acquired from cirrhotic patients. We examined the effects of liver cirrhosis on intestinal enzyme expression and activity. Our findings suggest that although cirrhosis has deleterious effects on hepatic CYP3A-dependent metabolism, no apparent effect was observed in the intestine.

Once metabolic differences were studied, our goal was to determine if a series of inhibitors behaved differently towards CYP3A4 and CYP3A5. For erythromycin, diltiazem, ketoconazole and nicardipine, affinities were higher towards CYP3A4 compared to CYP3A5. CYP3A5 also showed resistance to mechanism-based inactivation compared to CYP3A4.

In summary, no single mechanism seems responsible for CYP3A-dependent urinary recovery of midazolam. However, inhibitory differences do exist in time-dependent inhibition between CYP3A4 and CYP3A5.

TABLE OF CONTENTS

LIST OF FIGURES

LIST OF TABLES

LIST OF ABBREVIATIONS

1'-OH MDZ: 1'-hydroxymidazolam

4-OH MDZ: 4-hydroxymidazolam

AUC: area under the concentration-time curve

CYP: Cytochrome P450

DMSO: dimethyl sulfoxide

EDTA: ethylenediamine tetraacetic acid

EHR: entero-hepatic recycling

ERY: erythromycin

GC NCI-MS: gas chromatography-negative chemical ionization mass spectrometry

HL: human liver

KPi: potassium phosphate buffer

MDZ: midazolam

MIC: metabolite-inhibitor complex

MI-Complex: metabolite-inhibitor complex

mRNA: messenger ribonucleic acid

MRP: multidrug resistance protein

MTBSTFA: *N*-methyl-*N*-(*t*-butyl-dimethylsilyl)trifluoroacetamide

NADPH: nicotinamide adenine dinucleotide phosphate (reduced)

***N*-des-ERY:** *N*-desmethyl-erythromycin

PAGE: polyacrylamide gel electrophoresis

PMSF: phenyl methyl sulfonyl fluoride

PXR: Pregnane X receptor

RXR: Retinoid X receptor

SDS: sodium dodecyl sulfate

SNP: single nucleotide polymorphism

SPE: solid phase extraction

TAO: troleandomycin

Tris-HCl: tris (hydroxymethyl) amino methane hydrochloride

VDR: Vitamin D receptor

ACKNOWLEDGMENTS

I would first like to thank Dr. Ken Thummel for his years of guidance, support and encouragement throughout my training. He has truly served as a mentor, and is largely responsible for the scientist I have become. He seems to know when it is time to push and when to back off. This is a testament to him considering the variety of personalities that have been trained in his lab. I would also like to thank Drs. René Levy and Kent Kunze for serving on my thesis reading committee, and the remaining members of my committee, Drs. Danny Shen and King Holmes.

I would also like to thank my former labmates: Maurice Emery, Megan Gibbs, Mary Paine and Jeannine Fisher for my transition into this field and getting me started in the right way. I'd especially like to thank my current labmate Yvonne Lin for all her scientific contributions to my work, as well as being a good friend out of the lab. I'd also like to thank the College Inn Pub and Mr. Snappy soccer teams for keeping me sane.

Graduate school is tough enough, but Cathy Johnson made some of the rough points a little smoother. From general office help to emergency chocolate to baseball tickets, Cathy never turned me away. The little things do add up.

I'd like to thank my parents Donavon and Diane McConn for all their encouragement and support (moral and financial) over the years, as well as my wife's parents Joseph and Stephanie Zichichi. Lastly, I'd like to thank my wife Nicole for her infinite patience and support of me through some pretty rough times. She sacrificed a tremendous amount to be with me in Seattle, and I just hope I pay off in the long run.

CHAPTER 1

INTRODUCTION

1.1 PART I – Background and General Concepts Involving the Inhibitory and Metabolic Differences between CYP3A4 and CYP3A5

1.1.1 Cytochromes P450

The cytochromes P450 (CYP) are a large family of heme-thiolate proteins that are responsible for the biotransformation of numerous endogenous and exogenous compounds. Most P450 reactions involve the oxidation of lipophilic drug molecules, but reduction reactions can also occur. The result of the CYP-catalyzed oxidations is the formation of a more polar metabolite that is more apt to be renally excreted or conjugated to a polar endogenous molecule.

1.1.2 CYP3A

There are 14 CYP families in mammalian species, however; only three families (CYP1, CYP2 and CYP3) are generally responsible for xenobiotic metabolism in humans. The CYP3 family metabolizes over 50% of clinical medications cleared by biotransformation processes (Harris et al, 1995). Because of this fact, the CYP3 family is considered the most important and is the most widely studied family in human drug metabolism. The CYP3 family contains five known enzymes, all within the CYP3A subfamily: CYP3A3, CYP3A4, CYP3A5, CYP3A7 and CYP3A43 (Wrighton and Stevens, 1992; Domanski et al, 2001).

1.1.3 CYP3A3 and CYP3A4

CYP3A3 and CYP3A4 are 98% similar in their amino acid sequences (only 14 nucleotide differences), and are considered to be indistinguishable by standard separation and immunodetection techniques. However, the intestinal or hepatic expression of CYP3A3 has not yet been observed. Neither CYP3A3 protein nor mRNA has been detected in human liver or intestinal tissues (Kolars et al, 1994). This finding suggests that CYP3A3 may be a rare allelic variant of CYP3A4 or the result of a cloning artifact. For these reasons CYP3A3 and CYP3A4 will be considered as one enzyme.

CYP3A4 is the major CYP isoform in both adult human liver and small intestine. It constitutes approximately 30% of total CYP in the liver, and up to 70% in the small intestine (Shimada et al, 1994; Paine et al, 1997b; Watkins et al, 1987). The cDNA sequence for CYP3A4 is identical in both the liver and small intestine. However, the expression in each tissue appears to be differentially regulated (Lown et al, 1994; Lown et al, 1997). Regulation of hepatic CYP3A4 is primarily via Pregnane X receptor (PXR) dimerization with the Retinoid X receptor (RXR) followed by translocation of the dimer to the nucleus where it can bind to DNA and influence transcription of the *CYP3A4* gene (Lehmann et al, 1998; Xie et al, 2000). Intestinal CYP3A4 is also partially regulated by PXR:RXR, but the primary constitutive regulation mechanism is via the Vitamin D receptor (VDR) (Thummel et al, in press Mol Pharmacol). CYP3A4 can also be found in trace amounts in the kidney (Haehner

et al, 1996), the pancreas and colon where it is localized to cells of epithelial origin (e.g. ducts) (Kolars et al, 1994). CYP3A4 metabolizes a wide array of clinically important drugs, including calcium channel blockers, HMG-CoA reductase inhibitors, HIV protease inhibitors, antiarrhythmics, immuno-suppressants, opioid analgesics and benzodiazepine sedative/hypnotic agents.

CYP3A4 protein levels and enzyme activities show very large interindividual variability in the human population. This is due in part to the susceptibility of the enzyme to induction and inhibition phenomena. Common CYP3A4 inducers include the anticonvulsant drugs phenytoin, carbamazepine and phenobarbital, as well as the anti-tuberculosis agent rifampin. Although induction can occur by various processes including increased synthesis rate of the enzyme, stabilization of existing enzyme or increased transcription of the CYP3A4 gene, the effect of most inducers is likely mediated by ligand activation of PXR and transcriptional activation of the CYP3A4 gene (Lehmann et al, 1998). Since CYP3A4 binds to a large number of drugs from different therapeutic classes, there is a significant probability of enzyme inhibition in polytherapy drug regimens. CYP3A4 substrates are all potential competitive inhibitors, the likelihood of which depends on exposure concentrations and enzyme binding affinity. Common potent CYP3A4 inhibitors include the imidazole-containing antifungal agents fluconazole, itraconazole and ketoconazole (Back and Tjia, 1991); macrolide antibiotics erythromycin, clarithromycin, azithromycin and troleandomycin (Greenblatt et al, 1998); calcium channel blockers diltiazem and nicardipine (Ma et al, 2000); and bergamottins contained in grapefruit juice (Bailey et al, 1991). CYP3A4

inhibition occurs by a variety of different mechanisms including competitive and non-competitive binding to the enzyme or by time-dependent suicide inactivation of the enzyme.

In addition to exogenous factors that affect CYP3A expression, there are clearly interindividual differences in the "constitutive" level of CYP3A expression that is the result of variable transcriptional signals, protein degradation processes or genetic polymorphisms. Interestingly, all of the mutations in the CYP3A4 gene uncovered to date appear to be relatively rare (allele frequencies < 1-2%) (Sata et al, 2000; Eiselt et al, 2001; Lamba et al, 2001 in press-Pharmacogenetics), suggesting that the cause of individual enzyme expression differences lays with regulatory proteins, hormones and cytokines, and the genes that code for their production. The exception is a common mutation in the 5'-flanking region of the *CYP3A4* gene (-290 AG) (Tayeb et al, 2000) that has been associated with altered gene transcription rates. However, the data surrounding this mutation are conflicting (Wandel et al, 2000; Ball et al, 1999) and have uncertain significance.

1.1.4 CYP3A5

CYP3A5 is also expressed in the human liver and small intestine, but usually at lower levels than CYP3A4. It comprises approximately 10% of total CYP in the liver and 30% in the small intestine of individuals that express the enzyme (Paine et al, 1997b; Wrighton et al, 1989; Wrighton et al, 1990). In the University of Washington

School of Pharmacy liver bank approximately 10% of livers from Caucasian donors express CYP3A5 at levels **greater than** CYP3A4 (Gibbs et al, 1999; Paine et al, 1997a). In a population of African-American liver samples, 60% expressed significant levels of CYP3A5, and approximately 50% of the subjects expressed higher levels of CYP3A5 compared to CYP3A4 (Kuehl et al, 2001). CYP3A5 is the predominant isoform in the human colon, prostate, stomach and kidney (Haehner et al, 1996; Gervot et al, 1996; Yamakoshi et al, 1999; Kolars et al, 1994). It is also the only CYP3A isoform that is expressed in human lymphocytes (Janardan et al, 1996).

CYP3A5 shares approximately 84% amino acid similarity with CYP3A4, and is polymorphically expressed in the adult human population. CYP3A5 has a slightly different electrophoretic mobility than CYP3A4 (52 vs. 51 kDa, apparent MW), and will appear as a 'doublet' peak on protein immunoblots of liver samples that contain both isoforms. Approximately 25-33% of adult human livers express readily detectable levels of CYP3A5 (Wrighton et al, 1989; Aoyama et al, 1989; Kuehl et al, 2001). One group of investigators reported the detection of CYP3A5 protein in as much as 74% of the liver samples examined using a highly sensitive detection technique (Jounäidi et al, 1996). Moreover, variable levels of CYP3A5 mRNA were detected in 100% of liver samples tested in two different studies, implying that there is an intact gene in all individuals, but differences in formation and/or degradation of the mRNA (Kivisto et al, 1996; Zhang et al, 1999). Indeed, two polymorphisms have been discovered recently, and both result in alternative splicing of the CYP3A5 mRNA and production of a truncated, non-functional protein as the result (Kuehl et al, 2001). The

most common single nucleotide polymorphism (SNP) results in the incorporation of a portion of intron 3 into the transcript, thus creating a variant exon 3B (*CYP3A5*3*). The extra DNA sequence causes a frameshift mutation resulting in a premature stop codon at amino acid 109. The second SNP has only been detected in African-American subjects, and results in the deletion of exon 7, thus producing another truncated protein.

CYP3A5 differs from CYP3A4 in that it is far less susceptible to induction (Wrighton et al, 1989). This is somewhat of a surprise since the 5'-flanking region of the CYP3A5 gene contains a consensus ER-6 motif that binds the activated PXR:RXR complex. Presumably, induction requires involvement of other promoter/enhancer elements on the *CYP3A5* gene that are absent or non-functional, but present and functional on *CYP3A4*. CYP3A5 expression may also be affected by age. CYP3A5 protein was detected in a higher percentage of liver microsomes prepared from adolescents and children ($\leq$ 19 years) compared to adult liver microsomes (47% vs. 24%), and was also detected in 10% of fetal livers (Wrighton et al, 1990), however the sample size was small.

The substrate specificity of CYP3A5 is related to that of CYP3A4. To this date there is no known substrate that is selective for CYP3A5. All substrates of CYP3A5 are metabolized by CYP3A4. However, not all CYP3A4 substrates are metabolized equally well by CYP3A5 (Wrighton et al, 1990). All comparative studies to date have used purified or expressed enzymes. Activity of CYP3A5 towards common CYP3A4/CYP3A5 substrates is generally reduced (Wrighton et al, 1990; Gillam et al,

1995). However, reconstitution conditions (detergents, divalent cations, etc.) play an important role in the activity of recombinant CYP3A5. CYP3A5 was implicated in erythromycin metabolism at high substrate concentrations in one recombinant enzyme system (Gillam et al, 1995), yet was unable to metabolize erythromycin in another report (Wrighton et al, 1990). Interestingly, for the benzodiazepine midazolam (MDZ), CYP3A5-catalyzed formation of 1'-hydroxymidazolam was **greater** than that for CYP3A4. Also, the ratio of 1'-hydroxymidazolam to 4-hydroxymidazolam formation, another CYP3A-catalyzed reaction, was higher in CYP3A5-positive individuals (Paine et al, 1997a). To this date, no data are available with CYP3A4 or CYP3A5 selective human liver microsomes.

1.1.5 CYP3A7

CYP3A7 is the major CYP isoform expressed in the human fetal liver, comprising up to 50% of total fetal P450 (Wrighton and VandenBranden, 1989). It is also found in adult human endometrium and placenta (Schuetz et al, 1993). CYP3A7 protein has been detected in adult liver, although at levels far below that of CYP3A4 or CYP3A5 (Tateishi et al, 1999), therefore it will not be discussed further.

1.1.6 CYP3A43

CYP3A43 is a recent discovery in the CYP3A subfamily. CYP3A43 expression has been detected in liver, kidney, pancreas, and prostate, where its highest expression was observed (Gellner et al, 2001). The amino acid sequence is 76% identical to that of CYP3A4 and 3A5, and 71% identical to CYP3A7. CYP3A43 differs from CYP3A4 at six amino acid residues found within the putative substrate recognition sites of CYP3A4, and that are known to be determinants of substrate selectivity (Domanski et al, 2001). These changes may render the enzyme catalytically inactive. Immunoblot analyses revealed that CYP3A43 co-migrates with CYP3A4 in polyacrylamide gel electrophoresis but does separate from CYP3A5 (Gellner et al, 2001). CYP3A43 expression levels are approximately 0.1% of CYP3A4 and 2% of CYP3A5 in the liver, and were detectable in 70% of the livers examined (Westlind et al, 2001).

1.1.7 Other Cytochromes

1.1.7.1 Cytochrome b_5

Cytochrome b_5 is a small (17 kDa), membrane-bound protein (except in erythrocytes, where it is soluble) that is expressed in all eukaryotic tissues. The protein contains a heme group that lacks a free coordination position, thus allowing the protein to transfer electrons in a number of different reactions. Cytochrome b_5 is known to facilitate fatty acid elongation (Keyes et al, 1979), fatty acid desaturation (Shimakata et al, 1972) and also P450 monooxygenations (Hildebrandt et al, 1971). Cytochrome P450 reactions require the addition of 2 electrons in order to activate molecular oxygen, and these electrons must be added one at a time. Cytochrome b_5 has been shown to be the second electron donor in some P450 reactions, though it is isoform specific. Cytochrome b_5 can enhance, retard or have no effect on P450-mediated monooxygenation depending on the specific P450 enzyme responsible for oxidation (Schenkman and Jansson, 1999).

Cytochrome P450 3A4 is one isoform where enzyme activity is enhanced by cytochrome b_5 (Perret and Pompon, 1998). However, the increase in activity is dependent on the lipid composition of the membranes used for reconstitution (Basaran et al, 1999), and on the ratio of CYP3A4: cytochrome b_5: reductase (Yamazaki et al, 1999). Cytochrome b_5 has a higher affinity for mono-unsaturated acyl chains (DMPC),

and exerts its maximum facilitative effect on CYP3A4 at a ratio of 1 mole CYP3A4: 1 mole b_5: 2 moles reductase.

1.1.8 Involvement of CYP3A in First-Pass Drug Metabolism

1.1.8.1 First-Pass Metabolism

First-pass metabolism is defined as any irreversible loss of drug between the site of administration and the systemic arterial circulation (Tam, 1993). Intravenous administration is often considered to be void of first-pass metabolism, because the drug is infused directly into the systemic venous blood. However, since venous blood must travel to the right atrium, right ventricle and lungs before returning to the heart and becoming arterial flow, any metabolic loss in the lungs would be considered a first-pass loss as well. For most drugs (excluding those that undergo hydrolytic of sulfation reactions in blood), this loss is considered negligible, and therefore first-pass metabolism does not occur after intravenous administration.

Most drugs are given orally, and therefore must pass through several physical and metabolic barriers prior to reaching the systemic circulation. Further, drugs must survive the acidic environment of the stomach and undergo absorption through the gastrointestinal mucosa. Intestinal absorption can occur either paracellularly (between cells) or transcellularly (through cells), but transcellular uptake is considered to be the most efficient (Arturrson, 1991). While passing through the enterocyte, the drug can be

metabolized by enzymes present in the apical tips of the villi (Ilett et al, 1990). Drug molecules must then escape metabolic extraction by the liver before reaching the hepatic vein and the systemic circulation. Some drugs have such extensive first-pass metabolism (oxidative, reductive, hydrolytic or conjugative), that it precludes their use as oral medications, for example: naloxone, isoproterenol, lidocaine and nitroglycerin (Pond and Tozer, 1984). Both the liver and small intestine contain the highest levels of drug metabolizing enzymes, especially CYP3A, and therefore would be most implicated in any first-pass loss of orally administered drug. From the perspective of inter-individual differences in drug bioavailability (i.e. drug efficacy) and drug-drug interactions (i.e. drug safety), it is very important to know the extent of first-pass metabolism in these organs, and which factors, both endogenous and exogenous, can affect the overall first-pass effect.

1.1.8.2 Oral Bioavailability

The oral bioavailability (F) of a drug is often used as a quantitative measurement of the degree of first-pass metabolism. It is generally calculated as the ratio of the area under the plasma concentration vs. time curve following oral administration (AUC_{po}) to the area following intravenous administration (AUC_{iv}) after normalizing for dose (Gibaldi and Perrier, 1982):

$$F = AUC_{po} / AUC_{iv} * D_{iv} / D_{po} \qquad [1.1]$$

where D_{iv} and D_{po} represent the intravenous and oral dose, respectively. Since the bioavailability calculation compares oral to intravenous exposure, bioavailability can also be referred to as the fraction of oral dose that reaches the systemic circulation intact. Each drug-metabolizing organ has its own fraction of drug that can pass through it intact. When these organs are arranged in series, like the small intestine and liver, the overall systemic bioavailability can also be calculated as the product of each individual organ's bioavailability (Pond and Tozer, 1984):

$$F = F_a * F_g * F_h \qquad [1.2]$$

where F_a is the fraction of oral dose that gets absorbed through the gastrointestinal lumen, F_g is the fraction of oral dose that escapes biotransformation or efflux in the small intestine and F_h is the fraction of dose that remains intact after passage through the liver.

1.1.8.3 Extraction Ratio

Whereas bioavailability describes the fraction of dose that escapes loss through an organ, the extraction ratio (E) describes the fraction of dose that *does not escape* first-pass metabolism through an organ. The two parameters are related as follows:

$$F = 1 - E \quad \text{or} \quad E = 1 - F \qquad [1.3]$$

Since the extraction ratio is related to the bioavailability, it can also be calculated using the systemic exposure of the drug (AUC) during different types of drug administration (Ilett et al, 1990). Assuming rapid equilibrium between incoming and outgoing blood flows, no lung metabolism and equal doses of drug, intestinal (E_g) and hepatic (E_h) extraction can be calculated as follows:

$$E_g = 1 - (AUC_{po} / AUC_{ip}) \qquad [1.4]$$

$$E_h = 1 - (AUC_{ip} / AUC_{iv}) \qquad [1.5]$$

where AUC_{po}, AUC_{ip} and AUC_{iv} represent the area under the concentration vs. time curve after oral, intraportal and intravenous administration, respectively. These equations represent anatomical situations where drug is dosed afferent and efferent to the drug-metabolizing organ, and then sampled at a peripheral venous site. Thus, any loss of dose (i.e. differences in AUC by the two dosing routes) would be attributed to extraction by the organ in question. Although this method is appropriate for studies in animals, it is generally unsuitable for humans.

1.1.8.4 Factors that Affect AUC

The systemic AUC of a drug is a measure of its relative exposure to the body, and is inversely related to the systemic clearance of that particular drug (Gibaldi and Perrier, 1982):

$$AUC_{iv} = \text{Dose} / \text{Clearance} \qquad [1.6]$$

And if the drug is given orally, the relationship includes the bioavailability parameter.

$$AUC_{po} = F * \text{Dose} / \text{Clearance} \qquad [1.7]$$

Since dose is usually considered a constant value, clearance and bioavailability will influence the AUC after oral administration.

1.1.8.5 First-Pass Extraction Models

Up to this date, five models have been proposed to describe hepatic clearance and bioavailability in terms of three measurable physiological factors. These factors are: blood flow; the vehicle that presents drug to or removes drug from the

metabolizing organ; enzyme activity; the quantity, affinity and catalytic potential of the drug metabolizing framework; and the free fraction of drug, also referred to as the fraction of drug able to cross biological membranes and be metabolized. The first is the well-stirred (or venous equilibrium) (Rowland et al, 1973), followed by the parallel tube (or undistributed sinusoidal perfusion) (Winkler et al, 1979), the distributed sinusoidal perfusion (Bass et al, 1978), the dispersion (Roberts and Rowland, 1985) and the series-compartment model (Gray and Tam, 1987).

1.1.8.6 Well-Stirred Model of Extraction

1.1.8.6.1 Liver

As aforementioned, the well-stirred model of hepatic clearance was first discussed by Rowland (1973). This model considers the eliminating organ as a single homogeneous compartment, where the concentration of drug metabolizing enzymes and exogenous drug are considered constant throughout the organ. The well-stirred model also assumes that unbound drug concentration in the blood can freely diffuse into the organ, thus the unbound concentration in the blood reflects the unbound concentration inside the organ. Inherent to this stipulation is that there is no diffusional barrier to drugs entering the organ; thus, the diffusion of drug into the organ is not rate-limiting in its elimination. The relationship that describes hepatic extraction in the well-stirred model is shown below:

$$E_h = (f_u * Cl_{int}) / (Q_h + f_u * Cl_{int}) \quad [1.8]$$

where E_h, Q_h, f_u and Cl_{int} represent hepatic extraction ratio, hepatic blood flow, free fraction of drug in blood and unbound intrinsic clearance, respectively. The product of f_u and Cl_{int} is known as the total intrinsic clearance and is not solely dependent on enzyme parameters, but free fraction as well. The above relationship becomes a calculation for hepatic clearance if the equation is multiplied by hepatic blood flow (Q_h).

1.1.8.6.2 Intestine

Just as the well-stirred model can predict hepatic clearance for many drug compounds, it can also be used to predict intestinal extraction as well (Colburn, 1979; Klippert et al, 1983; Mistry and Houston, 1987).

$$E_g = (Cl_{int}) / (Cl_{int} + Q_{SMA} * f_s) \quad [1.9]$$

The above relationship incorporates many of the same parameters of the hepatic model in that intrinsic clearance and blood flow are represented. However, there are a few differences between the two models. The intrinsic clearance terms reflect *intestinal* enzyme parameters instead of the liver. Blood flow is represented by Q_{SMA}, referring to the superior mesenteric artery, the main blood supply to the small intestine. However, only a fraction of the SMA blood flow (f_s) actually goes to the mucosa.

Although SMA blood flow is not a relatively important vehicle to deliver drug to the drug metabolizing enzymes in the small intestine, it does affect residence time of the drug in the mucosa after oral administration. Blood flow in the intestinal model is counterproductive to drug metabolism after an oral dose, because it draws drug molecules away from the mucosal enzymes. The intestinal relationship is also absent a term for free fraction (f_u). The free fraction is absent primarily due to first-pass considerations where the drug has not been exposed to blood, and therefore has not been exposed to plasma proteins. However, from a theoretical consideration the f_u term can be included in the relationship, which would result in a decrease in intrinsic clearance, because it may exaggerate the sink effect of the SMA blood flow, and remove drug from the site of metabolism.

The pharmacokinetic effects of orally administered inducers or inhibitors can be observed in both the small intestine and the liver. The magnitude of an AUC change after treatment with an inhibitor or inducer is the product of the effect in the intestine and the effect in the liver, and the magnitude of AUC change depends on the bioavailability of the substrate. Various *in vivo* studies have confirmed this phenomenon (Table 1.1). The multiplicative relationship for a co-administered inhibitor is shown below:

$$AUC_{po(inh)}/AUC_{po} = F_{G(inh)}/F_G \bullet Cl_{int(inh)}/ Cl_{int} \qquad [1.10]$$

where $AUC_{po(inh)}$ represents the area under the plasma concentration versus time curve after oral administration of inhibitor, $F_{G(inh)}$ is the gut bioavailability during inhibitor treatment, [I] is the concentration of inhibitor and K_i is the inhibition constant for the inhibitor. AUC and F parameters without the (inh) notation represent parameter estimates during control (no inhibitor) phase. A similar relationship exists when an inducer is orally co-administered with a CYP3A substrate.

$$AUC_{po(ind)}/AUC_{po} = F_{G(ind)}/F_G \bullet Cl_{int(ind)}/ Cl_{int} \qquad [1.11]$$

The AUC ratio is as described for equation 1.10 except that the notation (ind) applies to an inducer rather than an inhibitor, and Cl_{int} represents the intrinsic hepatic clearance. Both relationships illustrate the multiplicative extraction in both the liver and small intestine.

1.1.8.7. Intrinsic Clearance and Enzyme Parameters

A single enzyme-single substrate system can be described by the following mass balance relationship (Segel, 1975):

$$[S] + [E] \underset{k_{-1}}{\overset{k_1}{\rightleftarrows}} [ES] \xrightarrow{k_{cat}} [P] \qquad [1.12]$$

where [S] and [E] are the substrate and enzyme concentrations, respectively. The rate constants k_1, k_{-1} and k_{cat} represent the on-rate of the enzyme-substrate complex, the off-rate of the same complex since they are in equilibrium, and the turnover number (moles of substrate converted to metabolite per unit time per mole of enzyme). However fundamental the above relationship is, it does not provide parameters that can be readily measured. The following relationship (the Michaelis-Menten equation) describes a one-enzyme system in parameters that are much more practical.

$$v = (V_{max} * [S]) / (K_m + [S]) \qquad [1.13]$$

In this relationship v, V_{max}, K_m and [S] are the velocity of metabolic turnover, the maximal rate at which drug can be metabolized, the substrate concentration that represents 50% of V_{max}, and the substrate concentration, respectively. V_{max} is only dependent on the quantity of enzyme present (E_{total}) and the turnover number (k_{cat}), and is the product of the two terms. K_m is a measure of the affinity of the drug and enzyme complex, and is therefore a ratio of the [enzyme-substrate complex] dissociation/association rate constants.

$$K_m = (k_{-1} + k_{cat}) / k_1) \qquad [1.14]$$

Although K_m is a measure of drug-enzyme affinity, it also incorporates the formation of product (k_{cat}). Intrinsic clearance is a relationship between all of the enzyme parameters

mentioned above, and is equal to the ratio of V_{max} to (K_m + [S]). Under first-order conditions prevalent *in vivo*, the intrinsic clearance (V_{max}/K_m) is independent of substrate concentration. This means that changes in intrinsic clearance *in vivo* can be attributed to changes in V_{max}, K_m or both. In general, inducers and inhibitors of drug metabolizing enzymes exert an effect by altering the intrinsic clearance (i.e. apparent K_m, V_{max} or both).

1.1.9 Enzyme Inhibition

Inhibition of drug-metabolizing enzymes occurs by various mechanisms ranging from rapidly reversible inhibition to slowly reversible inhibition up to irreversible inhibition. Competitive inhibition involves the substrate and inhibitor competing for a single catalytic site on the enzyme. Binding of both inhibitor and substrate to the enzyme are reversible and in equilibrium. Since the competition requires higher levels of substrate in the active site to achieve the same reaction velocity, the apparent K_m is increased. Moreover, since the maximum turnover rate would be unaffected by the competition, no change in V_{max} is observed. Equation 1.13 can be modified to include the effect of a competitive inhibitor.

$$v_{(inh)} = (V_{max} * [S]) / \{K_m \bullet (1 + [I]/K_i) + [S]\} \qquad [1.15]$$

The velocity of the reaction with concurrent administration of the inhibitor is described by $v_{(inh)}$. The K_m term has been modified by the $(1 + [I]/K_i)$ term, thus increasing its

apparent value by that relationship. One can also see how a competitive inhibitor affects the hepatic intrinsic clearance and AUC of an orally administered drug for equation 1.16.

$$AUC_{po(inh)}/AUC_{po} = F_{G(inh)}/F_G \bullet (1 + [I]/K_i) \qquad [1.16]$$

Another type of reversible inhibition involves the inhibitor and substrate binding to the enzyme in a non-mutually exclusive manner, and this type of inhibition is termed non-competitive. Equation 1.16 describes non-competitive inhibition.

$$v_{(inh)} = \{V_{max}/(1 + [I]/K_i) * [S]\} / (K_m + [S]) \qquad [1.17]$$

Whereas in competitive inhibition the inhibitor alters the apparent K_m, in non-competitive inhibition the reduction in reaction velocity cannot be overcome by adding excess substrate. The non-competitive inhibitor functions to reduce the maximal velocity that can be achieved at saturating substrate concentrations. At non-saturation substrate concentrations, the effect of a non-competitive inhibitor on the oral AUC of an inhibited substrate is also described by equation 1.16. Note though that inhibition of the intestinal component might be dependent on the inhibition mechanism, as substrate concentrations could transiently saturate the intestinal enzyme pool.

Many inhibitors exert an inhibitory effect that is irreversible or only reversible after long time periods. Some cytochrome P450 substrates form reactive intermediates

that can alkylate a heme nitrogen atom or apoprotein near the active site. Both processes form covalent bonds to the enzyme and render it terminally inactive. A more common mechanism of slowly reversible inhibition is by the formation of a heme ligand with the ferrous heme iron. The ligand can be a parent drug molecule or product of one or more metabolic reactions. A group of well-characterized ferrous heme ligands are substituted alkylamines. CYP3A4 catalyzes the successive *N*-demethylations, and the metabolism terminates at an *N*-oxide metabolite with a high affinity for ferrous heme (Pershing et al, 1982). This manner of inhibition is termed mechanism-based inactivation (Silverman, 1988), because it requires catalytic turnover of the parent drug to generate the inhibitory species. These mechanistic aspects of CYP3A4 and CYP3A5 dependent inhibition will be explored further in Chapter 4.

1.1.10 Midazolam as a Probe for CYP3A

Midazolam (8-chloro-6- (2-fluorophenyl)-1-methyl-4H-imidazo [1,5-a] [1,4] benzodiazepine) is a short-acting water-soluble benzodiazepine that is exclusively metabolized by CYP3A isoforms (Gorski et al, 1994). Midazolam is biotransformed *in vivo* predominantly to 1'-OH MDZ, and ~70% of the midazolam dose is excreted into the urine via that pathway (Heizmann and Ziegler, 1981). A second metabolite, 4-OH MDZ, accounts for ~3% of the recovered dose, and thus should not contribute significantly to midazolam clearance. However, Paine et al (1997a) showed that the importance of 4-OH MDZ, for both liver and intestinal tissue, increases with substrate concentration. For example, the 1'-OH/4-OH ratio was lowered 2-fold when the

concentration of midazolam was increased from 0.25 μM to 8 μM in liver and intestinal microsomes, irrespective of whether CYP3A5 was present or not. Indeed, Kronbach et al (1989) showed that at >32 μM midazolam, the 4-OH MDZ formation rate actually exceeded that of 1'-OH MDZ. Kronbach also calculated kinetic parameters for 1'-OH and 4-OH MDZ formation. The K_m for 1'-OH MDZ was found to be 3.5 μM, whereas the K_m for 4-OH MDZ was 40 μM. These studies and others demonstrate that 1'-OH and 4-OH MDZ formation proceeds through CYP3A4, but by different K_m values.

By most criteria midazolam appears to be an excellent probe substrate for CYP3A4. However, one further aspect of MDZ disposition still remains unresolved. Although Heizmann and Ziegler (1981) reported ~92-95% total dose recovery of radioactive midazolam, that value has never been equaled with a non-radioactive dose. Thummel et al (1996) showed that 50-95% of an intravenous and oral midazolam dose was recovered in the urine as 1'-OH MDZ, with a mean of 73%. Other investigators (Dundee et al, 1984) report a similar range and mean. Thus, a major question remaining to be addressed is the unexplained variability in urine recovery, especially when absorption appears to be complete.

Examination of urinary samples containing 1'-OH and 4-OH midazolam would reveal the relative selectivity of each pathway. However, urinary analysis of 4-OH midazolam has been problematic. At pH values less than 7, equilibrium favors the open-ring form of the molecule, which presumably precludes its further breakdown (Kronbach et al, 1989). Another report has confirmed that 4-OH midazolam and its

glucuronide conjugate are rapidly degraded in urine, with approximate half-lives of 4 and 7 hours for the metabolite and conjugate, respectively (Paine et al, 1997a). Even with frequent clinical urinary collection, a large and variable amount of 4-OH midazolam would be lost during each collection. The microsomal 4-OH midazolam formation data and the degree of chemical instability in the urine support the theory that 4-OH midazolam formation clearance *in vivo* is underestimated.

Chapter 3 describes the importance of 4-OH MDZ formation as a midazolam elimination pathway. An extensive examination of 1'-OH/4-OH MDZ metabolic ratios produced by 60 human liver microsomes, and the impact and relevance of CYP3A5 is also examined. This will allow for a more comprehensive examination of potential *in vivo* formation of 4-OH midazolam.

Another possible reason for the incomplete and variable urinary recovery of midazolam is biliary secretion. Previous studies have shown that glucuronide conjugates are readily excreted into bile via ATP-binding cassette transporters (Keppler et al, 1997; Zeng et al, 2000; Madon et al, 2000). It is possible that some variable fraction of the midazolam hydroxy conjugate(s) is excreted into bile. Chapter 2 details the examination of two aspects of this hypothesis. First, we determined whether or not midazolam and/or its metabolites were excreted into human bile. In addition, quantitative analysis of the fecal matrix from healthy volunteers receiving midazolam was performed. An assay was also developed to measure the quantity of metabolites present in human stool.

1.2 PART II-Organ- and Isoform-dependent Differences in Cirrhotic CYP3A-Mediated Drug Metabolism: Application of *In Vitro* Data to Clinical Disease State

1.2.1 Cirrhosis of the Liver

Cirrhosis of the liver causes a hardening and complete restructuring of the hepatic cellular framework. As the liver become fibrotic, the regenerating cells form architecturally different nodules. Cirrhosis most commonly develops from biliary occlusion, alcoholic or toxic chemical ingestion. Although development of cirrhosis can be much different depending on the manner of liver insult, in the latter stages of the disease it is nearly impossible to clinically distinguish the etiology. As the disease progresses, the fibrosis and nodular regeneration results in new blood vessels being formed that allow blood flow to bypass contact with hepatocytes. If blood containing drug molecules is unable to access the drug metabolizing enzymes in the hepatocytes, drug elimination can become severely compromised.

Primary biliary cirrhosis is a chronic cholestatic liver disease characterized by the destruction of interlobular and septal bile ducts. The blockage of bile ducts prevents bile acids from traveling to the gall bladder, and increases their residence time in the hepatocytes. Hydrophobic bile acids are toxic to liver cells, and their increased residence time cells allows for a self-perpetuating injury. Over time, the inflammation increases; fatty deposits and ascites commonly form, and cirrhosis develops when

groups of hepatocytes cluster into a fibrous bulb or nodule, and the nodules become vascularized via angiogenesis.

Cirrhosis caused from the repeated ingestion of toxic chemicals, such as alcohol, follows a similar pathway to that of primary biliary cirrhosis. Chronic ingestion of alcohol causes the formation of continuously high levels of acetaldehyde, the major oxidative metabolite of ethanol. Acetaldehyde is toxic to hepatocytes, and its chronic presence at high intracellular concentrations causes the hepatocytes to become inflamed over time. As the insults progress over time, the inflammation causes a disorder termed hepatomegaly, or enlarged liver. The swelling is due to inflammatory cytokines as well as increasing fat deposits. Progression to cirrhosis follows similarly to that of primary biliary disease. One difference is that alcoholic liver disease can be reversed by termination of alcohol ingestion. Since biliary cirrhotic insults arise from auto-developed bile acid toxins, treatment becomes increasingly difficult. Regardless of the etiology of the cirrhosis, the impact on hepatocyte structure and blood flow is the same.

Due to the fibrous nature of the liver cells in cirrhosis, it takes increased blood pressure to pump blood through a more restrictive organ. Often this results in a condition known as portal hypertension, where the hyper-dynamic changes in blood flow to the visceral organs (intestines, stomach, spleen and pancreas) are increased approximately 50% over control levels (Benoit et al, 1986).

Cirrhosis also affects the homeostatic functions of the liver, such as storage of sugar, neutralization of other systemic toxins, and synthesis of plasma proteins, such as

albumin. When albumin levels decrease, more drug molecules exist freely in the bloodstream, and can potentially exert more profound pharmacological or toxic effects.

1.2.2 Role of the Small Intestine in Cirrhosis

To date, the small intestine's role in the drug metabolism or clearance of a moderate-to-highly extracted CYP3A4 substrate in individuals with liver disease has not been explored. However, increased blood flow to the organ due to hypertension and a higher free drug concentration due to decreased albumin, may allow for increased intestinal drug metabolism in cirrhosis. A recent study showed that there was no change in oral clearance of midazolam between cirrhotics and healthy volunteers, yet cirrhotics showed significantly decreased intravenous clearance (Gorski et al, 2001). The intravenous clearance is a measure of liver clearance, whereas both the liver and small intestine describe the oral clearance. Since oral clearance did not change between the two groups, the data imply that the intestinal clearance increased. Thus, increased expression of drug metabolizing enzymes in the small intestine may be a compensatory response to the loss of drug metabolizing activity in the liver.

To test this hypothesis, intestinal biopsies from cirrhotic patients and control individuals were collected and compared based on midazolam metabolism and CYP3A4 and CYP3A5 content. These data are presented in Chapter 5.

Table 1.1. *In vivo* drug-drug interaction studies with various CYP3A substrates and the impact on the $AUC_{(inh)}/AUC$ ratio.

Substrate	*Bioavailability (F)*	*Ketoconazole Dose (mg)*	$AUC_{(inh)}/AUC$	*Reference*
terfenadine	< 5	200 mg bid	16-76	Honig et al, 1993
nisoldipine	~ 5	200 mg qd	25.3	Heinig et al, 1999
midazolam	44	400 mg qd	15.9	Olkkola et al, 1994
triazolam	~ 40	200 mg bid	13.7	Greenblatt et al, 1998
alprazolam	88	200 mg bid	1.8	Schmider et al, 1999
		200 mg bid	4.0	Greenblatt et al, 1998
quinine	76	100 mg bid	1.4	Mirghani et al, 1999
zolpidem	72	200 mg bid	1.7	Greenblatt et al, 1998

CHAPTER 2

ELUCIDATION OF THE EXCRETORY PROFILE OF MIDAZOLAM AND ITS METABOLITES: ROLE OF BILIARY EXCRETION

2.1 Introduction to Chapter 2

The effect of one drug on the clearance of another, a pharmacokinetically based drug-drug interaction, can be mediated through multiple pathways, including an alteration of drug metabolism and drug transport processes. Attention is generally given to drug biotransformation since it represents the dominant route of drug elimination *in vivo*. Less well studied are interactions that perturb the biliary excretion of unchanged drug or its metabolites.

Total urinary recovery of a midazolam dose varies from 48-95%, and is approximately normally distributed in the human population (Thummel et al, 1996). The dose is recovered almost exclusively as 1'-OH, 4-OH, 1',4-dihydroxy and the secondary glucuronide metabolites, with <1% recovered as unchanged midazolam (Heizmann & Zeigler, 1981; Thummel et al, 1996). To this date no satisfactory explanation for this interindividual variability in midazolam urinary recovery exists. Since previous oral and intravenous data show no route-dependent differences in recovery (Bauer et al, 1995; Thummel et al, 1996), we proposed that some variable fraction of the 1'-OH conjugate is excreted into bile. Midazolam exhibits biexponential kinetics following intravenous administration, with no clear evidence of entero-hepatic recycling (EHR). However, the process of EHR is often difficult to discern on a traditional concentration versus time profile. Unless biliary secretion is a relatively discrete and significant quantitative fraction, it can be masked by the terminal elimination phase.

Bile is produced by the liver in order to emulsify and digest fatty acids present in the diet, and is stored in the gall bladder. During the ingestion of food, bile is secreted into the lumen of the small intestine via the common bile duct for the digestion process. Bile components are extensively conserved by the digestive system, and are reabsorbed through the small intestine after digestion. Once reabsorbed, these components, mostly bile acids, are secreted into small ducts between hepatocytes termed canaliculi via active transport mechanisms. There are many transporter proteins present in the plasma membrane of the bile canaliculus, and these proteins can transport several anionic, cationic and neutral molecules. Once in the bile, the molecule can be stored in the gall bladder for extended periods of time or be secreted into the small intestine. Once in the small intestine, two things are possible. The compound can be absorbed and re-enter portal blood, or not be absorbed and be eliminated via the feces. Most endobiotic and xenobiotic compounds that are present in bile are glucuronide conjugates and have increased polarity, and thus lower membrane solubility. When glucuronides are secreted into the small intestine via bile, they are rarely reabsorbed due to the solubility issues concerning the attached sugar moiety. However, certain intestinal bacteria possess enzymes (β-glucuronidase) capable of hydrolyzing the glucuronic acid moiety from the molecule, thus allowing reabsorption across the enterocyte. Then the molecule visits the liver for a second time and the process can repeat itself, or the molecule can escape the liver and be exposed to the systemic circulation. In short, biliary excretion of a molecule can increase its residence time in the body by effectively increasing the volume of distribution through

the process of entero-hepatic recycling. It can also lead to terminal elimination of the molecule in the feces.

Many drugs or metabolites that undergo glucuronidation in the liver are subsequently excreted into the bile. After delivery to the small intestine, glucuronide conjugates may be excreted into feces or hydrolyzed by bacterial glucuronidase enzymes to regenerate parent drug or hydroxylated metabolite. This may lead to the phenomenon of entero-hepatic recycling (EHR), if the molecule is reabsorbed. Midazolam, 1'-OH midazolam and 1'-OH midazolam glucuronide are all potential substrates for bile canalicular transporters, and may subsequently undergo EHR or are eliminated in the feces.

Studies were conducted to examine this hypothesis. First, we determined whether or not midazolam or its major metabolite, 1'-OH midazolam, was excreted into human bile. The next step was to indirectly estimate the extent of entero-hepatic recycling by measuring midazolam and 1'-OH midazolam fecal elimination.

2.2 Materials and Methods

2.2.1 Materials

1'-OH midazolam and D_2-1'-OH midazolam were gifts from Roche Laboratories (Nutley, NJ). *N*-methyl-*N*- (t-butyl-dimethylsilyl) trifluoroacetamide (MTBSTFA) was purchased from Pierce Chemical (Rockford, IL). Acetonitrile and

ethyl acetate were purchased from Fisher Scientific (Santa Clara, CA). β-glucuronidase was purchased from Sigma Chemical (St. Louis, MO). Butylsilane (C4) columns were purchased from J.T. Baker (Phillipsburg, NJ). All other chemicals were of reagent grade or better.

2.2.2 Bile Collection and Analysis

Bile and plasma samples were collected from two human volunteers undergoing liver transplant surgery. The plasma and bile collection intervals were 60 and 90 minutes, respectively, with time zero defined as when the 1 mg intravenous dose of midazolam was administered. Midazolam was administered after reperfusion of the donor liver and after a steady production of bile was established (~1 hour post-reperfusion).

Bile and plasma were analyzed by the same procedure (Paine et al, 1996). Briefly, bile or plasma samples were incubated for 24 hours in 100 mM sodium acetate, pH = 5, containing 200 units/ml of β-glucuronidase and 40 ng of internal standard (D_2-1'-OH midazolam). The incubation was quenched by the addition of 1 ml 100 mM sodium carbonate, pH ~11. Ethyl acetate (5 ml) was then added to extract midazolam and 1'-OH midazolam. Samples were shaken for 20 minutes and then centrifuged for 20 minutes at 5000 rpm. A duplicate sample (bile or plasma) was subjected to the same procedure, but without the 24-hour β-glucuronidase incubation. This allowed for the quantitation of unconjugated 1'-OH midazolam in either matrix.

Conjugated 1'-OH midazolam was calculated by subtracting the non-hydrolyzed value from the hydrolyzed value (Conjugated = Total – unconjugated).

After removal of the ethyl acetate, all samples were evaporated to dryness under a nitrogen stream, followed by reconstitution in 100 µl of 10% MTBSTFA in acetonitrile. All samples were then incubated at 80 °C for two hours to complete the chemical derivitization. Samples were then analyzed by gas chromatography-negative chemical ionization mass spectrometry. Analysis was performed on a VG-model Trio 1000 mass spectrometer interfaced to a Hewlett-Packard 5890A gas chromatograph. Injections (3 µl) were made in the splitless mode and performed with a Hewlett-Packard 7376 auto injector. The column was a DB-17 fused capillary column (30 m x 0.32 mm i.d., 0.25 µm film thickness; J & W Scientific, Ventura, CA). Helium carrier gas was used at a head pressure of 5 psi. Injector temperature and transfer line temperatures were set at 260 °C and 280 °C, respectively. The oven temperature was held at 200 °C for 1.5 minutes, increased at 20 °C/min to 280 °C and held at 280 °C for the remaining 10 min. This profile elicited a retention time of 9.5 and 14.8 minutes for midazolam and 1'-OH midazolam, respectively. Methane was the moderating gas and electron energy was set at 75 eV. The source temperature was set at 200 °C and the source housing pressure was approximately 1 x 10^{-4} mm Hg. The ions monitored for 1'-OH midazolam were *m/z* = 455 and 459 for the *t*-butyl-dimethylsilyl derivitized compound and the ^{37}Cl signal for the D_2-1'-OH midazolam, respectively.

2.2.3 Stool Assay Methodology

Extraction of midazolam and its metabolites from the stool matrix was similar to that of bile. Since previous analyses confirmed high levels of conjugated 1'-OH-midazolam in urine samples from patients dosed with midazolam, blank stool samples were spiked with pooled urine (20 µl) from healthy volunteers that received a 1-2 mg intravenous midazolam dose. Different volumes (100 µl –1000 µl) of spiked stool homogenate (2 ml DI H_2O / 1 g stool wet weight) were combined with 1 ml 100 mM sodium carbonate, pH 11, and 40 ng of D_2-1'-OH midazolam as an internal standard. The basified mixture was vortexed and centrifuged at 5000 rpm for 20 minutes. The supernatant was added to 6 ml butylsilane (C4) solid phase extraction columns that were pretreated as follows: 5 ml acetonitrile followed by 10 ml (2 x 5 ml) 50% methanol in water, followed by 5 ml 10 mM K_2HPO_4. The elution protocol for the columns was the same as the pretreatment protocol, only in reverse order. The only fraction collected for further analysis was the final 5 ml acetonitrile eluant. Flow rate through the columns was ~ 1 ml/min. The collected acetonitrile fraction was evaporated under nitrogen to ~ 0.5 ml, then 1 ml KPi buffer, pH = 7.4 and 1 ml 100 mM sodium carbonate, pH ~11, were added to the tubes along with 5 ml ethyl acetate. The remainder of the procedure was identical to that previously described for the analysis of bile.

2.2.4 Stool Collection and *In Vivo* Analysis

Stool was collected from two healthy volunteers for a period of 24 hours after a 1 mg intravenous dose of midazolam. Samples were stored at 4 °C during the 24-hour collection, then at –20 °C until analysis. Stool samples were thawed in 2 volumes of DI water (as described above) homogenized and then analyzed as outlined above.

2.3 Results

2.3.1 Biliary Analysis

Analysis of bile collected from 2 liver transplant patients showed that 1'-OH midazolam glucuronide was excreted into bile after a 1-mg intravenous dose of midazolam was given to the patient (Figure 2.1). No parent midazolam was detected in biliary samples. The total biliary concentration of conjugated 1'-OH midazolam was 150 ng/ml and 80 ng/ml in the two subjects, respectively. Previous results show these values to be comparable to, but less than urine concentrations of 1'-OH midazolam glucuronide after similar doses of midazolam. However, the glucuronide metabolite was present in bile at a far greater concentration than found in plasma after intravenous administration of midazolam (Table 2.1).

2.3.2 Stool Recovery of Midazolam Metabolites *In Vivo*

One-milligram midazolam doses were given to two healthy male subjects, and stool was collected for 24 hours. Once determined that the 1'-OH midazolam glucuronide was secreted into the bile, an assay was developed to measure the quantity of metabolite that did not re-enter the bloodstream and become otherwise excreted. Stool collections were obtained from healthy volunteers, and recovery of 1'-OH midazolam and its conjugate from the fecal matrix was determined via solid phase extraction (SPE). SPE was required due to the amount of interfering organic compounds present in the fecal matrix. The goals of the assay were to remove as much interference as possible, while still achieving a quantitative assay.

Initial method development involved selection of the optimum solvents, both organic and aqueous, for rinsing impurities from the column and for elution of the desired analyte(s). Since midazolam has unique solubility properties, we were able to use certain solvents and pH adjustment to purify the metabolites out of stool. Midazolam is water-soluble at mildly acidic pH due to protonation of the two diazepine nitrogen atoms, and due to the formation of a ring-opened conformation in which a terminal primary amine is formed. At elevated pH, the nitrogen atoms are not positively charged, and the ring structure remains intact, thus confirming solubility in low molecular weight organic solvents. Since our goal was to extract a hydroxylated or glucuronidated metabolite, knowledge of solubility characteristics are vital due to the molecule's increased water solubility.

Method development was conducted on blank human stool spiked with pooled human urine known to contain high levels of 1'-OH midazolam glucuronide. The solid phase extraction protocol typically involves four steps:

1) Elution of blank column to remove any interferences inherent to the column
2) Application of matrix containing analyte(s) of interest
3) Rinse away impurities
4) Elution of analyte(s) of interest from column

Due to the increased water solubility of the midazolam metabolites, we believed that a weak organic solvent would elute our analyte(s) with the best efficiency. Moreover, as the solvent gets increasingly non-polar, the probability of eluting organic contaminants increased. Therefore, our initial solvents for elution were acetonitrile or methanol. Due to simplicity, our initial rinse solvent was deionized water. Flow rate was set at ~1 ml/min via vacuum pump.

Stool homogenate supernatant (1 ml) was applied to columns after initial pretreatment with 5 ml of methanol or acetonitrile. Repeated deionized water rinses (up to 20 ml) were unable to remove any of the dark brown coloration from the columns. Analysis of the rinsate found no detectable levels of any midazolam species. Elution with acetonitrile or methanol (5 ml) removed all coloration within 1-5 minutes time. Methanol was less able to elute any contaminants compared to acetonitrile. Acetonitrile elution rarely took greater than 90 seconds, whereas methanol elution approached five minutes in all cases. Once all contaminants were removed, additional elutions were performed to determine if any metabolites were still present on the

columns. Unfortunately, no detectable midazolam species were present in the additional eluted fractions. Previous control experiments with urine-spiked water showed that both acetonitrile and methanol were able to elute 1'-OH midazolam and its glucuronide. These findings suggest that the methanol and acetonitrile were eluting the analyte(s) of interest, but also eluting the unwanted interferences.

The next obstacle was to find a rinse solvent that would remove the interferences and leave sufficient metabolites bound to the column. We constructed a matrix of various combinations of methanol, acetonitrile and water. Acetonitrile was able to elute the brown contaminants down to a concentration of 10% in water, but methanol could not elute any contamination below 50%. Control experiments were then performed to determine if 50% methanol in water could elute midazolam metabolites from the columns. Less than 5% of the spiked analytes were recovered from the columns after two-5 ml rinses with 50% methanol. Additional elution with acetonitrile found that no analytes remained on the columns, suggesting that 50% methanol could also elute the analytes in question.

To increase binding affinity of the midazolam metabolites, an additional rinse step with a low ionic strength base was added. By increasing the pH of the column environment, the midazolam nitrogen atoms become protonated and less soluble in 50% methanol solution. Immediately after pretreatment with acetonitrile, we rinsed the columns with two-5 ml rinses with 50% methanol followed by 5 ml of 10 mM K_2HPO_4, prior to sample application. After the stool supernatant was applied, the pretreatment procedure was duplicated in reverse starting with application of the weak

phosphate solution. Visual inspection was identical to the previous experiments, but elution of the analyte increased to almost 30%. Presumably, at pH values of ~10, the midazolam species were bound to the column with higher affinity.

Analysis of the stool matrix found that neither midazolam nor any of its metabolites were detected in stool from either subject, although plasma concentrations of midazolam and 1'-OH midazolam were within normal parameters (data not shown). The extraction efficiency varied from 23.9 – 45.5 % (Table 2.2). Solid phase extraction efficiency increased as the amount of stool applied to the columns decreased. The lowest limit of detection observed was ~ 1ng/ml (24.8% x 2 ng / 0.5 ml).

The metabolic scheme for midazolam, based on literature data and those presented in this report, is shown in Figures 2.2. Midazolam can be metabolized by CYP3A4 or CYP3A5 to two hydroxylated metabolites, 1'-OH midazolam and 4-OH midazolam. A third oxidative metabolite, 1',4-dihydroxy midazolam, is also formed via CYP3A, but only from the 4-OH midazolam precursor (Podoll, 1996). All three metabolites are extensively conjugated with glucuronic acid, and excreted into urine. Data from this study demonstrate that the conjugated 1'-OH metabolite is excreted into bile, but is either subsequently reabsorbed from the gastrointestinal tract or is decomposed or altered by gut bacteria.

2.4 Discussion

2.4.1 Presence of Midazolam Metabolites in Human Bile

Biliary concentrations of 1'-OH midazolam glucuronide were found to be higher than what was observed in plasma after intravenous midazolam administration. Previous studies have shown that glucuronide conjugates are readily excreted via ATP-binding cassette transporters (ABC) MRP-1, MRP-2 or cMOAT (Keppler et al, 1997), MRP-3 (Zeng et al, 2000), and MRP-6 (Madon et al, 2000). The ABC transporters are well characterized with respect to endogenous hormone and bile acid glucuronide export, but drug glucuronide excretion data are sparse. To date, only MRP-1, MRP-2 and MRP-6 are known to be located within the bile canalicular membrane, and thus are the only candidates for potential xenobiotic elimination into bile. Previous work in the rat shows midazolam is primarily excreted into the feces and not into urine (Woo et al, 1981), unlike the excretion profile for humans. However, in both species there is very little excretion of unchanged midazolam. Our data from humans suggest that 1'-OH midazolam is secreted into bile primarily in the form of a glucuronide conjugate, with no detectable export of unchanged midazolam. This is consistent with previous data showing that unconjugated biliary secretion of benzodiazepine-like drugs or metabolites in humans is negligible (Hellstern et al, 1990; Tse et al, 1983).

Only a small percentage of the total administered midazolam dose entered the bile. From mass balance calculations, we estimate that only 10.8 μg of the 1 mg

midazolam dose (~1.1%) was excreted into bile through 90 minutes (assuming maximum bile flow of 0.8 ml/min and a bile concentration of 150 ng/ml). Bile flow remains generally constant at 0.5 – 0.8 ml/min. Although the concentration of conjugated 1'-OH midazolam is much greater than found in plasma, indicative of active transport, the total amount of metabolite in the bile was only a fraction of the dose. Although the full plasma midazolam and metabolite concentration-time profiles were not determined, approximately 50% of a midazolam dose will be eliminated after 90 minutes. However, only ~33% of the glucuronide conjugate AUC will be accounted for in the first 90 minutes after an intravenous dose (Thummel Lab, unpublished data). Since the elimination of conjugated 1'-OH midazolam is not complete after 90 minutes post dose, the biliary excretion (1.1%) reflects only the glucuronide that has been eliminated in that time period. Thus, the 1.1% biliary excretion may actually represent up to 36% (33% x 1.1%) of excreted drug/metabolite.

2.4.2 Entero-Hepatic Recycling of Midazolam

We demonstrated that 1'-OH midazolam glucuronide was secreted into bile. Previous groups have also detected benzodiazepine glucuronides in bile (Hellstern et al, 1990; Tse et al, 1983). Since both 1'-OH midazolam and 1'-OH midazolam glucuronide are active metabolites, it is relevant to determine their disposition characteristics. By collecting bile samples from patients receiving intravenous midazolam, we were able to confirm that 1'-OH midazolam glucuronide was present in

bile in relatively high concentrations compared to plasma. No unconjugated 1'-OH midazolam was detected in bile, suggesting that hydrolytic cleavage of the glucuronide does not occur in the biliary matrix. Interestingly, significant biliary hydrolytic activity has been previously reported (Pappo et al, 1967; Ho et al, 1979). Hydrolysis of the glucuronide metabolite will also occur in the gastrointestinal tract. Indeed, in an experiment involving human stool spiked with human urine containing high doses of 1'-OH midazolam glucuronide, only 1'-OH midazolam was recovered. This implies that hydrolysis of the sugar occurred in the stool matrix, and any remaining conjugated 1'-OH midazolam was below the limit of detection. As with bile, human feces contain numerous bacteria that possess β-glucuronidase activity. Though we did not test β-glucuronidase activity in our biliary samples, the literature and the spiked stool results suggest complete hydrolysis occurs in the fecal matrix or along the gastrointestinal tract.

Although high concentrations of 1'-OH midazolam glucuronide were found in human bile, we were unable to quantify any of the metabolites in human stool samples. These findings suggest that the entero-hepatic recycling of 1'-OH midazolam glucuronide is complete; all glucuronide is hydrolyzed and 1'-OH midazolam is reabsorbed, where it could be re-conjugated in the liver and eventually eliminated via the urine. This theory is quite plausible considering the solubility and membrane permeability of midazolam and 1'-OH midazolam. Midazolam is rapidly absorbed on oral dosing, and therefore it is likely that 1'-OH midazolam would also share some of its absorption characteristics. No data are available concerning the fraction of 1'-OH

midazolam that can cross the gut lumen ($F_A \cdot F_G$). However, experiments conducted with Caco-2 cell cultures demonstrate rapid transcellular permeability, a process that is enhanced by extensive binding to plasma proteins in the receiver (i.e. vascular) compartment (H. Ishizuka, unpublished data).

In our study of liver transplant patients, both had relatively normal levels of midazolam present in plasma, and biliary 1'-OH midazolam glucuronide concentrations that were 5 – 10 fold higher than plasma. The data suggest active transport of 1'-OH midazolam glucuronide into the bile, and that perhaps ~36% of the dose is involved in the entero-hepatic recycling distributive phenomenon. Although our fecal recovery data come from only two subjects, the data suggest that the interindividual variability seen in 1'-OH midazolam urinary recovery cannot be explained by differing degrees of biliary excretion and fecal elimination in the population, since none of this metabolite was found in feces. However, it is possible that other midazolam metabolites were excreted into the bile. Biliary samples were not analyzed for 4-OH midazolam levels. Previous data have shown the 4-OH midazolam is chemically unstable to acidic hydrolysis conditions (Paine, 1997a). Admittedly, all of the 4-OH midazolam glucuronide could have been degraded by the hydrolysis treatment in bile. The possibility that variable 1'-OH midazolam recovery is a result of variable 1'-OH/4-OH midazolam formation will be explored in Chapter 3.

Future *in vivo* studies to further examine the role of EHR in midazolam disposition could be performed using cholestyramine and neomycin concomitantly as a model for an EHR-deficient individual. Cholestyramine is a bile acid binding resin

that binds anionic compounds secreted into the small intestine via the bile (Zhu et al, 2000). Since the midazolam doses in these studies are intravenous, any drug or metabolite bound up by the resin would be of biliary origin. Concomitant neomycin treatment would ablate the bacteria that possess β-glucuronidase activity (Remmel et al, 1981), thus rendering the patient unable to hydrolyze glucuronides even if some were to escape the binding resin. By comparing the urinary recovery of a midazolam dose in individuals with impaired and intact EHR, the relative contribution of midazolam biliary disposition could be elucidated. In addition, development of a direct 4-OH midazolam glucuronide assay would help address the quantitative significance of biliary and renal excretion of this metabolite.

2.5 Summary

Analysis of human bile following intravenous administration revealed relatively high levels of 1'-OH midazolam glucuronide compared to those found in plasma. These data strongly suggest that 1'-OH midazolam glucuronide is excreted into bile. *In vivo* stool analysis, however, revealed no detectable 1'-OH midazolam glucuronide in two human subjects. These results suggest that any 1'-OH midazolam glucuronide that is presented to the gastrointestinal lumen on biliary secretion is reabsorbed into portal blood, and not eliminated in the stool.

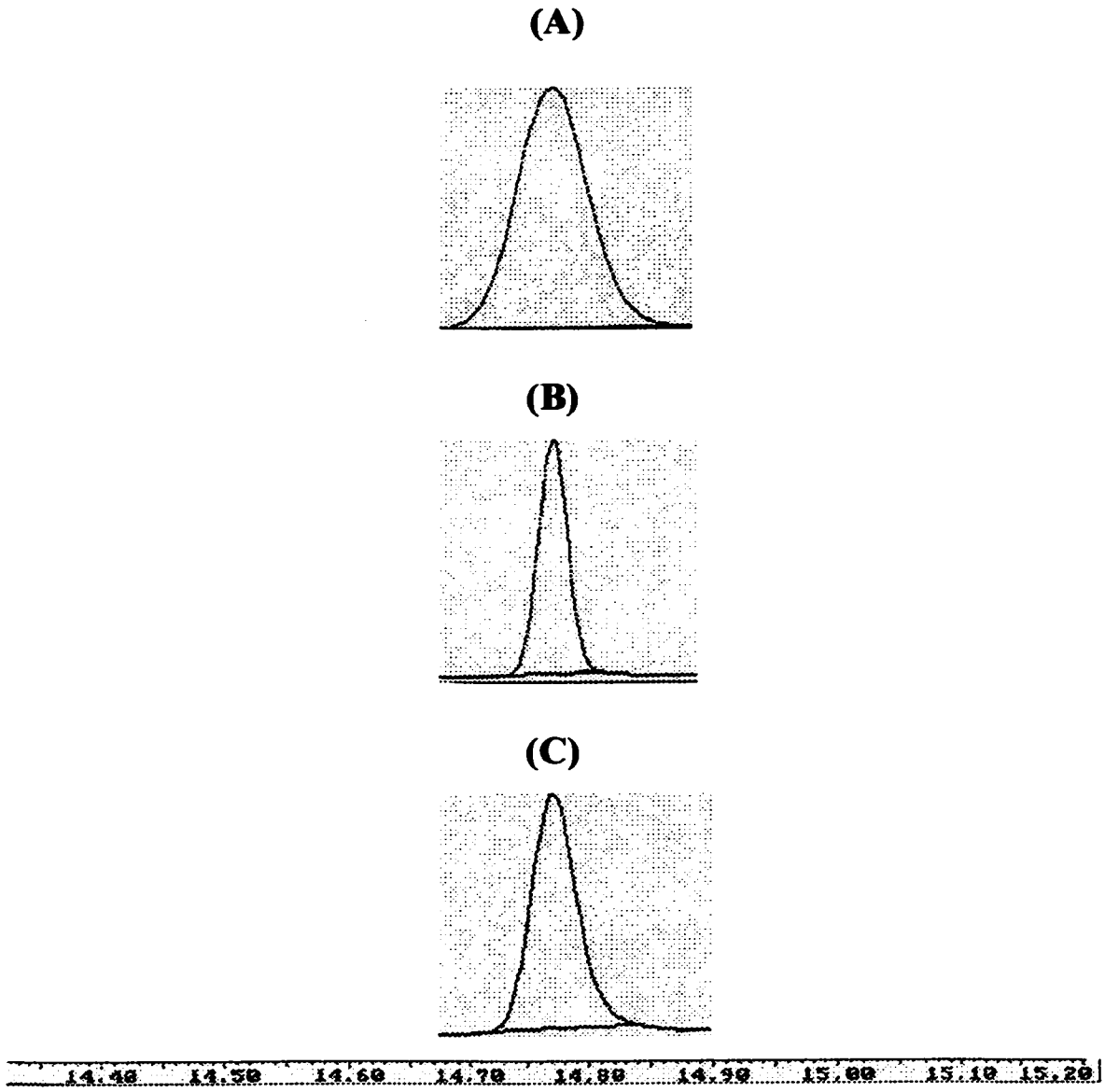

Figure 2.1. Mass spectral analysis of TBDMS derivative of 1'-OH midazolam in (A) bile, (B) feces and (C) urine (m/z = 455).

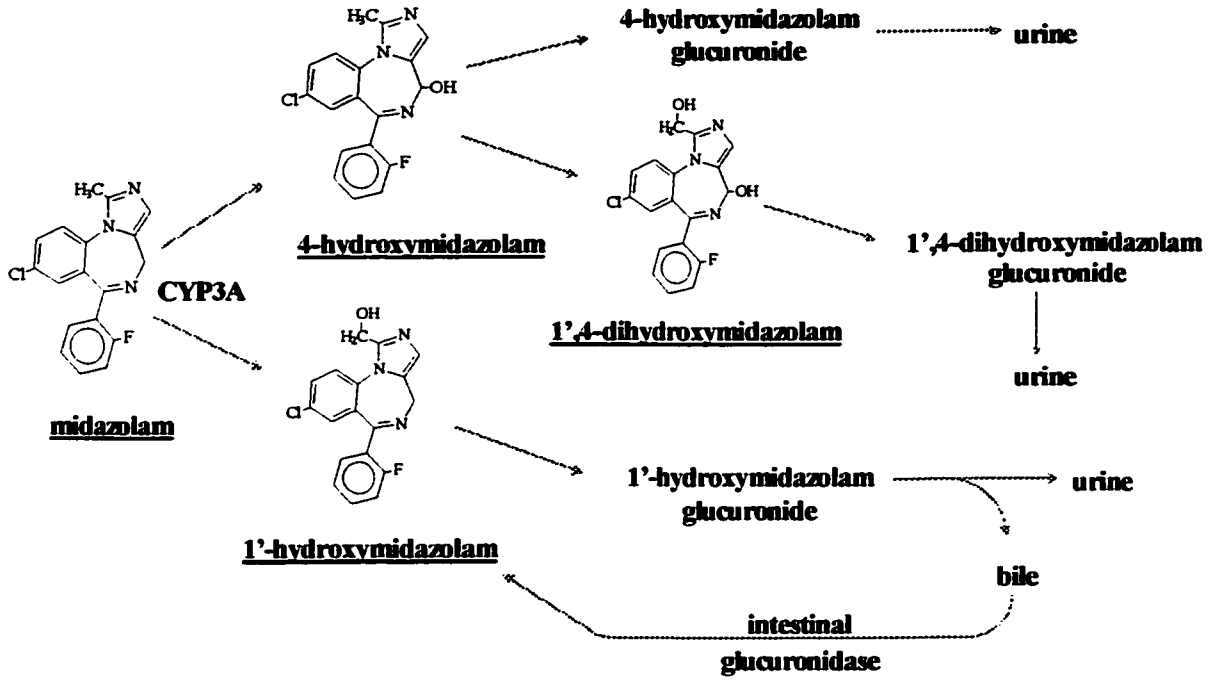

Figure 2.2. Metabolic scheme for midazolam and its metabolites [adapted from Gerecke, 1983; Podoll, 1996].

Table 2.1. Biliary and plasma analysis of 1'-OH midazolam and 1'-OH midazolam glucuronide.

		1'-OH midazolam (nM)	*1'-OH midazolam glucuronide (nM)*
Patient	*plasma*	7.9	39.0
1	*bile*	ND	235
Patient	*plasma*	3.8	30.0
2	*bile*	BLD	440

ND = not determined due to sample volume.
BLD = below limit of detection (~ 1.5 nM).

Table 2.2. Extraction Efficiency of Total 1'-OH Midazolam Species.

Stool Homogenate Volume (ml)	*Spike (ng)*	*Column Extraction Efficiency (%)*
1000 µl	25, 50	23.9, 28.0
500 µl	2, 25	24.8, 37.2
250 µl	2, 25	25.2, 37.9
100 µl	2, 25	33.2, 45.5

Efficiency was calculated as the ratio of recovered drug relative to known spike amount multiplied by 100. Columns were butylsilane (C_4).

CHAPTER 3

INTERINDIVIDUAL VARIABILITY IN THE 1'-OH MIDAZOLAM / 4-OH MIDAZOLAM METABOLIC RATIO

3.1 Introduction to Chapter 3

In vivo metabolism of midazolam (MDZ) is mediated by cytochrome P450 3A (CYP3A4 and CYP3A5), and results in formation of 1'- and 4-hydroxylated metabolites, which are subsequently excreted primarily as glucuronides. Hydroxylation at the 1'-position is dominant in humans, and constitutes ~70% of the Phase I metabolism at low *in vivo* systemic concentrations (range = 55-99%)(Heizmann et al, 1981; Thummel et al, 1996). The other 30% of Phase I metabolism is assumed to occur through hydroxylation at the 4-position, but this contribution is minimal as judged by urinary recovery *in vivo*. However, at high concentrations of MDZ *in vitro*, 4-OH MDZ is a significant clearance pathway for the parent drug (Gorski et al, 1998).

Chapter 2 described studies in which we determined whether or not midazolam or its major metabolite, 1'-OH midazolam, was excreted into human bile, and to indirectly estimate the extent of entero-hepatic recycling by measuring midazolam and 1'-OH midazolam fecal elimination. Those results suggested that any 1'-OH midazolam glucuronide that is presented to the gastrointestinal lumen on biliary secretion is reabsorbed into portal blood, and not eliminated in the stool. However, 4-OH midazolam was not quantitated in plasma or bile in our previous study.

CYP3A4 has been implicated in the formation of multiple metabolites from a single substrate. Aflatoxin B_1 (Gallagher et al, 1996), 17β-estradiol (Lee et al, 2001),

amitriptyline (Venkatakrishnan et al, 2001) and progesterone (Yamazaki et al, 1997) are just a few examples of multiple CYP3A-dependent metabolites from a single substrate. Coincidentally, these substrates also show homotropic cooperativity in the CYP3A-dependent formation of such metabolites. In some cases such cooperativity appears to influence the metabolic ratio of the multiple reaction products.

It is possible that variability in 1'-OH MDZ recovery *in vivo* is due to concentration-dependent product selectivity. Concentration dependent product ratios may result from multiple substrate molecules simultaneously binding to the CYP3A enzyme. CYP3A4 has been previously reported to bind more than one substrate simultaneously in its active site (Korzekwa et al, 1998; Shou et al, 1999; Tang et al, 2001), and multiple binding domains in the CYP3A4 active site have been described (Schrag and Weinkers, 2001). It is likely that metabolite specificity can be altered depending on the presence of one or more identical substrate molecules in the active site.

The dependence of product ratios on substrate concentration can possibly have organ-specific effects. Since the concentration of substrate in the small intestine can be far greater than that in the hepatocyte, the site of metabolism could influence a CYP3A-dependent product ratio. For midazolam, a high gut wall first pass extraction may promote greater 4-OH midazolam production based on the high concentrations of midazolam in the enterocyte. However, *in vivo* data with midazolam do not support this theory. Recovery of 1'-OH midazolam in urine from individual subjects was not

dosing route dependent (Thummel et al, 1996), although a tendency toward higher recovery after oral dosing was observed.

Less is known regarding CYP3A5 substrate regioselectivity or active site dynamics. CYP3A5 is a polymorphically expressed isoform that shares 84% amino acid sequence with CYP3A4. Traditionally regarded as a small quantitative contributor to *in vivo* CYP3A-dependent metabolism, its role in the metabolism of midazolam has recently been discovered to be increasingly important (Kuehl et al, 2001). In addition, limited data suggest that heterotropic cooperativity can also be manifested with CYP3A5 (Korzekwa et al, 1998).

Although the 1'-OH/4-OH midazolam ratio product ratio is known to be substrate concentration-dependent *in vitro*, it is also possible that it is not constant between individuals at a given MDZ concentration. In addition to the high levels of variability observed in CYP3A4-dependent metabolism, the presence of CYP3A5 in approximately 1/4 of the Caucasian population may add more variability to the midazolam metabolic ratio. Thus, interindividual differences in the urinary recovery of 1'-OH midazolam may be a result of polymorphic CYP3A5 expression. A more thorough examination of the regioselective metabolism of midazolam was undertaken to test this hypothesis.

3.2 Materials and Methods

3.2.1 Materials

NADPH and alkaline phosphatase-labeled secondary antibodies were obtained from Sigma Chemical Company (St. Louis, MO). Midazolam, 1'-OH midazolam, 4-OH midazolam and $^{15}N_3$-midazolam were kindly provided by Roche Laboratories (Nutley, NJ). Acetonitrile and ethyl acetate were purchased from Fisher Scientific (Santa Clara, CA). *N*-methyl-*N*-(*t*-butyl-dimethylsilyl) trifluoroacetimide (MTBSTFA) was obtained from Pierce Chemical (Rockford, IL). Expressed CYP3A4 (P207), CYP3A5 (P235) and a CYP3A5-selective antibody (A235) were purchased from Gentest Corporation (Woburn, MA). Cytochrome b_5 was purchased from Panvera Corporation (Madison, WI). SDS-polyacrylamide gel electrophoresis reagents (37.5:1 bis-acrylamide, ammonium persulfate and *N,N,N',N'*-tetra-methyl-ethylene-diamine) were purchased from Bio-Rad Laboratories (Hercules, CA). Nitrocellulose was purchased from Schliecher and Schuell (Keene, NH). BCIP/NBT reagents were purchased from Kirkegaard and Perry (Gaithersburg, MD). All other reagents were reagent grade or better.

3.2.2 Methods

Protein determinations were performed by the method of Lowry et al (1951). All human liver specimens were analyzed for CYP3A4 and CYP3A5 immunoreactive protein by Western blot, and quantitation was done via alkaline phosphatase detection. To determine an accurate ratio of 1'-OH midazolam /4-OH midazolam, incubations were performed with microsomes from 60 different human livers at three different MDZ concentrations. The formation of 1'-OH midazolam and 4-OH midazolam were monitored, and the metabolic ratio was calculated from the initial formation velocities of each. Incubations with 0.5 μM, 8 μM and 40 μM midazolam as the CYP3A4 / CYP3A5 substrate and 50 μg of microsomal protein were performed at 37 °C for 4, 2 and 1 minute, respectively. Similar experiments, as described for human liver microsomes, were performed with expressed CYP3A enzyme systems. In addition to experiments containing each recombinant isoform, CYP3A4 and CYP3A5 were mixed and titrated between 0 and 100% CYP3A4, and were incubated in isolation with all three midazolam concentrations to determine the rate of change in the metabolic ratio as a function of relative CYP3A4/CYP3A5 content. For the cDNA-expressed microsomal experiments, 10 pmol of total enzyme was used in lieu of microsomal protein. At lower concentrations of midazolam, longer incubation times insured sufficient detectable product formation. Previous experiments confirmed that the incubation reaction was linear through at least 6 minutes for the lower concentrations of midazolam (data not shown). At 40 μM midazolam, incubation times longer than

one minute caused significant mechanism-based inactivation of CYP3A. Assays for 1'-OH midazolam and 4-OH midazolam were performed using GC/MS as described previously (Paine et al, 1997b). Metabolic ratios were calculated from the initial velocity of 1'-OH and 4-OH midazolam formation.

Cytochrome P450 and cytochrome b_5 levels were determined from CO-difference and reduced-oxidized difference spectra, respectively, using extinction coefficients of 91 and 185 $mM^{-1} \cdot cm^{-1}$ (Omura and Sato, 1964).

3.3 Results

A panel of 60 different human liver microsomal samples was incubated with three concentrations of midazolam. Of the 60 livers 43 contained only CYP3A4, whereas 17 expressed CYP3A4 and CYP3A5. CYP3A4 specific content ranged in the 60 livers from 5 - 376 pmol/mg protein (~75 fold range), and CYP3A5 specific content ranged from 6.7 - 329 pmol/mg protein (~50 fold range) (Table 3.1). Cytochromes P450 and b_5 ranged from 110 - 510 and 210 - 550 pmol/mg protein, respectively (Table 3.1).

Interindividual variability and concentration dependence in the 1'-OH / 4-OH metabolic ratio were observed in the panel of 60 livers. As the concentration of midazolam increased, the metabolic ratio decreased (Figure 3.2). Midazolam 1'-and 4-hydroxylation, markers for CYP3A4/3A5 activity, varied in the microsomal samples from 200 - 8400 pmol/min/mg protein (~42 fold variability) at 8 μM midazolam. At

0.5 μM the variability was similar to 8 μM: the velocity range was 20.4 - 842 pmol/min/mg protein. For the 40 μM incubations, the range was reduced to ~15 fold (499 - 7450 pmol/min/mg protein) (Table 3.2). The cDNA-expressed isoforms, supplemented with a 3:1 molar ratio of cytochrome b_5, also showed concentration dependence in the 1'-OH / 4-OH midazolam metabolic ratio (Table 3.3). Metabolic ratios calculated from recombinant CYP3A4 were 10.6, 3.9 and 1.8 at 0.5 μM, 8 μM and 40 μM, respectively. For recombinant CYP3A5 the ratios were 26.5, 8.0 and 4.7 for the increasing concentrations of midazolam. At all three concentrations of midazolam, the 1'-OH / 4-OH metabolic ratio decreased as the relative amount of CYP3A5 to CYP3A4 increased (Table 3.3).

To determine what factor(s) influenced the 1'-OH / 4-OH ratio, correlations were performed with the velocity data, CYP3A4 and CYP3A5 content, total CYP protein and cytochrome b_5 levels (Figure 3.1). Correlations of the 1'-OH / 4-OH ratios with the absolute concentrations of CYP3A4 or CYP3A5 showed no dependence of the ratios on either parameter alone (Figure 3.3). The 1'-OH / 4-OH ratios also did not correlate with total cytochrome P450 or cytochrome b_5 levels. However, the 1'-OH / 4-OH ratio did correlate with relative CYP3A5 content (Figure 3.2). There is a clear relationship between the 1'-OH / 4-OH metabolic ratio at 8 μM midazolam (r^2 = 0.599), but no relationship was observed at 40 μM midazolam (r^2 = 0.082). A relationship also exists at 0.5 μM midazolam, although the relationship is not linear, thus revealing higher variability at lower midazolam concentrations.

Concentration dependence in the 1'-OH / 4-OH metabolic ratio was confirmed by incubating human liver microsomes with three different concentrations of midazolam (Table 3.4). For the entire panel of livers, the metabolic ratio decreased from 11.54 to 2.76 as the midazolam concentration increased from 0.5 μM to 40 μM. For livers that contained CYP3A5, the metabolic ratio was significantly higher than the ratio for livers that only contained CYP3A4, regardless of midazolam concentration (Table 3.4). Both 1'-OH and 4-OH midazolam formation at 0.5, 8 and 40 μM midazolam were correlated with total CYP3A levels: r^2 = 0.748-0.924 for total CYP3A; r^2 = 0.635-0.754 for CYP3A4; r^2 = 0.342-0.787 for CYP3A5 (Table 3.5).

Figure 3.1 shows how the presence of CYP3A5 affected the metabolic ratio at a midazolam concentration of 8 μM. Similar results were seen at 0.5 μM (data not shown). At 40 μM midazolam there was no significant velocity difference between livers expressing CYP3A5 and livers that did not, but the livers that expressed CYP3A5 showed a higher 1'-OH / 4-OH metabolic ratio than livers that did not express CYP3A5.

Figure 3.2 shows the dramatic effect of CYP3A5 expression on the 1'-OH / 4-OH metabolic ratio, especially at the two lower concentrations of midazolam. The metabolic ratio increased in a non-linear fashion as the relative amount of CYP3A5 increases. At 40 μM midazolam difference between the metabolic ratio for CYP3A4 and CYP3A5 was greatly masked. Presumably, at such a high midazolam concentration (40 μM), saturation of binding site(s) has occurred for both CYP3A4 and CYP3A5 and the metabolic ratios for the two enzymes converge.

3.4 Discussion

Experimental results reported in this chapter, examined the differential regiospecificity in midazolam metabolism by CYP3A4 and CYP3A5, and the effect of differing substrate concentrations on the regiospecificity. The incubation concentrations were chosen to mimic as closely as possible the peak unbound plasma (0.5 μM), GI lumenal (40 μM) and an intermediate (8 μM) midazolam concentration following oral administration. The low and high concentrations would represent the minimal and maximal peak concentrations of midazolam one might expect for the liver and small intestine, respectively, following ingestion of 2 mg midazolam syrup. The experiments were performed with a panel of microsomes prepared from 60 different human liver samples. The large sample size allowed us to address interindividual variability in reaction rates and product ratios in addition to regioselective metabolism.

CYP3A5 was quantitatively expressed in 17/60 liver samples (28%). Comparison of the 1'-OH midazolam /4-OH midazolam ratio in CYP3A5 positive and CYP3A5 negative livers indicated that a significant difference existed between the two groups (Table 3.4). Michaelis-Menten parameters for the CYP3A5-dependent metabolism of midazolam are similar to those of CYP3A4, except that CYP3A5 has an approximately 2-fold higher affinity and 2-fold higher V_{max} with regards to 1'-hydroxylation (Gorski et al, 1994). These data confirm the previous findings in that

the 1'-OH/4-OH ratio was significantly higher in microsomal samples expressing both CYP3A4 and CYP3A5.

These data also show that at high concentrations of midazolam, hydroxylation at the 4-position could be a significant clearance pathway for midazolam *in vivo*. Following intravenous therapeutic administration, plasma concentrations of midazolam would fall short of a concentration of 40 μM. However, after oral dosing of midazolam, the lumenal concentration in the small intestine can approach 40 μM (Fisher et al, 1999). At such a high concentration of midazolam, *in vivo* formation of 4-OH midazolam may be a significant but highly variable elimination pathway. As concentrations of midazolam increase, there is the possibility of saturation of the active site. Previous data suggest that two midazolam molecules can fit in the CYP3A4 active site at the same time (Korzekwa et al, 1998). These data strongly suggest that as the midazolam concentration increases from 0.5 μM to 40 μM, the 4-OH pathway becomes more favored. This is most likely due to the fact that CYP3A4-dependent midazolam 4-hydroxylation has a K_m value approximately 10-fold higher than for 1'-hydroxylation, although V_{max} estimates are comparable for both pathways (Gorski et al, 1994). Therefore, 1'-hydroxylation predominates at the lower concentrations of midazolam, and 4-hydroxylation becomes a more important pathway as the substrate concentration increases. Theoretically, once the midazolam concentration reached a high enough level, both pathways would be at V_{max}, and the metabolic ratio would approach unity. However, CYP3A5 kinetics becomes increasingly difficult to understand due to the homotropic and heterotropic changes in metabolism commonly

apparent with CYP3A4 kinetics. Although the effects are not as well characterized as CYP3A4 kinetics, CYP3A5 activity was increased by α-naphthoflavone (Baune et al, 1999; Korzekwa et al, 1998). Considering potential non-linear metabolite formation, multiple midazolam molecules in the active site or differential activation of metabolic activity, it is clear that the catalytic differences between CYP3A4 and CYP3A5 should be explored further.

Midazolam metabolic ratios for the CYP3A5-containing microsomes were significantly higher than those only expressing CYP3A4. The difference between the two populations of microsomes diminished as the midazolam concentration increased, suggesting that CYP3A5 preferentially oxidizes midazolam at the 1'-position at low substrate levels, and that 4-hydroxylation becomes more quantitative as the active site becomes more crowded with midazolam molecules. Since CYP3A5 favors hydroxylation at the 1'-position of midazolam, especially at low concentrations found *in vivo*, it is possible that individuals expressing significant levels of CYP3A5 may produce a higher fraction of 1'-OH midazolam as a metabolic product than individuals who only express CYP3A4. Moreover, if more 1'-OH midazolam is formed by CYP3A5 *in vivo*, it may be possible to quantitate the 1'-OH midazolam in the urine and use the percentage of dose recovered in the urine as a phenotypic marker for CYP3A5 expression.

One *in vivo* study (Thummel et al, 1996) compared urinary recovery of 1'-OH midazolam in 20 healthy volunteers after oral and intravenous administration of midazolam. Although CYP3A5 genotype was not determined in that study, 6 possible

outliers were detected on the basis of urinary recovery. Mean urinary recovery was 71.1 ± 12.9 percent of dose as 1'-OH midazolam and its glucuronide conjugate. Three men and three women exhibited urinary recovery greater than one standard deviation above the mean (> 84%). Although the genotypes of these six individuals is not known, it is an interesting finding that the percentage of individuals with such high urinary recovery of 1'-OH midazolam (30%) corresponds well to the approximate prevalence of the *CYP3A5*1* allele in the Caucasian population (33%) (Kuehl, et al, 2001). Indeed, it is plausible to suggest that the individual with a urinary 1'-OH midazolam recovery of >85% was homozygous for the functional *CYP3A5*1* allele.

It is likely that the variable recovery observed in 1'-OH midazolam urinary excretion is in part due to the expression of CYP3A5. Our data show that at midazolam concentrations comparable to that of plasma, CYP3A5 microsomes produce a significantly higher ratio of 1'-OH/4-OH midazolam.

Since CYP3A5 is found in both liver and intestine, the effect of the enzyme on total 1'-OH midazolam formation *in vivo* should not be dosing route specific, as was observed. Previous *in vivo* data (Thummel et al, 1996) show an interesting pattern of individuals that have a relatively higher degree of 1'-OH midazolam excretion. In all three male subjects, the excretion of 1'-OH midazolam was lower after oral administration compared to intravenous dosing. Considering the higher enterocyte concentration of midazolam following oral dosing, and the importance of midazolam 4-hydroxylation at high substrate levels, this finding is consistent. It is possible that the discrepancy in the 1'-OH midazolam urinary recovery, and perhaps the 1'-OH/4-

OH ratio, between oral and intravenous dosing was masked by the presence of significant CYP3A5 expression is some subjects. Unfortunately, the limited population sample size (n = 20) and the lack of genotypic information does not allow for an accurate characterization of the potential CYP3A5 effect on the 1'-OH/4-OH midazolam ratio or in 1'-OH midazolam urinary recovery. To accurately assess if CYP3A5 expression does indeed impact the 1'-OH midazolam urinary recovery, a prospective study in which persons expressing the *CYP3A5*1* allele are recruited prior to commencement of the study would ensure the necessary statistical power for a comparison.

The prospective recruitment of 20 individuals expressing at least one *CYP3A5*1* allele and 20 matched control subjects who are homozygous for the *CYP3A5*3* allele, would address the variability in 1'-OH midazolam urinary recovery and its possible dependence on CYP3A5 genotype. Buccal swabs would provide genomic DNA from the cheek epithelial cells of prospective subjects. Once genotyping analysis determines which individuals express at least one *CYP3A5*1* allele, corresponding control subjects could be matched for gender, age and ethnicity. Once the two populations were selected, a similar study to Thummel et al, (1996) could be conducted, and the CYP3A5 effect on 1'-OH midazolam urinary recovery could be determined.

Since there is large interindividual variability in both CYP3A4 and CYP3A5 expression and activity, a convenient phenotyping assay would be very useful. Although these data are preliminary, they show that it may be possible to phenotype for

CYP3A5 expression using midazolam as the CYP3A5 probe and analyzing the urinary 1'-OH / 4-OH metabolic ratios as previously suggested (Gorski et al, 1994) or the fraction of dose metabolized to 1'-OH midazolam. These data could be applied to *in vivo* phenotyping by analysis of a single urine or plasma sample, and subsequent calculation of the 1'-OH / 4-OH metabolic ratios. Unfortunately, urinary analysis of 4-OH midazolam has been complicated due to instability of the molecule at pH values less than 7 (urine pH ~6) (Paine et al, 1997a). Perhaps loss of 4-OH midazolam due to chemical instability or biotransformation to 1',4-di-OH midazolam contributes to lack of total midazolam recovery seen in the human population. A direct assay for the glucuronide conjugates may overcome this problem, however mass spectrometry analysis of urine containing midazolam metabolites suggests that the 4-OH midazolam glucuronide may be unstable as well. A recent publication (Lin et al, 2001 Pharmacogenetics *in press*) validates the use of a 4-hour plasma sample as a phenotypic marker for CYP3A-dependent clearance; it is possible that the same plasma sample can be used to determine the significant expression of CYP3A5 as well.

Although these data reveal a description of the interindividual variability in regiospecific midazolam metabolism, we were unable to determine a marker that would allow for the prediction of the metabolic ratio *in vivo*. Since CYP3A4 and CYP3A5 are expressed in at least two clearance organs, and their content and activity are widely variable in those organs, it is likely that many different factors are responsible for the metabolic differences observed in the population. Although total cytochrome P450, CYP3A4, CYP3A5 or cytochrome b_5 did not predict the magnitude or variation in the

midazolam 1'-OH / 4-OH metabolic ratio, these data show that the CYP3A5 content relative to CYP3A4 is responsible for the some of the variability observed in the metabolic ratios.

3.5 Summary

In this report the regioselectivity of midazolam hydroxylation by CYP3A4 and CYP3A5 was examined in a panel of human liver microsomes from 60 organ donors. Hydroxylation activities at the 1'- and 4-positions of midazolam were measured at three substrate concentrations, and the ratio of velocities at each position was calculated. Livers that expressed CYP3A5 in addition to CYP3A4 had significantly higher 1'-OH/4-OH metabolic ratios at all three midazolam concentrations studied. For all livers, the metabolic ratio decreased as the concentration of midazolam increased, thus suggesting that 4-hydroxylation is not as favored at low midazolam concentrations. Individual parameter estimates did not correlate with the 1'-OH/4-OH metabolic ratio. These findings imply a complicated mechanism involving the metabolism of midazolam.

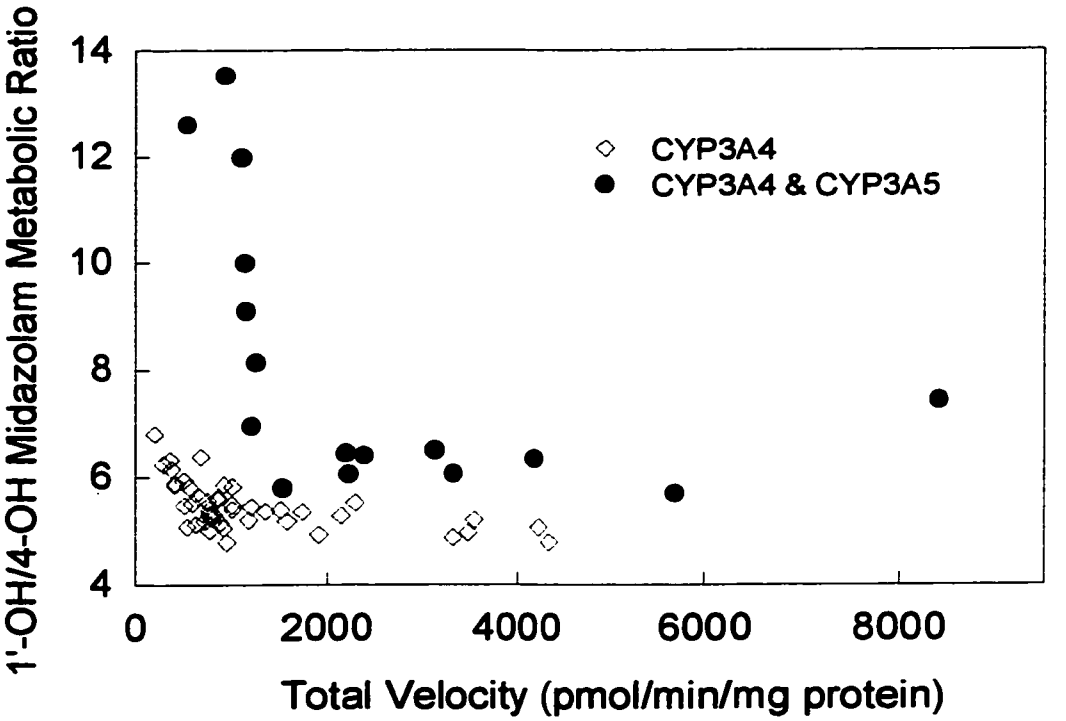

Figure 3.1. Total midazolam hydroxylation velocity versus the 1'-OH to 4-OH midazolam metabolic ratio. Dark circles denote livers that express CYP3A5 in addition to CYP3A4.

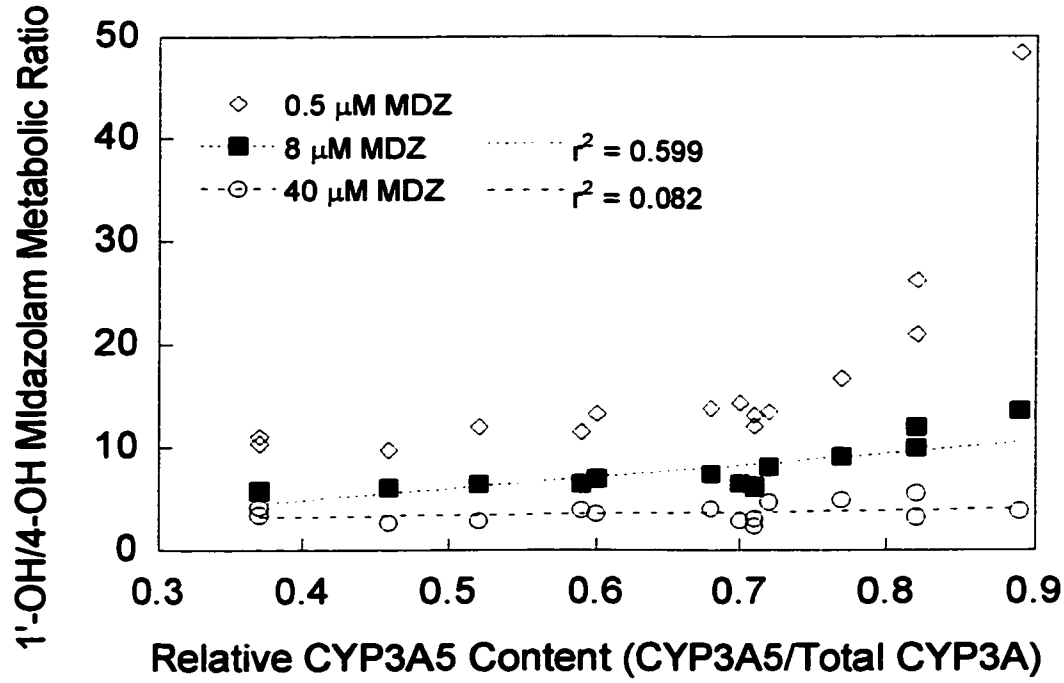

Figure 3.2. Relative CYP3A5 content versus the 1'-OH to 4-OH midazolam metabolic ratio. Relative CYP3A5 content is reported as the fraction of total CYP3A (CYP3A4 + CYP3A5).

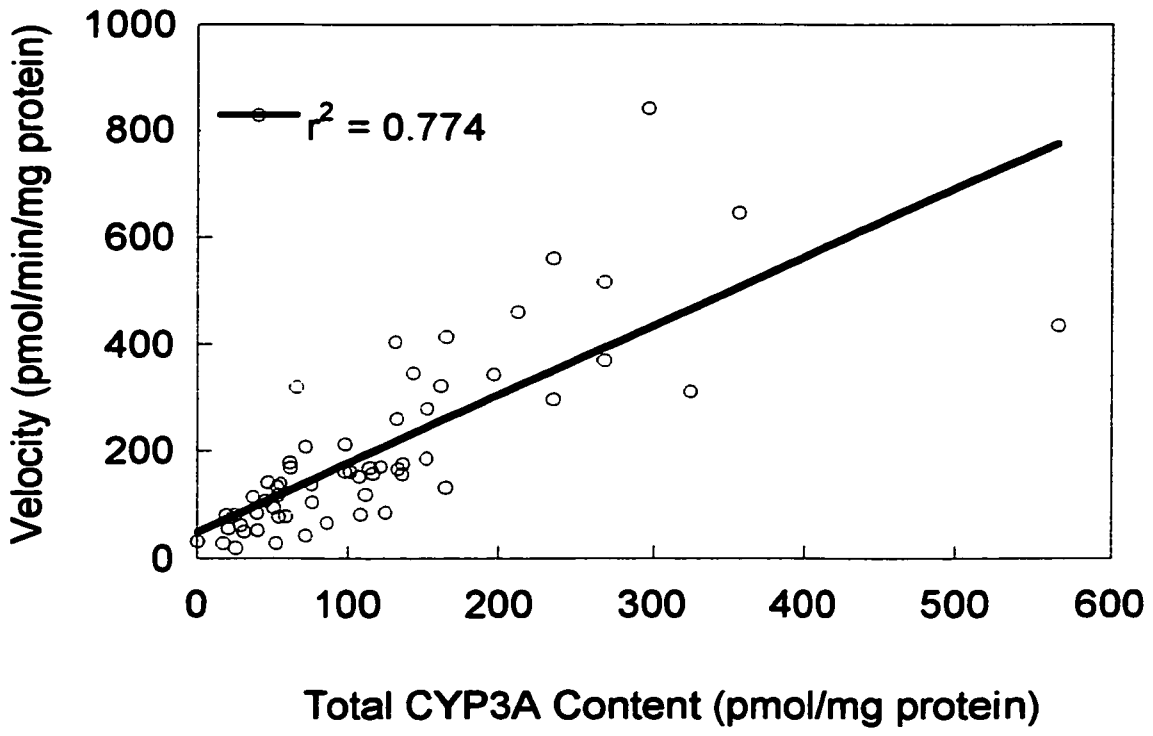

Figure 3.3A. Correlation between CYP3A content and total midazolam hydroxylation velocity at 0.5 μM MDZ concentration.

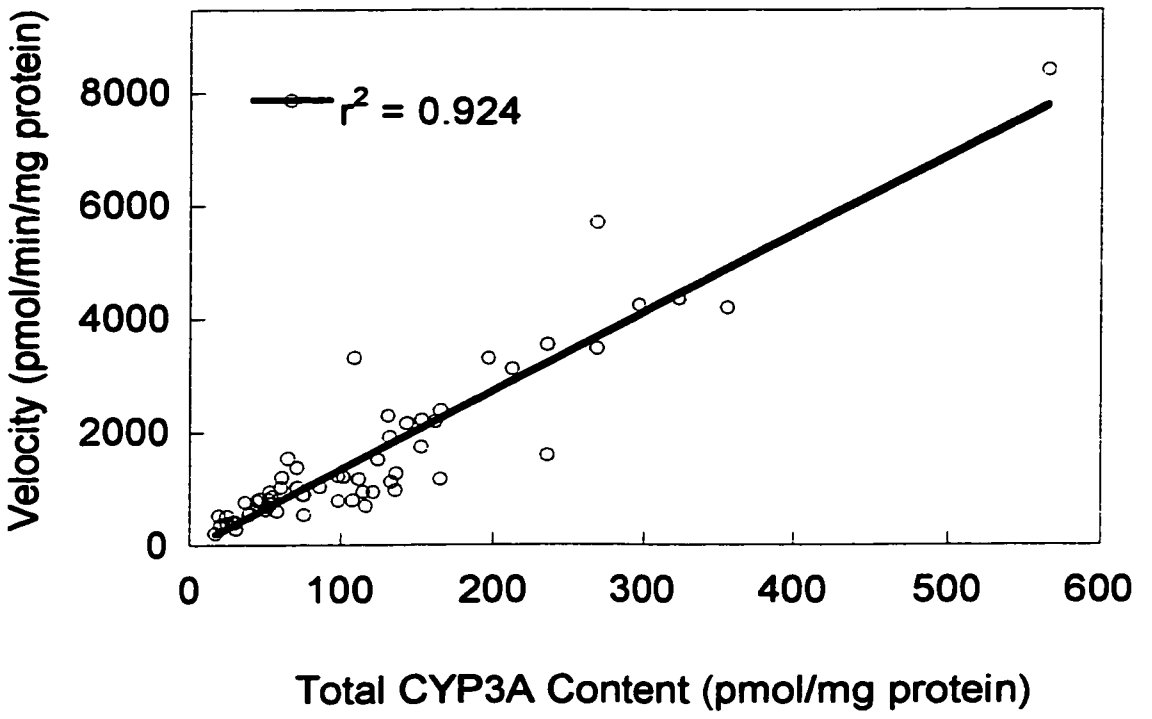

Figure 3.3B. Correlation between CYP3A content and total midazolam hydroxylation velocity at 8 μM MDZ concentration.

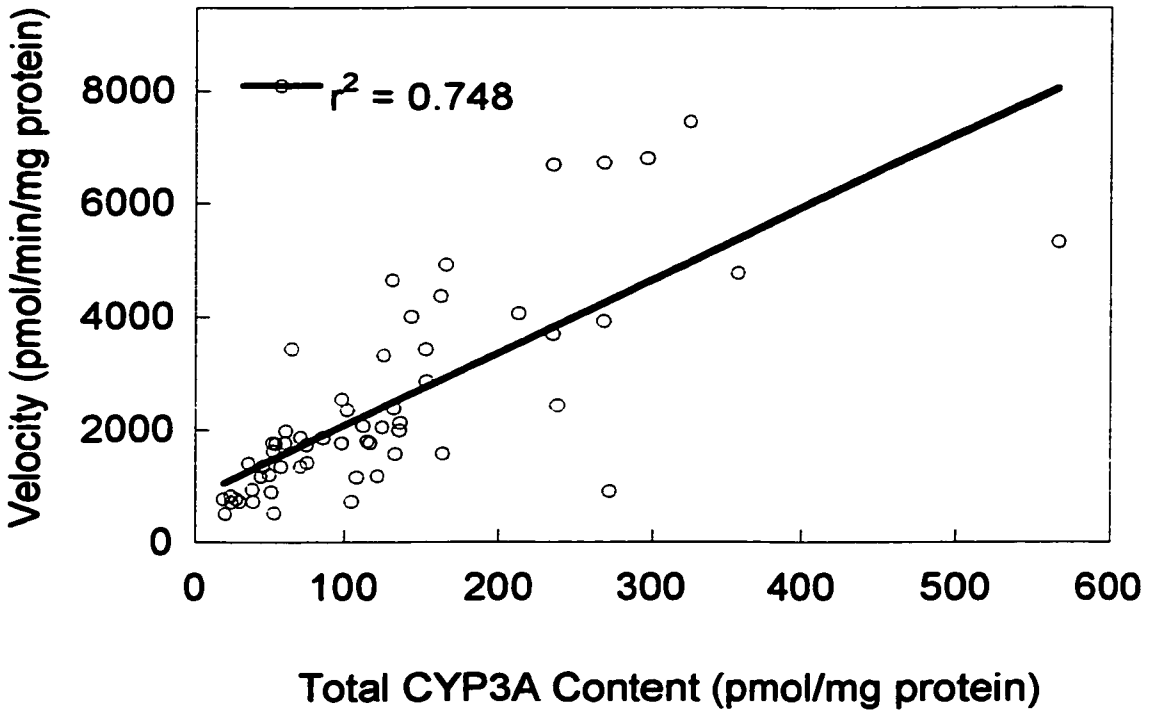

Figure 3.3C. Correlation between CYP3A content and total midazolam hydroxylation velocity at 40 μM MDZ concentration.

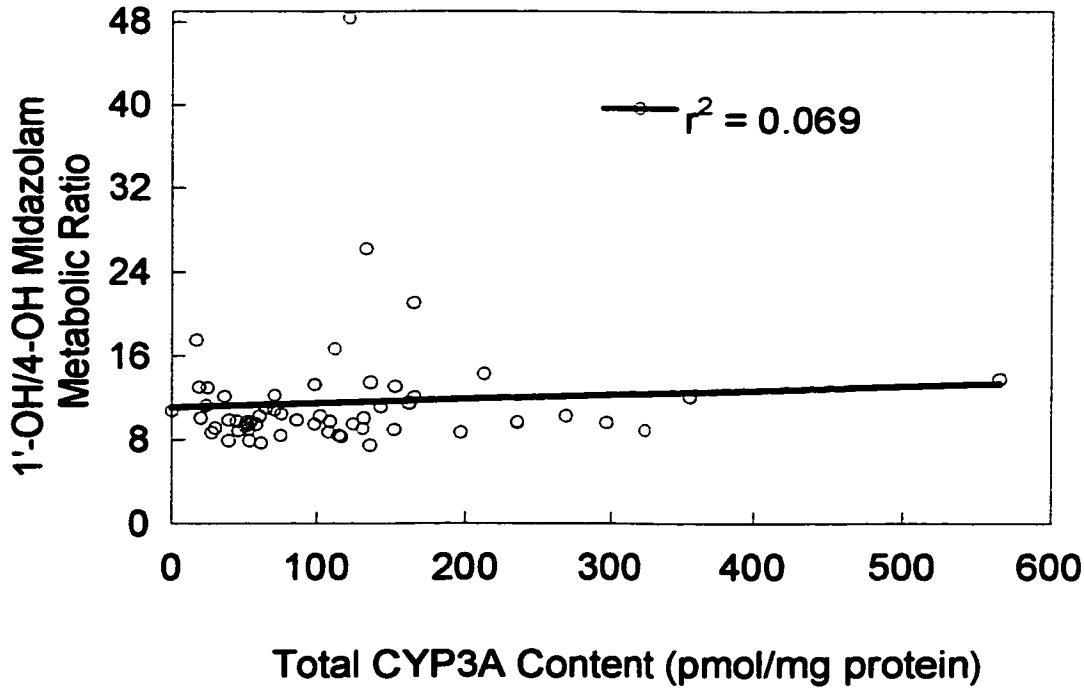

Figure 3.3D. Correlation between CYP3A content and the 1'-OH/4-OH midazolam metabolic ratio at 0.5 μM MDZ concentration.

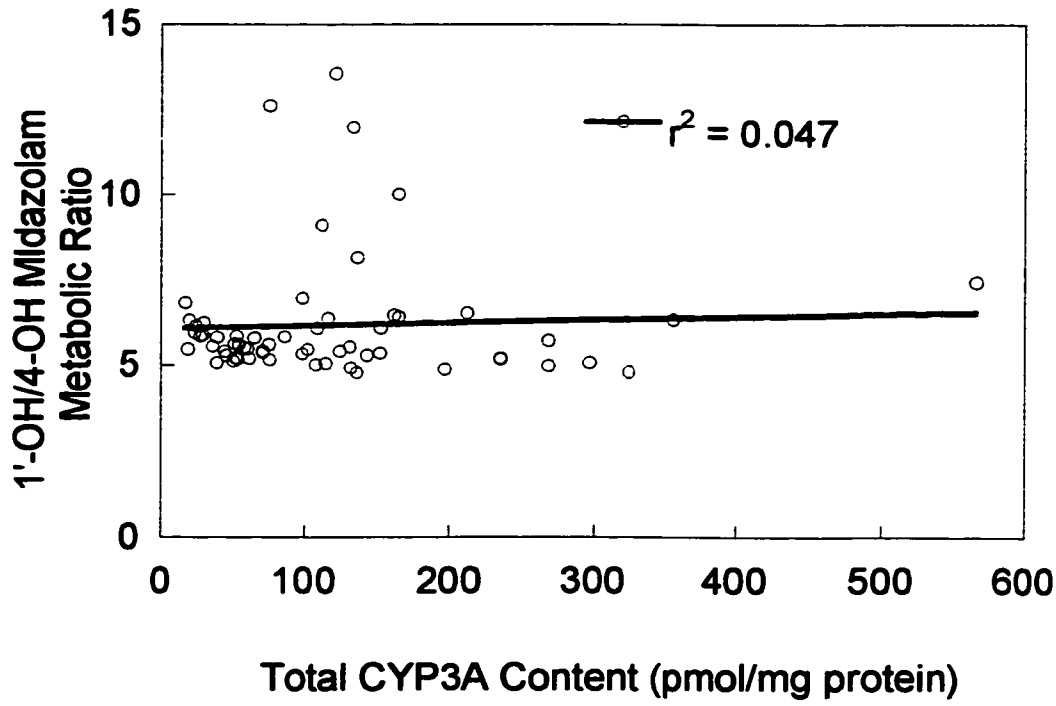

Figure 3.3E. Correlation between CYP3A content and the 1'-OH/4-OH midazolam metabolic ratio at 8 μM MDZ concentration.

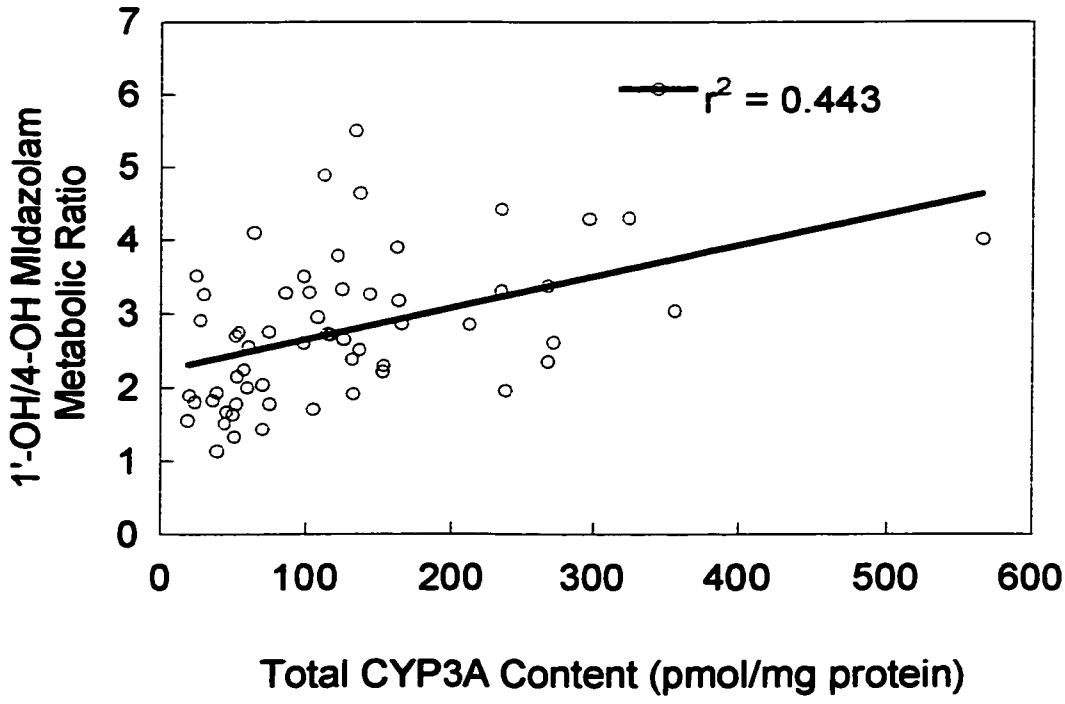

Figure 3.3F. Correlation between CYP3A content and the 1'-OH/4-OH midazolam metabolic ratio at 40 μM MDZ concentration.

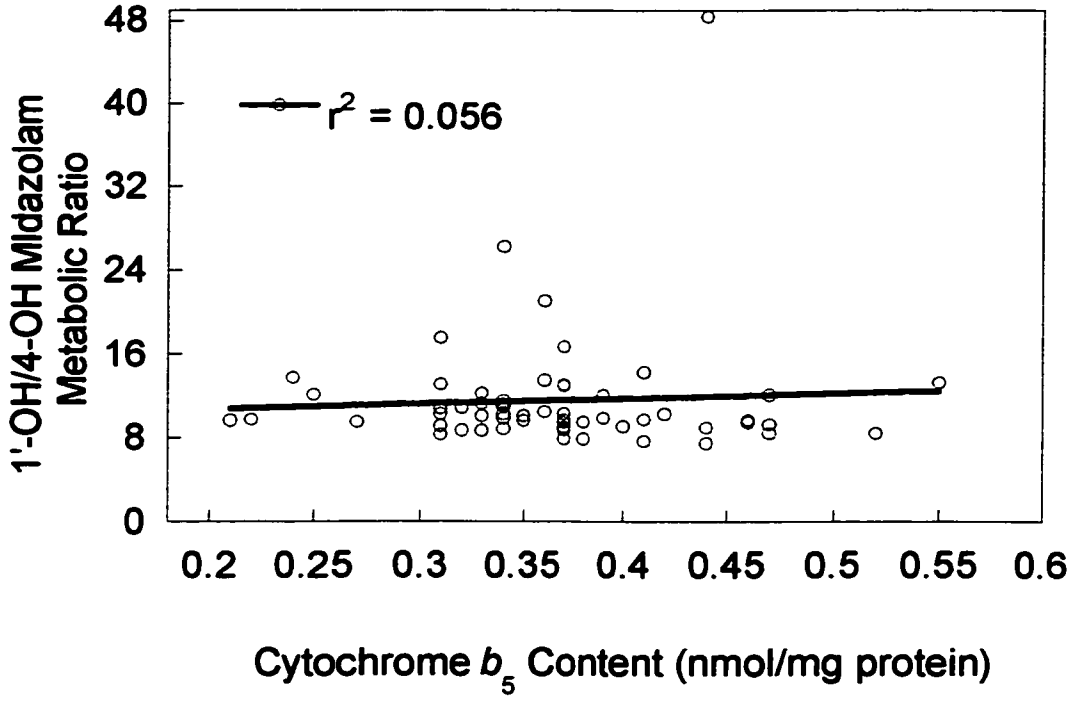

Figure 3.3G. Correlation between Cytochrome b_5 content and the 1'-OH/4-OH midazolam metabolic ratio at 0.5 μM MDZ concentration.

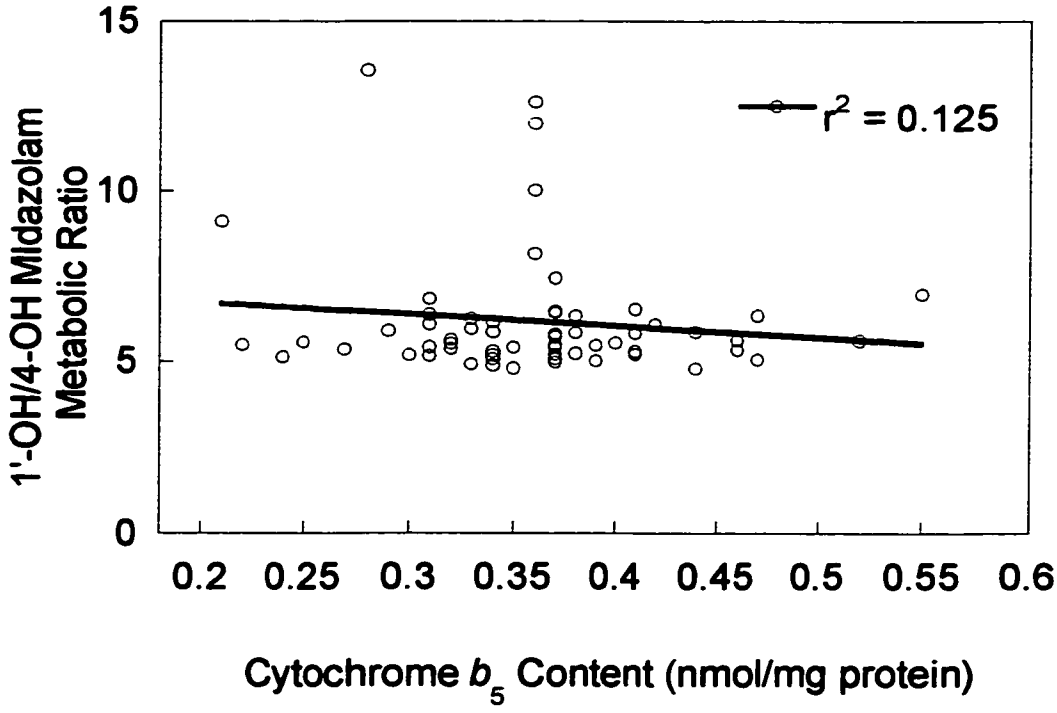

Figure 3.3H. Correlation between Cytochrome b_5 content and the 1'-OH/4-OH midazolam metabolic ratio at 8 μM MDZ concentration.

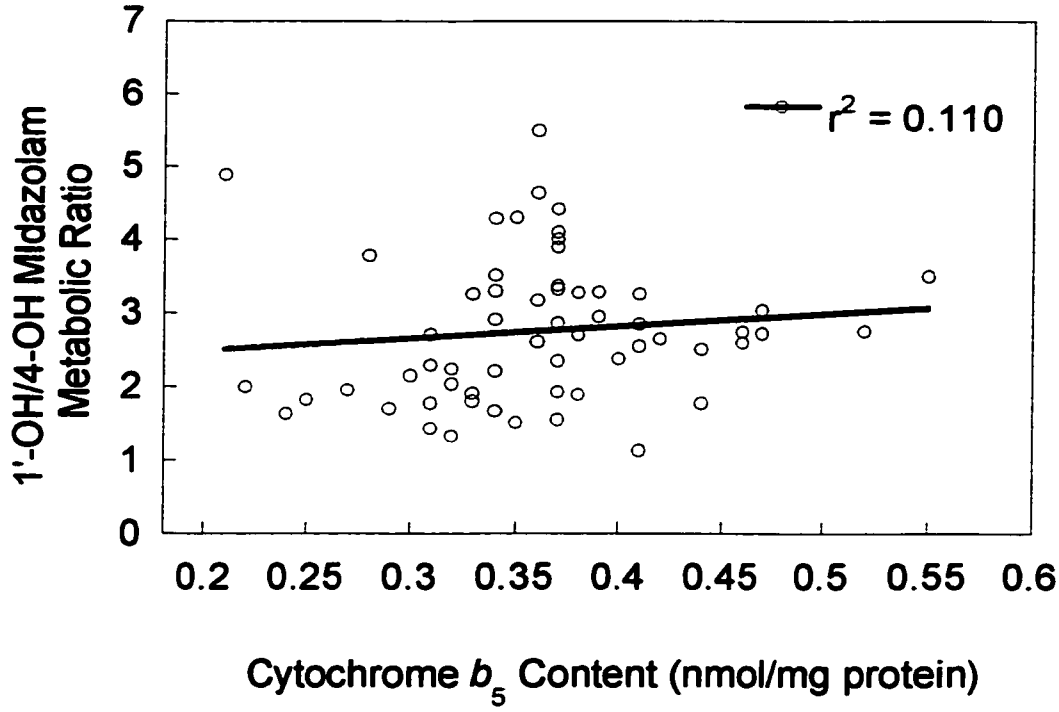

Figure 3.3I. Correlation between Cytochrome b_5 content and the 1'-OH/4-OH midazolam metabolic ratio at 40 μM MDZ concentration.

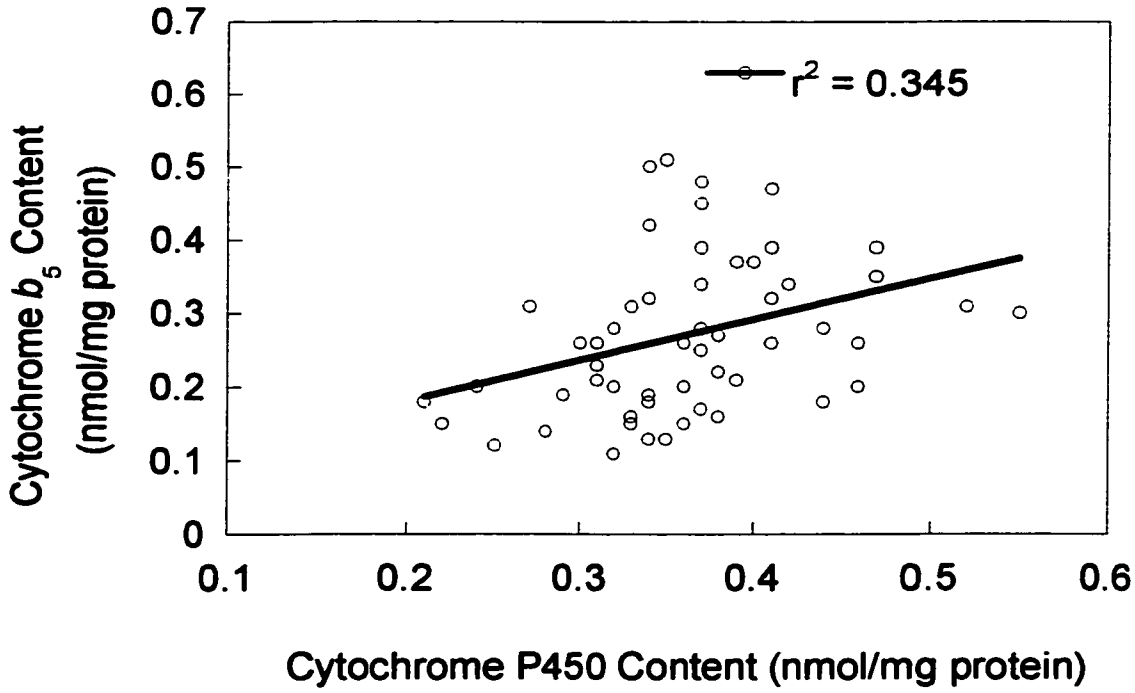

Figure 3.3J. Correlation between Cytochrome P450 content and Cytochrome b_5 content in human liver microsomes.

Table 3.1. Human Liver Bank Characteristics

Liver #	*CYP3A4 Specific Content (nmol/mg)*	*CYP3A5 Specific Content (nmol/mg)*	*Total CYP Specific Content (nmol/mg)*	*Cytochrome b_5 (nmol/mg)*
HL-102	85.3	BLD	0.47	0.41
HL-103	78.5	BLD	0.31	0.52
HL-106	130	6.7	0.37	0.40
HL-108	57.2	71	0.26	0.36
HL-109	102	BLD	0.23	0.31
HL-111	95.0	BLD	0.39	0.47
HL-112	57.7	BLD	0.20	0.46
HL-113	51.5	BLD	0.20	0.32
HL-114	86.1	BLD	0.26	0.46
HL-115	51.9	BLD	0.27	0.38
HL-118	20.1	BLD	0.25	0.37
HL-119	106	79.3	0.39	0.37
HL-120	68.5	BLD	0.21	0.39
HL-121	74.5	51.3	0.25	0.37
HL-124	171	BLD	0.42	0.34
HL-125	71.6	57.8	0.28	0.37
HL-126	46.0	BLD	0.26	0.30
HL-127	21.1	40.9	0.20	0.36
HL-128	19.5	BLD	0.16	0.38
HL-129	133	BLD	0.39	0.41
HL-130	23.6	BLD	0.13	0.34
HL-131	281	BLD	0.48	0.37
HL-132	59.0	BLD	0.22	0.38
HL-133	20.6	BLD	0.18	0.34
HL-134	332	BLD	0.51	0.35
HL-135	376	BLD	0.50	0.34
HL-136	23.9	BLD	0.16	0.33

BLD = Below limit of detection

Table 3.1. (continued) Human Liver Bank Characteristics

Liver #	*CYP3A4 Specific Content (nmol/mg)*	*CYP3A5 Specific Content (nmol/mg)*	*Total CYP Specific Content (nmol/mg)*	*Cytochrome b_5 (nmol/mg)*
HL-138	84.4	BLD	0.39	0.37
HL-139	67.2	BLD	0.37	0.34
HL-140	16.3	BLD	0.41	0.26
HL-141	90.1	329	0.37	0.45
HL-142	31.8	BLD	0.35	0.13
HL-143	37.9	BLD	0.31	0.21
HL-144	187	121	0.37	0.45
HL-145	17.2	BLD	0.32	0.11
HL-146	5.0	BLD	0.31	0.17
HL-147	86.2	65.6	0.42	0.34
HL-148	170	BLD	0.27	0.31
HL-149	151	BLD	0.34	0.32
HL-150	5.0	21.7	0.36	0.20
HL-151	13.2	BLD	0.29	0.19
HL-152	24.9	BLD	0.24	0.20
HL-153	52.8	BLD	0.22	0.15
HL-154	5.0	33.6	0.28	0.14
HL-155	16.0	BLD	0.33	0.15
HL-156	43.4	BLD	0.31	0.23
HL-157	165	BLD	0.37	0.39
HL-158	102	92.5	0.41	0.32
HL-159	11.4	BLD	0.37	0.17
HL-160	57.8	BLD	0.32	0.28
HL-161	24.5	BLD	0.25	0.12
HL-162	48.1	37.5	0.31	0.26
HL-163	106	129	0.47	0.35
HL-164	33.9	BLD	0.34	0.19
HL-166	144	BLD	0.33	0.31
HL-167	19.2	33.4	0.36	0.15

BLD = Below limit of detection

Table 3.2A. Midazolam hydroxylation velocities and 1'-OH/4-OH midazolam metabolic ratios at 0.5 μM midazolam.

	*Velocity**		
Liver #	*1'-OH*	*4-OH*	*1'-OH/4-OH Metabolic Ratio*
HL-102	148.5	19.3	7.7
HL-103	124.0	14.8	8.4
HL-104	197.6	14.9	13.3
HL-105	137.2	18.4	7.5
HL-106	364.0	40.0	9.1
HL-108	163.8	12.2	13.5
HL-109	140.5	17.0	8.3
HL-111	150.0	17.9	8.4
HL-112	126.3	13.1	9.7
HL-113	70.2	7.4	9.5
HL-114	146.1	15.4	9.5
HL-115	119.2	12.7	9.4
HL-118	73.8	9.4	7.9
HL-119	381.8	31.8	12.0
HL-120	136.1	15.6	8.7
HL-121	293.3	26.6	11.0
HL-124	268.8	27.8	9.7
HL-125	295.4	25.8	11.5
HL-126	68.2	8.6	7.9
HL-127	158.7	6.1	26.2
HL-128	49.6	4.9	10.1
HL-129	318.5	28.6	11.2
HL-130	54.6	6.3	8.7
HL-131	507.2	52.6	9.6
HL-132	60.6	6.1	9.9
HL-133	19.0	1.5	12.9
HL-134	279.5	31.4	8.9
HL-135	762.3	79.7	9.6
HL-136	44.3	4.9	9.1

*Velocity was measured as pmol/min/mg protein

Table 3.2A. (continued) Midazolam hydroxylation velocities and 1'-OH/4-OH midazolam metabolic ratios at 0.5 μM midazolam.

	*Velocity**		
Liver #	*1'-OH*	*4-OH*	*1'-OH/4-OH Metabolic Ratio*
HL-137	110.7	6.6	16.7
HL-138	147.4	14.3	10.3
HL-139	77.3	8.1	9.5
HL-140	47.5	4.8	9.9
HL-141	405.4	29.5	13.7
HL-142	96.7	9.9	9.7
HL-143	38.5	3.2	12.2
HL-144	338.0	32.7	10.3
HL-145	25.0	2.6	9.6
HL-146	25.0	1.4	17.5
HL-147	74.2	7.6	9.7
HL-148	167.5	18.7	9.0
HL-149	307.7	35.5	8.7
HL-151	28.7	2.7	10.8
HL-152	83.0	9.0	9.2
HL-153	162.0	15.8	10.3
HL-154	165.9	3.4	48.4
HL-155	73.2	6.5	11.3
HL-156	95.2	9.1	10.5
HL-157	470.4	45.5	10.3
HL-158	430.3	30.2	14.3
HL-159	74.5	5.7	13.0
HL-160	191.1	17.6	10.8
HL-161	105.7	8.7	12.1
HL-162	259.0	19.8	13.1
HL-163	594.6	49.3	12.1
HL-164	125.7	14.3	8.8
HL-165	104.6	11.7	9.0
HL-166	236.7	23.5	10.1
HL-167	125.5	6.0	21.0

*Velocity was measured as pmol/min/mg protein

Table 3.2B. Midazolam hydroxylation velocities and 1'-OH/4-OH midazolam metabolic ratios at 8 μM midazolam.

	*Velocity**		
Liver #	*1'-OH*	*4-OH*	*1'-OH/4-OH Metabolic Ratio*
HL-102	1001.6	192.7	5.2
HL-103	744.6	133.1	5.6
HL-104	1071.2	154.1	7.0
HL-105	800.2	167.4	4.8
HL-106	1936.8	350.9	5.5
HL-108	1130.7	139.0	8.1
HL-109	596.2	93.6	6.4
HL-111	782.7	155.1	5.1
HL-112	739.2	131.5	5.6
HL-113	509.6	92.4	5.5
HL-114	661.6	124.7	5.3
HL-115	679.3	130.0	5.2
HL-118	456.8	90.1	5.1
HL-119	2059.6	322.0	6.4
HL-120	657.8	131.2	5.0
HL-121	1318.8	227.5	5.8
HL-124	1328.4	256.7	5.2
HL-125	1893.5	294.1	6.4
HL-126	619.0	119.5	5.2
HL-127	1032.7	86.1	12.0
HL-128	310.2	49.2	6.3
HL-129	1804.3	341.6	5.3
HL-130	355.5	60.8	5.9
HL-131	2965.3	570.5	5.2
HL-132	877.2	150.6	5.8
HL-133	328.2	53.4	6.2
HL-134	3596.7	751.2	4.8
HL-135	3537.5	699.1	5.1
HL-136	246.3	39.5	6.2

*Velocity was measured as pmol/min/mg protein

Table 3.2B. (continued) Midazolam hydroxylation velocities and 1'-OH/4-OH midazolam metabolic ratios at 8 μM midazolam.

	*Velocity**		
Liver #	*1'-OH*	*4-OH*	*1'-OH/4-OH Metabolic Ratio*
HL-137	1049.0	115.2	9.1
HL-138	1027.0	188.4	5.5
HL-139	1284.1	238.1	5.4
HL-140	487.0	83.8	5.8
HL-141	7411.6	997.9	7.4
HL-142	664.6	123.3	5.4
HL-143	863.8	159.9	5.4
HL-144	4842.0	849.8	5.7
HL-145	578.4	102.7	5.6
HL-146	174.3	25.6	6.8
HL-147	2841.7	469.6	6.1
HL-148	1466.3	273.9	5.4
HL-149	2741.2	561.5	4.9
HL-150	504.6	40.0	12.6
HL-151	357.8	60.8	5.9
HL-152	537.8	105.1	5.1
HL-153	864.4	157.9	5.5
HL-154	881.9	65.1	13.5
HL-155	435.0	73.2	5.9
HL-156	747.5	145.2	5.2
HL-157	2885.6	581.7	5.0
HL-158	2699.4	415.4	6.5
HL-159	435.6	79.7	5.5
HL-160	1152.5	215.1	5.4
HL-161	644.2	116.1	5.6
HL-162	1904.9	313.8	6.1
HL-163	3614.5	571.1	6.3
HL-164	690.7	130.3	5.3
HL-165	800.3	136.6	5.9
HL-166	1586.5	322.7	4.9
HL-167	1047.0	108.7	10.0

*Velocity was measured as pmol/min/mg protein

Table 3.2C. Midazolam hydroxylation velocities and 1'-OH/4-OH midazolam metabolic ratios at 40 μM midazolam.

	*Velocity**		
Liver #	*1'-OH*	*4-OH*	*1'-OH/4-OH Metabolic Ratio*
HL-102	1534.8	446.5	2.6
HL-103	1374.4	354.5	2.8
HL-104	2057.3	475.5	3.5
HL-105	1533.5	453.2	2.5
HL-106	3276.1	1377.4	2.4
HL-108	1817.8	306.1	4.6
HL-109	1391.8	367.0	2.7
HL-111	1413.7	374.5	2.7
HL-112	1384.8	360.5	2.7
HL-113	1045.7	290.3	2.2
HL-114	1382.9	379.1	2.6
HL-115	1285.9	476.3	2.7
HL-118	612.0	316.5	1.9
HL-119	3649.1	1273.8	2.9
HL-120	857.2	290.3	3.0
HL-121	2757.5	672.5	4.1
HL-124	2832.4	856.2	3.3
HL-125	3463.6	891.4	3.9
HL-126	348.4	162.3	2.2
HL-127	1314.3	239.6	5.5
HL-128	326.5	172.3	1.9
HL-129	3058.8	938.8	3.3
HL-130	588.4	167.5	2.9
HL-131	5448.2	1232.6	4.4
HL-132	1414.0	430.8	3.3
HL-133	533.3	163.4	3.5
HL-134	6043.4	1406.4	4.3
HL-135	5505.0	1283.2	4.3
HL-136	526.3	181.0	3.3

*Velocity was measured as pmol/min/mg protein

Table 3.2C. (continued) Midazolam hydroxylation velocities and 1'-OH/4-OH midazolam metabolic ratios at 40 μM midazolam.

	*Velocity**		
Liver #	*1'-OH*	*4-OH*	*1'-OH/4-OH Metabolic Ratio*
HL-137	1710.5	350.7	4.9
HL-138	1799.4	546.7	3.3
HL-139	1566.4	471.2	3.3
HL-140	383.9	335.8	1.1
HL-141	4253.9	1063.0	4.0
HL-142	693.7	460.6	1.5
HL-143	784.8	547.4	1.4
HL-144	5177.8	1534.7	3.4
HL-145	501.3	378.3	1.3
HL-147	2406.8	909.7	2.7
HL-148	1608.6	822.4	2.0
HL-149	2354.8	1067.0	2.2
HL-150	647.1	248.3	2.6
HL-151	445.2	261.8	1.7
HL-152	735.8	450.1	1.6
HL-153	1173.9	591.4	2.0
HL-154	921.8	243.5	3.8
HL-155	529.6	292.2	1.8
HL-156	898.3	504.6	1.8
HL-157	2752.5	1172.6	2.4
HL-158	3001.2	1052.1	2.9
HL-159	463.7	298.3	1.6
HL-160	1250.1	614.0	2.0
HL-161	896.1	493.2	1.8
HL-162	1988.1	863.5	2.3
HL-163	3580.5	1177.0	3.0
HL-164	834.9	499.1	1.7
HL-165	1026.7	576.5	1.8
HL-166	1563.7	819.0	1.9
HL-167	1182.4	372.7	3.2

*Velocity was measured as pmol/min/mg protein

Table 3.3. Midazolam metabolic ratios in cDNA-expressed CYP3A4 and CYP3A5.

Enzyme Composition		*1'-OH/4-OH Midazolam Ratio*		
CYP3A4 (%)	*CYP3A5 (%)*	*0.5 μM MDZ*	*8 μM MDZ*	*40 μM MDZ*
100	0	10.6	3.9	1.8
75	25	9.9	4.5	2.1
50	50	12.4	5.1	2.2
25	75	13.9	6.4	3.3
0	100	26.5	8.0	4.7

Incubations contained 10 pmol total CYP3A enzyme per incubation tube plus an additional 30 pmol cytochrome b_5.

Table 3.4. Mean 1'-OH/4-OH midazolam metabolic ratios in human liver microsomes at differing concentrations of midazolam.

	1'-OH/4-OH Metabolic Ratio		
HL Microsomes	*0.5 μM MDZ*	*8 μM MDZ*	*40 μM MDZ*
CYP3A4 only (n = 43)	9.8 ± 1.8*	5.5 ± 0.5†	2.5 ± 0.8†
CYP3A4 + CYP3A5 (n = 17)	16.5 ± 9.8	7.9 ± 2.6	3.5 ± 1.0
Total Livers (n = 60)	11.5 ± 5.8	6.2 ± 1.8	2.8 ± 1.0

Values are expressed as the mean metabolic ratio ± s.d.

* $p < 0.05$ for comparison between the two groups of microsomes.

† $p < 0.005$ for comparison between the two groups of microsomes.

Table 3.5. Correlation coefficients (r^2) for 1'-OH and 4-OH midazolam turnover velocities versus CYP3A4 and CYP3A5 content at differing concentrations of midazolam.

	1'-OH Velocity (pmol/min/mg)			*4-OH Velocity (pmol/min/mg)*		
(pmol/mg)	*0.5 μM*	*8 μM*	*40 μM*	*0.5 μM*	*8 μM*	*40 μM*
CYP3A4	0.677	0.635	0.750	0.754	0.751	0.707
CYP3A5	0.586	0.787	0.442	0.453	0.680	0.342
Total CYP3A	0.742	0.742	0.806	0.663	0.724	0.735

CHAPTER 4

DIFFERENCES IN THE INHIBITION OF CYTOCHROMES P450 3A4 AND 3A5 BY METABOLITE-INHIBITOR COMPLEX FORMING DRUGS

The data and content of Chapter 4 have been submitted

to

Drug Metabolism and Disposition

4.1 Introduction to Chapter 4

Although CYP3A4 and CYP3A5 share 84% amino acid sequence, the two isoforms behave differently with respect to substrate turnover and susceptibility to inhibition. Information addressing the impact of CYP3A5 expression and its importance to *in vivo* drug metabolism is limited. Although hepatic and intestinal expression of CYP3A5 has been recognized for many years, CYP3A5 has generally been considered less important than CYP3A4 because of its polymorphic and relatively low level of hepatic and intestinal expression. However, recent reports indicate that a majority of individuals express some CYP3A5 protein (Jounäidi et al, 1996), and that it can be found at relatively high levels in individuals with a heterozygous or homozygous *CYP3A5*1* genotype (Kuehl et al, 2001). Moreover, the frequency of polymorphic CYP3A5 expression differs among ethnic groups. For example, hepatic CYP3A5 is found at high levels in only 33% of Caucasians but >50% of African-Americans (Kuehl et al, 2001). Thus, CYP3A5 expression may play a major role in determining interindividual and interracial variability with respect to metabolic drug elimination.

CYP3A4 and CYP3A5 exhibit similar K_m and V_{max} values for midazolam 1'-hydroxylation (Gibbs et al, 1999; Gorski et al, 1995). In addition, both enzymes appear similarly efficient at metabolizing nifedipine (Aoyama, 1989; Gillam, 1995), lidocaine (Bargetzi et al, 1989) etoposide (Relling et al, 1994) and dextromethorphan (Gorski et al, 1994). In contrast, significant differences in the turnover of other CYP3A4/5 substrates have been described, including testosterone (Waxman et al,

1991; Wrighton et al, 1989), progesterone (Waxman et al, 1991; Aoyama et al, 1989), cyclosporine (Aoyama et al, 1989; Fisher et al, 1998), valspodar (Fischer et al, 1998) and erythromycin (Gillam et al, 1995).

There have been only a few studies comparing the inhibition kinetics for CYP3A4 and CYP3A5, but when studied, differences in inhibition potency were reported. For example, both ketoconazole and fluconazole are more potent inhibitors of CYP3A4 than of CYP3A5 (Gibbs et al, 1999). Also, studies with diltiazem revealed a lower amount of MI-complex formation, higher partition ratio (k_{cat}/k_{inact}) and a lower *N*-demethylation rate for CYP3A5, compared to CYP3A4 (Jones et al, 1999).

Mechanism-based inactivation is not uncommon for CYP3A substrates that contain an amine functional group and undergo *N*-dealkylation (Pershing and Franklin, 1982; Bensoussan et al, 1995). The process by which amine-containing compounds inactivate CYP3A is presumed to involve four consecutive CYP3A-dependent oxidations at the amine nitrogen, eventually forming a nitroso compound that binds tightly to the ferrous heme iron (Ortiz de Montellano, 1995). Erythromycin, diltiazem and nicardipine have been shown to form CYP3A4 MI-complexes *in vitro* (Periti et al, 1995; Jones et al, 1999; Ma et al, 2000), and thus have the potential ability to inhibit the enzyme in a reversible manner or by mechanism-based inactivation. Moreover, Sutton et al, (1997) showed that the two successively *N*-demethylated diltiazem metabolites were more potent inhibitors of CYP3A4 than the parent molecule. Accordingly, *N*-desmethyl-erythromycin (*N*-des-ERY), the major CYP3A-dependent metabolite of erythromycin, would be likely to inhibit CYP3A4 as well. Since

erythromycin can inhibit CYP3A4 by either reversible or mechanism-based processes, perhaps *N*-desmethyl-erythromycin can inhibit in a similar fashion. Thus, accumulation of inhibitory erythromycin metabolites may contribute to reversible enzyme inhibition *in vivo*.

The goal of this study was to compare the effects of erythromycin, *N*-desmethyl-erythromycin, diltiazem and nicardipine on CYP3A4 and CYP3A5 catalyzed midazolam hydroxylation, and to determine whether there is a difference in the binding affinity or inactivation kinetics. Inhibitory effects of the potent but reversible CYP3A ligand, ketoconazole, were also studied for comparison to the putative mechanism-based inhibitors.

4.2 Materials and Methods

4.2.1 Reagents

NADPH, erythromycin, diltiazem, nicardipine, troleandomycin and alkaline phosphatase conjugated secondary antibodies were obtained from Sigma Chemical Company (St. Louis, MO). Ketoconazole was obtained from Research Diagnostics, Inc. (Flanders, NJ). Midazolam, 1'-OH midazolam, 4-OH midazolam and $^{15}N_3$-midazolam were kindly provided by Roche Laboratories (Nutley, NJ). $^{15}N_3$ –labeled 1'-OH and 4-OH midazolam were generated enzymatically from $^{15}N_3$-midazolam as described (Paine et al, 1997a). *N*-desmethyl-erythromycin was a gift from Jason Boer (UW Medicinal Chemistry, Seattle, WA). Acetonitrile and ethyl acetate were

purchased from Fisher Scientific (Santa Clara, CA). *N*-methyl-*N*-(*t*-butyl-dimethylsilyl) trifluoroacetimide (MTBSTFA) was obtained from Pierce Chemical (Rockford, IL). cDNA-expressed CYP3A4 (P207), CYP3A5 (P235) and a CYP3A5-selective antibody (A235) were purchased from Gentest Corporation (Woburn, MA). Cytochrome b_5 was purchased from Panvera Corporation (Madison, WI). SDS-polyacrylamide gel electrophoresis reagents (37.5:1 bis-acrylamide, ammonium persulfate and *N,N,N',N'*-tetra-methyl-ethylene-diamine) were purchased from Bio-Rad Laboratories (Hercules, CA). Nitrocellulose was purchased from Schliecher and Schuell (Keene, NH). BCIP/NBT reagents were purchased from Kirkegaard and Perry (Gaithersburg, MD). All other reagents were reagent grade or better.

4.2.2 Tissue Collection and Microsomal Preparation

Human livers were obtained through the Solid Organ Transplant Program at the University of Washington Medical Center and LifeCenter Northwest (Seattle, WA). Liver microsomes were prepared as described elsewhere (Paine et al, 1997b), and stored at –80 °C until analysis. Protein concentrations were determined by the method of Lowry et al, (1951). All experiments with cDNA-expressed enzymes were supplemented with a 3:1 molar ratio of cytochrome b_5 to enzyme.

4.2.3 CYP3A4 and CYP3A5 Western Blot Analysis

Human livers used in the following experiments were selected based on the relative abundance of CYP3A4 and CYP3A5. Immunoquantitation of CYP3A4 and CYP3A5 content in the human microsomal preparations was performed as described previously (Kuehl et al, 2001). Purified human liver CYP3A4 and purified cDNA-expressed CYP3A5 were used as reference standards to quantitate both enzymes. Integrated optical density measurements were obtained from a BioRad ChemiDoc system and Quantity One Software (Hercules, CA).

4.2.4 Kinetic Protocols for IC_{50} and Reversible K_i Measurements

These experiments determined the effect of various concentrations of inhibitor on the formation of 1'- and 4-OH midazolam. Incubations were conducted in solutions containing 1 mM EDTA and 100 mM potassium phosphate (KPi) buffer at pH = 7.4 in a final volume of 0.5 ml. All incubations were performed in triplicate. Ketoconazole and erythromycin solutions were prepared in acetone and after addition to the reaction vessel; the solvent (50 µl) was allowed to evaporate prior to the addition of any other reagents. Nicardipine was dissolved in dimethyl sulfoxide (DMSO); the final concentration of solvent never exceeded 1%. Midazolam and diltiazem were dissolved in KPi buffer.

Substrate, inhibitor, buffer and CYP3A enzyme (50 μg protein for microsomes, or 10 pmol expressed enzyme) were pre-incubated for 5 minutes at 37°C prior to the addition of NADPH (1 mM final concentration). After four minutes, reactions were terminated with the addition of 1 ml of 100 mM Na_2CO_3, pH ~11. Internal standards ($^{15}N_3$-1'- and $^{15}N_3$-4-OH midazolam solution) were added to all tubes, followed by extraction with 5 ml of ethyl acetate. Standard curves were prepared with known amounts of 1'- and 4-OH midazolam. Both 1'- and 4-OH midazolam were measured by gas chromatography-negative chemical ionization mass spectrometry as described previously (Paine et al, 1996). The ions monitored for 1'-OH midazolam were *m/z* = 455 and 460 for the *t*-butyl-dimethylsilyl derivitized compound and the ^{37}Cl isotope for the $^{15}N_3$-labeled metabolite, respectively. The ions for 4-OH midazolam were *m/z* = 323 and 328, representing a loss of water from 4-OH midazolam (MW = 341) and the ^{37}Cl signal for the $^{15}N_3$-labeled metabolite, respectively.

Ketoconazole concentrations ranged from 0.005 – 0.25 μM for co-incubation inhibition experiments. The concentrations of erythromycin used for co-incubation inhibition experiments were between 10 – 500 μM for human liver microsomal experiments, and from 2 - 150 μM for cDNA-expressed enzyme experiments. The diltiazem concentration range for human liver microsomes and cDNA-expressed enzymes varied from 0.5 – 100 μM and from 20 – 1000 μM, respectively. Nicardipine concentrations varied from 0.005 – 1 μM for cDNA-expressed enzymes and from 0.05 – 10 μM for human liver microsomes. Midazolam concentrations were 4 μM (IC_{50} experiments) or varied between 2 and 16 μM (K_i experiments).

4.2.5 Kinetic Protocols for Irreversible k_{inact} and $K_{I(app)}$ Measurements

Experiments were conducted to determine the effect of various concentrations of inhibitor and pre-incubation times on the formation of 1'- and 4-OH midazolam. Incubations were performed in solutions of 100 mM KPi, pH = 7.4, and 1 mM EDTA. To assess time- and concentration-dependent inhibition, a 5 x 5 matrix of inhibitor concentration and NADPH-dependent incubation time was implemented for each inhibitor. Briefly, 180 µl of a solution containing enzyme (200 pmol cDNA-expressed CYP3A4 or CYP3A5 supplemented with 600 pmol cytochrome b_5, or 1 mg human liver microsomal protein), inhibitor, EDTA and buffer were pre-incubated at 37 °C for 5 minutes prior to the addition of 20 µl of 10 mM NADPH (200 µl total volume). The concentrations of erythromycin and *N*-desmethyl-erythromycin (prepared in acetone) used for inactivation experiments were between 2 – 100 µM for microsomal experiments, and from 2 - 50 µM in cDNA-expressed enzymes. The diltiazem and nicardipine concentrations ranged from 0.5 – 100 µM and from 0.2 – 10 µM for microsomes and cDNA-expressed enzymes, respectively.

Following the addition of NADPH, 25 µl aliquots were transferred to pre-warmed tubes containing 475 µl of 1 mM EDTA, 100 mM KPi buffer, 1 mM NADPH and 8 µM MDZ (all final concentrations) at time intervals of 0, 1, 6, 12 and 25 minutes. A higher concentration of midazolam (8 µM vs. 4 µM) was used to displace residual inhibitor that was present in the 25 µl transfer volume. After a four-minute incubation

with midazolam, the reactions were terminated with 100 mM Na_2CO_3, pH ~11. Addition of internal standard and work-up of incubation samples was as described in the previous section (4.2.4).

4.2.6 Determination of Kinetic Parameters

For ketoconazole, the inhibition mechanism was determined by graphical analysis using Dixon and Lineweaver-Burk plots. Inhibition constant (K_i) estimates were obtained by fitting to either competitive or non-competitive models (Segel, 1975) using SAAM II statistical software (Seattle, WA). For all inhibitors co-incubated with midazolam, concentrations of inhibitor required for half-maximal substrate turnover (apparent IC_{50}) were determined based on a one-enzyme Michaelis-Menten model (Kaleidagraph; Synergy Software).

For time-dependent enzyme inactivation, the pseudo first-order rate constant for enzyme inactivation (λ) was estimated from Equation 1.

$$E_{(t)} = E_0 \cdot e^{-\lambda t} \qquad [4.1]$$

$E_{(t)}$ is the percent of active enzyme remaining at time t, and E_0 was set at 100%. The pseudo first-order rate constant (λ) was estimated from the slope at t = 1–12 minutes (See Figure 4.1, for example). To determine inactivation kinetic constants ($K_{I(app)}$ and k_{inact}), λ and inhibitor concentration [I] were fitted to Equation 2.

$$\lambda = k_{inact} \cdot [I] / (K_{I(app)} + [I]) \qquad [4.2]$$

where k_{inact} represents the constant for the maximal rate of enzyme inactivation and $K_{I(app)}$ is the concentration of inactivator that produces half-maximal rate of inactivation (Silverman, 1988). A kinetic representation of metabolic inactivation is given in Scheme 4.1.

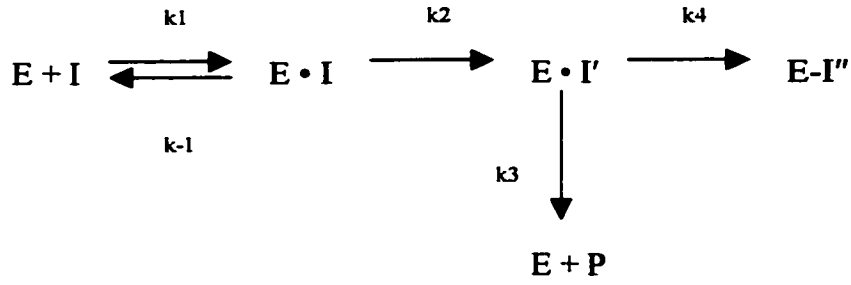

[Scheme 4.1]

In Scheme 4.1 the initial step describes enzyme (E) and inhibitor (I) binding, with respective on- and off-rate constants k_1 and k_{-1}, respectively. The second step describes the catalytic event (k_2) that produces the inhibitory metabolite. Once the metabolite is formed, it can be released as product (k_3) or can inactivate the enzyme (k_4). This scheme is clearly an oversimplification of the events that occur during the conversion of a dialkyl-substituted amine to a nitroso-like MI-complex, since 4 successive oxidations must occur in the process. This will be discussed further with the interpretation of experimental results.

4.2.7 K_S Binding Determinations

To determine absolute binding differences between CYP3A isoforms, K_S values were determined from difference spectra for expressed and human liver microsomal

systems. Human liver microsomes containing no immunodetectable CYP3A5 or >85% of total CYP3A as CYP3A5 were suspended in 50 mM Tris-HCl, 1 mM EDTA, pH = 7.4 to a concentration of 1 mg/ml total protein (expressed isoforms were diluted to 200 pmol/ml CYP3A). The solution (1 ml) was equally divided between sample and reference cuvettes and a baseline was recorded. Aliquots (1 – 16 μl) of an erythromycin or *N*-desmethyl erythromycin solution were added to the sample cuvette, whereas the reference cuvette received an equal volume of vehicle (acetone). After 3 min the difference spectra were recorded between 350 and 520 nm (Cary 9E double beam UV/VIS Spectrometer, Varian Corporation). Measurements were carried out at 25 °C. A concentration range of 0 – 223 μM was examined for both substrates. No measurements were performed with nicardipine or diltiazem due to UV instability of the compounds.

4.2.8 Metabolite-Intermediate Complex (MIC) Formation

MIC formation was determined for cDNA-expressed CYP3A4 and CYP3A5, as well as for human liver microsomes. MIC formation was characterized by difference spectroscopy (Cary 9E double beam UV/VIS Spectrometer, Varian Corporation) over a wavelength range of 390-500 nm. Formation of an MIC was evident by the appearance of a peak absorbing at λ = ~452 nm (Bensoussan et al, 1995), and was quantitated from absorbance difference spectra (λ_{490} - λ_{452}). Sample cuvettes contained 1 mg microsomal protein (HL microsomes) or 200 pmol CYP3A (cDNA-expressed

enzyme), NADPH (1 mM final concentration) and inhibitor [erythromycin, 50 μM; *N*-desmethyl erythromycin, 50 μM; diltiazem, 50 μM; nicardipine, 5 μM; troleandomycin, 20 μM], whereas reference cuvettes contained identical contents except inhibitor was replaced with the appropriate vehicle solvent. Reactions containing expressed enzymes were supplemented with 600 pmol cytochrome b_5. Reactions were initiated by addition of NADPH, and were conducted for 30 minutes at 37 °C. For one set of experiments, erythromycin (50 μM) was incubated with CYP3A4, CYP3A5 and cytochrome b_5, in molar ratio of 200:200:1200, and the resulting difference spectra was compared to that produced from an incubation of erythromycin (50 μM) and 200:600 CYP3A4 and cytochrome b_5 alone.

4.3 Results

Apparent IC_{50} values were calculated for ketoconazole, diltiazem, erythromycin and nicardipine in populations of human liver microsomes that were classified as positive (readily detectable band by Western blot) or negative (no detectable band) for CYP3A5.

The mean IC_{50} values are shown in Table 4.1. Ketoconazole was the most potent inhibitor of liver microsomal midazolam 1'-hydroxylation, followed by nicardipine, erythromycin and diltiazem. Compared to CYP3A5-negative microsomes, the mean IC_{50} value was significantly higher ($p < 0.05$) for CYP3A5-containing microsomes and all inhibitors except diltiazem, where no statistical difference was

observed. Using midazolam 4-hydroxylation as a marker reaction gave similar results for the IC_{50} experiments. Since midazolam 4-hydroxylation provided no additional inhibitory or mechanistic insight, only data for 1'-hydroxylation are reported.

IC_{50} experiments were also conducted for cDNA-expressed CYP3A4 and CYP3A5 microsomes supplemented with a 3:1 molar ratio of cytochrome b_5. Compared to CYP3A4, the apparent potency of CYP3A5 inhibition was lower for ketoconazole (5.8-fold higher IC_{50}, $p < 0.05$), erythromycin (1.9-fold higher IC_{50}, $p < 0.05$), and diltiazem (1.9-fold higher IC_{50}, N.S.). In contrast, the apparent IC_{50} for CYP3A4 and CYP3A5 was comparable for nicardipine. However, it was noted that the apparent IC_{50} value for nicardipine and cDNA-expressed enzymes was approximately 15-fold lower than the value generated for liver microsomes (e.g., 24.5 $\pm$ 4.3 nM *vs.* 363 $\pm$ 21 nM for CYP3A4). This observation may reflect a difference in a non-specific binding effect between human liver microsomes and insect cell microsomes expressing CYP3A. However, this binding difference should not impact the comparison between the two CYP3A isoforms.

Irreversible inhibition of CYP3A4 and CYP3A5 was also examined in human liver microsomes and expressed enzyme systems. Three human liver microsomal preparations that contained only CYP3A4 (HL-114, HL-155, HL-166), and the three microsomal samples with the highest molar abundance of CYP3A5 [HL-127 (86% CYP3A5), HL-154 (95% CYP3A5), HL-167 (89% CYP3A5)] were pre-incubated with erythromycin, diltiazem and nicardipine in the presence of NADPH for varying amounts of time. Data were fit to equations 4.1 and 4.2 (Figure 4.2) to determine

inactivation kinetic parameters. The parameters obtained from the inactivation experiments are shown in Tables 4.2 and 4.3. In contrast to the reversible IC_{50} data, no difference was observed between the model-fitted $K_{I(app)}$ value for erythromycin in microsomes expressing only CYP3A4, compared to those dominated by CYP3A5 expression. However, insufficient time-dependent inactivation with diltiazem and nicardipine in CYP3A5-containing microsomes rendered the k_{inact} values below the limit of detection, which made $K_{I(app)}$ estimates unavailable.

No such complications were observed for cDNA-expressed $K_{I(app)}$ experiments. $K_{I(app)}$ estimates were calculated for each of the four inhibitors and both expressed isoforms. $K_{I(app)}$ values for erythromycin and nicardipine were not different between the two expressed isoforms, which was similar to human liver microsomal data (Table 4.2). The $K_{I(app)}$ for erythromycin and CYP3A4-dominated and CYP3A5-dominated human microsomal samples was not significantly different from each other ($p > 0.05$). In contrast, the $K_{I(app)}$ for diltiazem and expressed CYP3A4 was lower than that obtained for CYP3A5 (1.23 μM vs 8.70 μM, respectively).

Inactivation experiments demonstrated significant differences in the rate of CYP3A4 and CYP3A5 inactivation (k_{inact}) for all inhibitors studied. The k_{inact} values for erythromycin was $\geq$ 2.5-fold lower for both CYP3A5-containing microsomes and for expressed CYP3A5, compared to the respective expressed CYP3A4 and CYP3A4-dominated liver microsomes (Table 4.3). No k_{inact} parameters for diltiazem or nicardipine were obtained for CYP3A5-dominated microsomes because of the failure

of the drugs to inhibit the enzyme, but the lack of enzyme inactivation clearly suggests that both inhibitors inactivate CYP3A5 at a much slower rate than CYP3A4.

Additional experiments were conducted to directly compare time-dependent loss of metabolic activity in a sample (n = 4) of human liver microsomes expressing either high levels of CYP3A5 or non-detectable CYP3A5. These experiments were similar to the previous time-dependent experiments, except that inhibition was examined at t = 0 and 30 minutes. The decline in activity from t = 0-30 minutes was assessed for erythromycin (50 μM) and a prototypical mechanism-based inhibitor, troleandomycin (20 μM). Figure 4.5 shows the comparative loss of enzyme activity in both panels of microsomes. In the two sets of human liver microsomes, approximately 1/3 additional CYP3A4 was inactivated by both troleandomycin and erythromycin compared to CYP3A5.

We also examined the effect of the primary erythromycin metabolite, *N*-desmethyl erythromycin, on CYP3A4 and CYP3A5-catalyzed midazolam hydroxylation. In contrast to results obtained with erythromycin, the metabolite exhibited a higher affinity for expressed CYP3A4 than for CYP3A5 ($K_{I(app)}$ = 2.79 μM *vs.* 7.98 μM, respectively) (Table 4.2). Moreover, the k_{inact} for expressed CYP3A4 was 5.4-fold higher than the value obtained for CYP3A5 (0.062 ± 0.002 *vs.* 0.012 ± 0.001 min^{-1}, respectively; $P < 0.05$) (Table 4.3). Similarly significant differences in the k_{inact} and $K_{I(app)}$ was observed for CYP3A4-dominated liver microsomes, compared to CYP3A5-dominated microsomes (Tables 4.2 and 4.3).

Additional experiments were performed to elucidate any enzyme-substrate binding differences independent of interferences that may be present during incubation. Addition of erythromycin or *N*-desmethyl erythromycin to cDNA-expressed CYP3A4 or human liver microsomes containing predominantly CYP3A4 led to the appearance of a difference spectrum characterized by a peak at 390 nm and a trough at 420 nm (Figure 4.6), which is typical of P450-Fe(III) complexes in which H_2O is displaced from the sixth ligand site (Type I). The apparent spectral dissociation constant, K_S, which was calculated from the increase in spectral intensity as a function of erythromycin concentration, was found to be 26.7 ± 5.5 μM and 49.4 ± 12.9 μM for cDNA-expressed CYP3A4 and human liver microsomes, respectively (Table 4.4). K_S values for *N*-desmethyl erythromycin were 70.5 ± 17 μM and 17.1 ± 8.7 μM for cDNA-expressed CYP3A4 and human liver microsomes, respectively. These values are slightly higher that $K_{I(app)}$ values previously reported (Table 4.2). For the expressed enzyme, erythromycin exhibited a higher affinity for CYP3A4 compared to its metabolite, but the opposite was true in microsomes. Therefore, no conclusion can be made regarding affinity differences between erythromycin species. Table 4.5 summarizes all three affinity measurements (IC_{50}, $K_{I(app)}$ and K_S) for erythromycin, diltiazem and nicardipine in the cDNA expressed microsomes.

Although binding experiments were performed in cDNA-expressed CYP3A5 and human liver microsomes expressing a majority of CYP3A5, no binding spectra were observed for erythromycin or *N*-desmethyl erythromycin at concentrations up to 223 μM. Since erythromycin can be metabolized by CYP3A5, a binding event must

occur. However, it is possible that the binding event that allows metabolism to occur, albeit at a slower rate, does not produce a visible binding spectrum (i.e. does not displace the sixth Fe^{+3} ligand). It is also possible that CYP3A5 heme in the correct iron oxidation state (Fe^{+3}) required for binding spectra is at levels that are too low to detect by our methods. It is also possible that the solvent (acetone) may bind preferentially, since no reducing equivalents are present.

To investigate the possible mechanistic differences between the inactivation of CYP3A4 and CYP3A5, spectral analyses were performed with human liver microsomes and expressed isoforms. MIC formation was used as the surrogate marker for inactivation. Microsomes or expressed enzymes were incubated with each inhibitor, and time- and concentration-dependent MI-Complex formation was measured by the absorbance difference between 452 nm and 490 nm. We were unable to detect MI-complex formation between 452-455 nm for expressed and microsomal CYP3A5 and erythromycin, *N*-desmethyl-erythromycin or diltiazem (Figure 4.3). In contrast, representative CYP3A4 spectra for all inhibitors show clear absorbances in that region typical of an MI-Complex (Figure 4.3). Only nicardipine gave a small MI-complex peak for CYP3A5-containing samples, but it was minimal compared to CYP3A4.

To test the hypothesis that CYP3A5 is deficient at generating reactive inhibitory metabolites, but capable of forming an MI-Complex, we conducted experiments where 50 μM erythromycin was co-incubated with either CYP3A5 + CYP3A4 + cytochrome b_5 (200:200:1200) or CYP3A4 + cytochrome b_5 alone

(200:600) alone. Although an erythromycin-dependent MI-Complex was non-detectable with CYP3A5 (Figure 4.3), the absorbance difference ($\lambda_{452-490}$ nm) produced from the CYP3A5:CYP3A4 co-incubation was 21% greater than that observed from an incubation of inhibitor with CYP3A4 alone (Figure 4.4).

4.4 Discussion

4.4.1 CYP3A4 and CYP3A5 Inhibition Kinetics

There were major differences between the interactions of known P450 inhibitors with CYP3A4 and CYP3A5. In general, the catalysis of midazolam 1'-hydroxylation was less susceptible to the inhibitory effects of erythromycin, diltiazem and nicardipine. These findings are in agreement with our previous results demonstrating higher K_i values for the inhibition of CYP3A5, compared to CYP3A4, by ketoconazole and fluconazole (Gibbs, 1998). A difference in IC_{50} for CYP3A4 and CYP3A5 was observed for all inhibitors except diltiazem when compared in human liver microsomes (Table 4.1). These data suggest that there is a difference in the binding affinity of inhibitor for the enzymes (ketoconazole, erythromycin and nicardipine) or irreversible inactivation kinetics (erythromycin, *N*-desmethyl-erythromycin, diltiazem and nicardipine) or both. These findings point towards active site residue differences, as well as potential alterations in allosteric binding pockets.

Although the IC_{50} results for expressed enzymes were not identical to that obtained with liver microsomes, the relationships between CYP3A4 and CYP3A5 did not change for the four inhibitors tested. The IC_{50} results for expressed enzymes were within 2-3 fold of the microsomal results for three inhibitors with nicardipine being the exception. The nicardipine IC_{50} results were ~15 fold lower in expressed enzymes compared to microsomes. Nicardipine has been shown to inhibit other P450 enzymes besides CYP3A (Katoh et al, 2000). It is possible that nicardipine has a high affinity for CYP3A4 and CYP3A5, but can be metabolized by other CYP isoforms, thus lowering the actual concentration of nicardipine available to inhibit CYP3A. Nicardipine undergoes CYP3A-dependent *N*-debenzylation and *N*-demethylation, but also can be sequentially hydrolyzed to a carboxylic acid metabolite. These metabolites may also undergo CYP oxidation by isoforms other than CYP3A. It is possible that these competing pathways effectively reduce the amount of nicardipine in the system. It is also possible that a high degree of non-specific binding to the microsomes exists for nicardipine. Felodipine, a calcium-channel blocker with similar structural characteristics, has been shown to exhibit high non-specific binding (>93%) in microsomal systems (Bäärnhielm et al, 1986).

Theoretically, the IC_{50} estimates obtained in reversible inhibition experiments should be similar to the $K_{I(app)}$ from time-dependent data if there is little inactivation during the reversible experiment, if the formation rate of the reactive metabolite is rate-limiting in the time-dependent reaction, and substrate concentration is equal to K_m. For non-competitive inhibitors like ketoconazole, the IC_{50} equals the $K_{I(app)}$ (Gibbs *et al*,

1999). Competitive inhibitors like diltiazem, erythromycin and nicardipine would theoretically have IC_{50} values equal to twice the $K_{I(app)}$, given that substrate concentration was equal to K_m (Segel, 1975). However, these inhibitors can also inhibit by MI-Complex formation, even over a short 4-minute co-incubation interval. Thus, the differences in IC_{50} values may simply reflect the difference in MIC formation, which was demonstrated from spectral experiments.

The IC_{50} value is not derived from a kinetic model nor does it imply an inhibitory mechanism, whereas the $K_{I(app)}$ is obtained by examining the effect of inhibitor concentration on rate of inactivation (Silverman, 1988). In the inactivation kinetics experiments the $K_{I(app)}$ is equal to $[(k_{-1} + k_2)/k_1][(k_3 + k_4)/(k_2 + k_3 + k_4)]$ (Scheme 4.1). It is clear that the $K_{I(app)}$ not only depends on the behavior of the E·S complex, but also on the rate of release of product (k_3) and on the rate of enzyme inactivation (k_4). If k_2 is rate-limiting in the time-dependent experiments, the $K_{I(app)}$ expression reduces to the identical expression for a reversible K_i. If the release rate of product from the active site (k_4) or the rate of inactivation by the activated inhibitor (k_3) are at least partially rate-limiting, then $K_{I(app)}$ will be greater than K_i. It is important to note that the above scheme is simplified to a single k_2 term, whereas all three mechanism-based inhibitors employed in this study undergo at least 4 consecutive oxidations (k_2, k_2', k_2'', k_2''', etc.) before inactivation occurs, thus further complicating the estimates. The k_2 in Scheme 4.1 represents the slowest of all inactivation steps.

A different picture emerged from time-dependent experiments to determine the $K_{I(app)}$ and k_{inact} values (Table 4.2). $K_{I(app)}$ and k_{inact} parameters were very difficult to

measure in the CYP3A5 human liver microsomes, due to limited time- and concentration-dependent inactivation. Indeed, for nicardipine and diltiazem, we were unable to generate parameters. Erythromycin and *N*-desmethyl-erythromycin were the only inhibitors where CYP3A5 microsomal parameters could be estimated.

$K_{I(app)}$ values for erythromycin were obtained from 2 out of 3 CYP3A5-containing human livers, but *N*-desmethyl-erythromycin estimates came from only one CYP3A5-containing liver due to aforementioned model fitting difficulties. For the livers where estimates were available, the standard deviation (or standard error) measurements for $K_{I(app)}$ were quite large, thus preventing the determination of a difference between CYP3A4 and CYP3A5 (Table 4.2). However, one can assume empirically that a large difference in either $K_{I(app)}$, k_{inact} or both existed. Inactivation parameters $K_{I(app)}$ and k_{inact} were available for all four inhibitors using the expressed enzyme systems. Diltiazem and nicardipine showed higher affinity ($K_{I(app)}$) for expressed CYP3A4 compared to expressed CYP3A5, and erythromycin showed no quantitative difference between the two isoforms. Taken together, the microsomal and cDNA-expressed enzyme data strongly suggest that the principal difference between CYP3A4 and CYP3A5 is the reduced ability of CYP3A5 to generate inhibitory metabolites or to form an inhibitory MI-complex from the bioactivated metabolites.

Results from the spectral inactivation experiments further suggest that CYP3A5 is not efficient at forming an MI-Complex from erythromycin, diltiazem or nicardipine. It is possible that CYP3A5 cannot form the demethylated metabolite, the terminal *N*-oxide metabolite responsible for the complex, or that the terminal metabolite cannot

bind productively to the CYP3A5 heme. Indeed, neither erythromycin nor *N*-desmethyl erythromycin binds to CYP3A5 in a way that elicits a Type I or Type II spectrum. This suggests a favored active site orientation that is displaced from the sixth heme ligand.

Unpublished data from our lab reveal a 3-4 fold difference in erythromycin *N*-demethylation between expressed CYP3A4 and CYP3A5. At an erythromycin concentration of 1 mM, the formation rate of *N*-desmethyl erythromycin was 2.0 nmol/min/nmol CYP3A4 and 0.6 nmol/min/nmol CYP3A5. Data from time-dependency experiments showed that inactivation did occur for expressed CYP3A5, but that it occurred at a much slower rate than that observed for CYP3A4. However, it is unclear whether inhibition of CYP3A5 occurs by MI-Complex formation, since no MI-complex spectra could be discerned. To address this question, equal amounts of CYP3A4 and CYP3A5 were incubated with erythromycin and the MIC was measured (Figure 4.3). Since no detectable complex was formed with CYP3A5 alone, the increase observed with co-incubation suggests that CYP3A5 can be inactivated as well, but may not be able to generate the inhibitory metabolites in high enough concentrations without aid from CYP3A4. It also suggests that the secondary or tertiary metabolites of erythromycin leave the active site prior to further oxidation and formation of an MI-complex. Apparently, CYP3A4 may generate high enough concentrations of erythromycin metabolites to inactivate itself, in addition to CYP3A5 when time and substrate availability are not constrained.

If CYP3A5 cannot produce significant concentrations of the inhibitory metabolites, it is possible that CYP3A5 would be more resistant to mechanism-based inactivation in individuals who carry at least one *CYP3A5*1* allele and are relatively deficient in CYP3A4 expression. To determine if any catalytic differences exist in the first demethylation reaction, *N*-desmethyl-erythromycin inactivation data were employed. For both CYP3A4 and CYP3A5-containing microsomes, no statistical difference ($p > 0.05$) in inactivation rate was observed between ERY and N-des-ERY (CYP3A4 mics k_{inact} = 0.046 vs. 0.052 min^{-1} for ERY and *N*-des-ERY; CYP3A5 mics k_{inact} = 0.015 vs. 0.014 for ERY and *N*-des-ERY, respectively). For expressed CYP3A5, data were similar for erythromycin and *N*-desmethyl-erythromycin (k_{inact} = 0.0113 vs. 0.0115 min^{-1}), and the expressed CYP3A4 showed slightly faster inactivation for the *N*-desmethyl metabolite (k_{inact} = 0.062 vs 0.042) compared to parent erythromycin.

Since the inactivation rates were not different for ERY and *N*-des-ERY regardless of isoform, it suggests that the first demethylation reaction is not rate limiting in the inactivation of either CYP3A isoform; the rate-limiting step (k_{inact}) is merely slower for CYP3A5 (Figure 4.5). Further evidence that the first demethylation is not the key reaction to the isoform-specific difference comes from spectral data. Both erythromycin and *N*-desmethyl-erythromycin showed similar MI-complex formation at λ = ~452 nm for expressed CYP3A4, and both showed no detectable complex for expressed CYP3A5 (Figure 4.2). These data also suggest that the major discriminating step in CYP3A4/5 inactivation may lay downstream from the first

demethylation reaction. More specifically, it is possible that CYP3A5 can produce all of the intermediary oxidation metabolites (*N*-desmethyl, *N,N*,-di-desmethyl, *N*-hydroxyl or *N*-oxide) but at reduced rates compared to CYP3A4. The observation that time-dependent inactivation of CYP3A5 can occur (at 1/3 the rate of CYP3A4) but not MI-complex formation, suggests an alternative mechanism of "pseudo-irreversible" inhibition of CYP3A5. Extrapolating from the k_{inact} parameters, a discernable spectral change should have occurred, albeit at a slower rate than for CYP3A4. However, the absence of such findings suggests the nature of such a putative inhibitory species is unknown.

To explore CYP3A binding differences independent of incubation-induced confounders, spectral binding experiments were performed and K_S values were estimated for erythromycin and *N*-desmethyl-erythromycin. Type I spectra were observed for both compounds in both CYP3A4-containing systems. Although both erythromycin and its metabolite are demethylated at the amine nitrogen by CYP3A4, it appears as if the amine nitrogen does not serve as a sixth ligand to the heme. The Type I spectra observed are indicative of ligands that displace the H_2O from the heme, without themselves serving as strong field ligands, and that become subsequently oxidized. The complete absence of binding spectra for erythromycin and *N*-desmethyl erythromycin and CYP3A5 suggests something unusual in the orientation of the substrate in the enzyme active site. Perhaps this phenomenon is linked to enzyme inactivation without MI-complex formation.

4.4.2 *In Vitro-In Vivo* Predictions

The literature values for k_{inact} vary widely. Kanamitsu et al, (2000) obtained erythromycin k_{inact} values of 0.062 min^{-1} and 0.097 min^{-1} in human liver microsomes and expressed CYP3A4, respectively. The erythromycin values from this study are slightly lower (0.046 min^{-1} and 0.042 min^{-1}, respectively). With regard to diltiazem, Jones et al, (1999) obtained k_{inact} of 0.17 min^{-1} in expressed CYP3A4 compared to 0.030 min^{-1} in this study. Ma et al (2000) obtained a k_{inact} for diltiazem (0.01 min^{-1}) closer to the estimate in this report, but reported a result for nicardipine (2 min^{-1}) much higher than we report.

It is also possible that the discrepant findings in k_{inact} are due to differences in the estimation of the pseudo-first order rate constant (λ). Kanamitsu et al (2000) estimated λ using the "initial linear phase", and Jones et al (1999) measured λ using the initial phase as well (0-5 minutes). It is not uncommon for time-dependent inactivation experiments to become biphasic over time, and as Figure 4.1 shows, our data appear biphasic as well. Traditional analysis of non-pseudo first-order kinetic data suggests the use of the initial linear phase because later time points may be compromised by increasing concentrations of "true" inhibitor, and thus the inactivation may not be solely due the initial inactivator. However, this theory applies to a one-step inactivation process whereby the initial burst of enzyme inactivation is likely due to the inhibitor. The four inhibitors chosen for this study all undergo at least three CYP3A-dependent oxidations prior to inactivation of the enzyme. Quantitatively, more CYP3A

is inactivated from 1-12 minutes than from 0-1 minute, which is the extent of our initial phase. It is unlikely that the 0-1 minute burst seen in these data is the best marker for the inactivation rate of the enzyme. To avoid problems involving metabolite buildup that arise using later time points, we truncated the terminal time point at 12 minutes.

The reason for the burst phenomenon remains unexplained. The pre-incubation tubes were diluted 1:20 (25 μl to 500 μl) to eliminate possible competitive inhibition resulting from the carry-over of residual inhibitor, and the midazolam concentration was 2-3 fold higher than the approximate K_m. Ideally, higher concentrations of substrate would be employed, except that midazolam itself can inactivate CYP3A at higher concentrations (Podoll, 1995). However, it is possible that a burst amount of metabolite is formed initially, and the metabolite concentration is high enough to be a complicating factor in the pre-warmed incubation tubes.

In order to show further that inhibitor metabolism is sequential, linearity experiments were performed with variable enzyme concentration. If the rate of inactivation does not change with variable enzyme concentration, that would suggest that the steady-state rate of metabolite dissociating away from the enzyme does not change as a function of inhibitor concentration, and therefore supports the theory that metabolism is sequential. If the metabolite's dissociation off rate was significant, then the metabolites would actually behave as affinity-labeling agents that inhibit the enzyme by initiating binding from outside the active site. No change in inactivation rate as a function of enzyme concentration was observed (data not shown). Thus, these data are consistent with downstream metabolites that have increasing affinity for

CYP3A4. Unfortunately, only *N*-desmethyl-erythromycin was available for testing this hypothesis. Limited data suggest a slightly greater affinity of the metabolite for CYP3A4 compared to the parent molecule. If more of the metabolites in the erythromycin:CYP3A cascade become available, it may be possible to elucidate the mechanism further.

To evaluate the *in vivo* relevance of our inactivation estimates, we calculated the effect of erythromycin on *in vivo* CYP3A4-dependent metabolism using a formula presented by Mayhew et al (2000). The formula estimates the effect of a mechanism-based inactivator on steady-state CYP3A4 levels and is shown below.

$$[E]_t = [k_{syn}/k_{deg} - k_{syn}/(k_{deg} + \lambda)] \cdot e^{-\lambda t} + k_{syn}/(k_{deg} + \lambda) \qquad [4.3]$$

$[E]_t$ represents the concentration of enzyme at any time t, λ is the first-order rate constant for enzyme inactivation in the presence of an inactivator, and k_{syn} and k_{deg} are the rate constants for enzyme synthesis and degradation, respectively.

Based on our estimates of $K_{I(app)}$ and k_{inact} for erythromycin (10.9 μM and 0.046 min^{-1}, respectively) and an unbound plasma concentration of 0.66 μM (Olkkola et al, 1993; Goodman & Gilman, 1996), we were able to calculate a value for λ using equation 4.2. Using our value for λ and equation 4.3, we calculate that steady-state hepatic CYP3A4 levels will drop approximately 75% during multiple dose erythromycin therapy (Figure 4.7). An *in vivo* study with erythromycin and midazolam (Olkkola et al, 1993) showed a 54% reduction in systemic midazolam clearance during

erythromycin treatment, and suggested a midazolam dose reduction of 50 – 75% if erythromycin is concurrently administered. Both estimates concur with the simulations produced from these data presented here.

4.5 Summary

The inhibitory differences between CYP3A4 and CYP3A5 were examined with 4 time-dependent inhibitors. Inhibition differences under co-incubation conditions were substrate dependent, however, there was a trend toward higher affinity of the inhibitors towards CYP3A4. Irreversible inhibitory differences were more profound. Under pre-incubation conditions CYP3A5 was inactivated at a slower rate than CYP3A4 for all inhibitors tested and did not form visible MI-complexes under the conditions employed, thus implying potential for less severe drug:drug interactions with compounds during multiple dosing regimens. However, further MI-complex data suggested that CYP3A5 can form MI-complexes and be inactivated as long as significant levels of CYP3A4 are co-expressed. Overall, these data show that reversible drug:drug interactions may be less severe in individuals expressing high levels of CYP3A5 relative to CYP3A4.

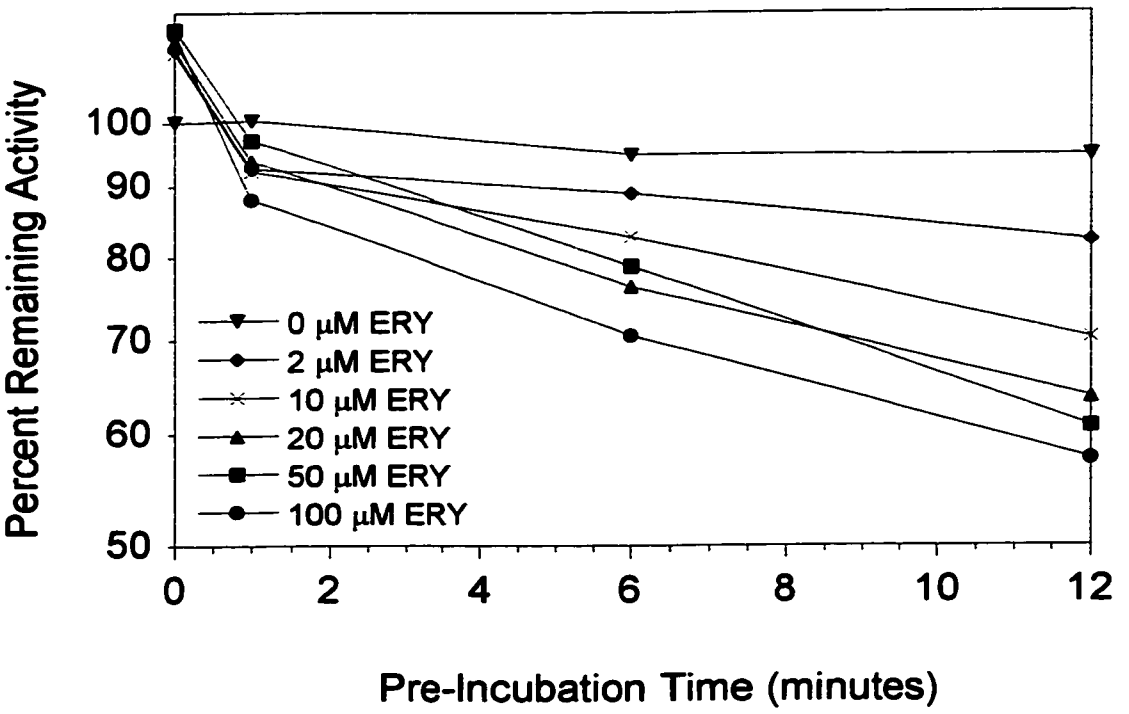

Figure 4.1A. A, Time-dependent loss of enzyme activity by different concentrations of erythromycin. Human liver microsomes (HL-166 shown) were incubated with erythromycin (0-100 μM), buffer and NADPH from 0-12 minutes followed by 4-minute incubations with 8 μM midazolam to assess loss of midazolam 1'-OHlase activity.

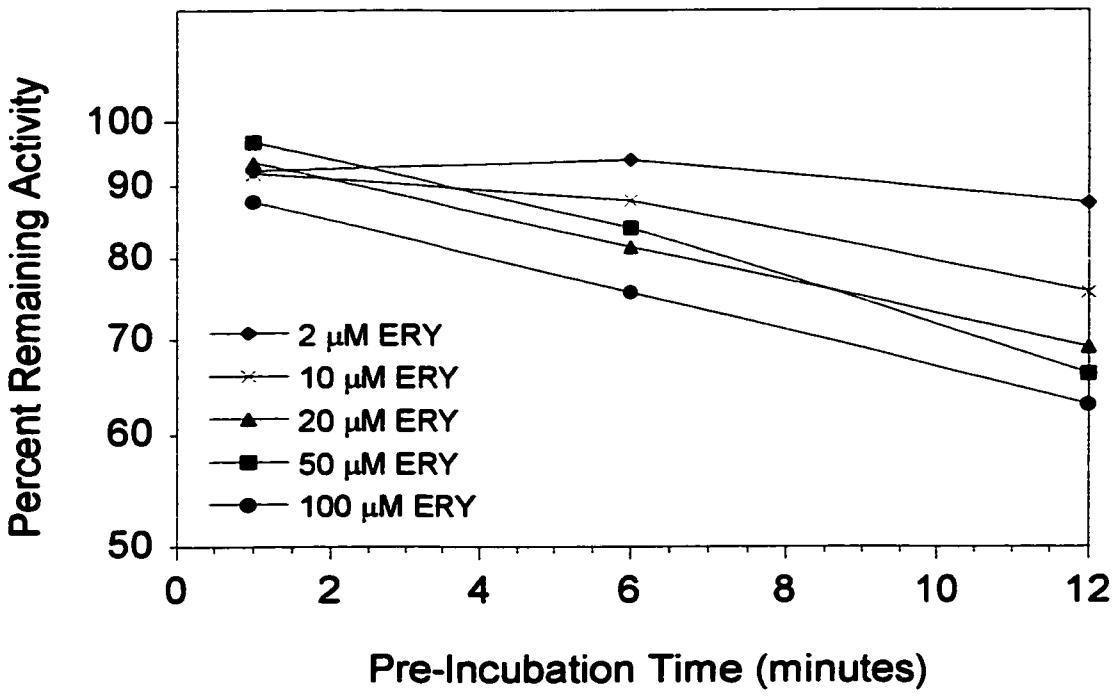

Figure 4.1B. Corrected time-dependent loss of enzyme activity by different concentrations of erythromycin. Human liver microsomes (HL-166 shown) were incubated with erythromycin (0-100 μM), buffer and NADPH from 0-12 minutes followed by 4-minute incubations with 8 μM midazolam to assess loss of midazolam 1'-OHlase activity. The erythromycin concentrations were corrected for control loss of activity (0 μM ERY).

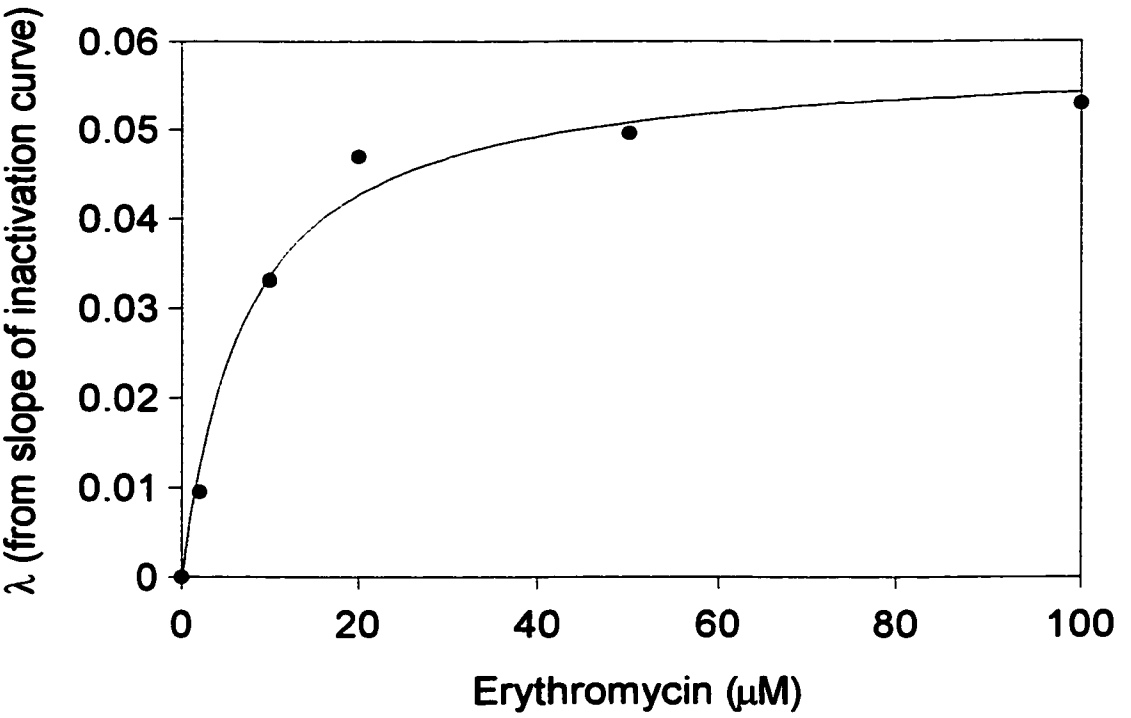

Figure 4.2. Rate of enzyme inactivation by erythromycin in human liver microsomes (HL-166) containing no detectable CYP3A5. Microsomes (50 μg protein) were incubated with erythromycin (0-50 μM), buffer and NADPH for differing incubation times. Estimates of λ from enzyme degradation data (Eq. 4.1) were plotted versus erythromycin concentration. The curve represents the line of best fit with Eq. 4.2. $K_{I(app)}$ = 14.4 μM; k_{inact} = 0.045 min^{-1}.

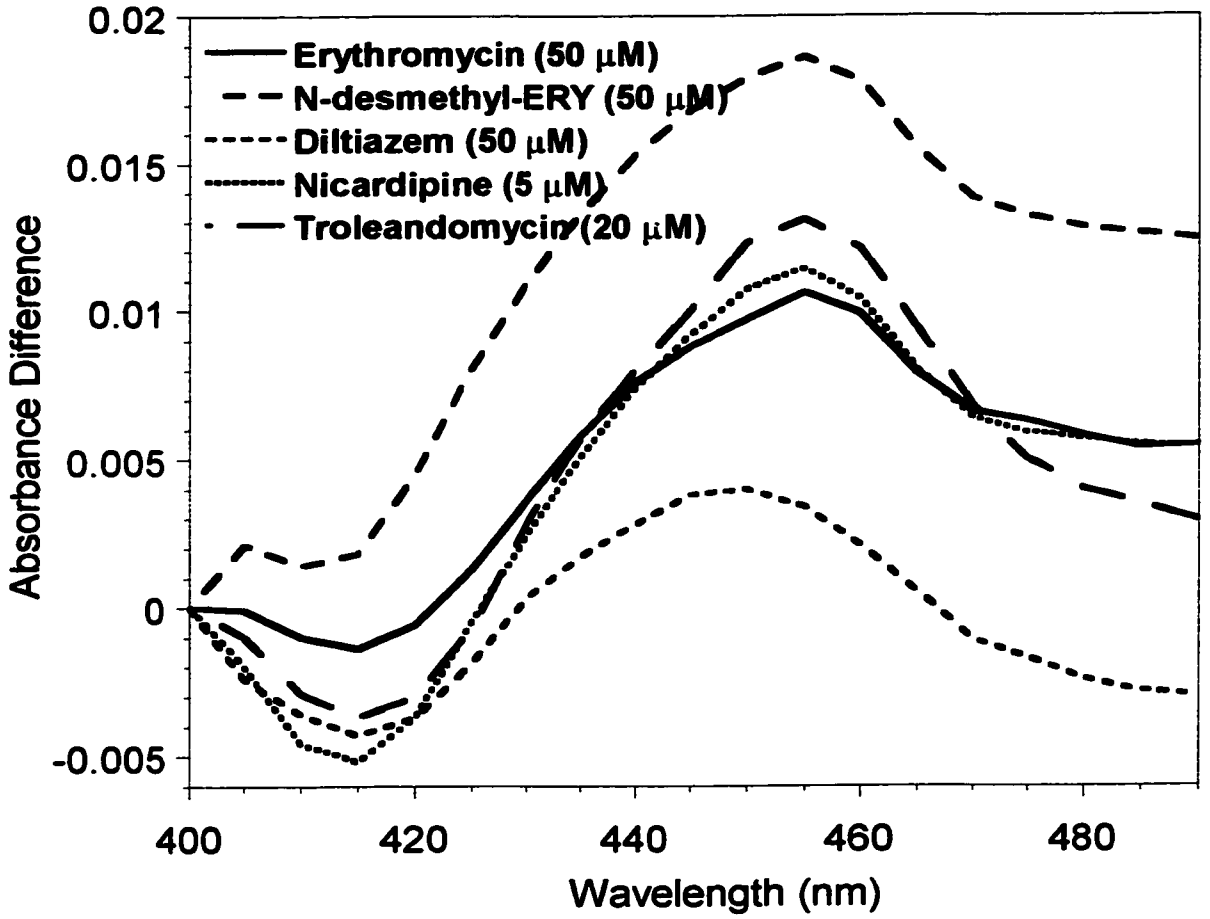

Figure 4.3A. Metabolite-intermediate complex (MIC) formation by erythromycin (50 μM), *N*-desmethyl erythromycin (50 μM), diltiazem (50 μM), troleandomycin (20 μM) and nicardipine (10 μM) in cDNA-expressed CYP3A4 **(A)** and CYP3A5 **(B).** Sample cuvettes contained expressed enzyme, erythromycin, buffer and NADPH, whereas reference cuvettes contained expressed enzyme, buffer, NADPH and evaporated inhibitor vehicle (acetone). Absorbance was monitored from 0-40 minutes; t = 40 minute scans are shown. All cuvettes were supplemented with cytochrome b_5 at a 3:1 cytochrome b_5:CYP3A molar ratio.

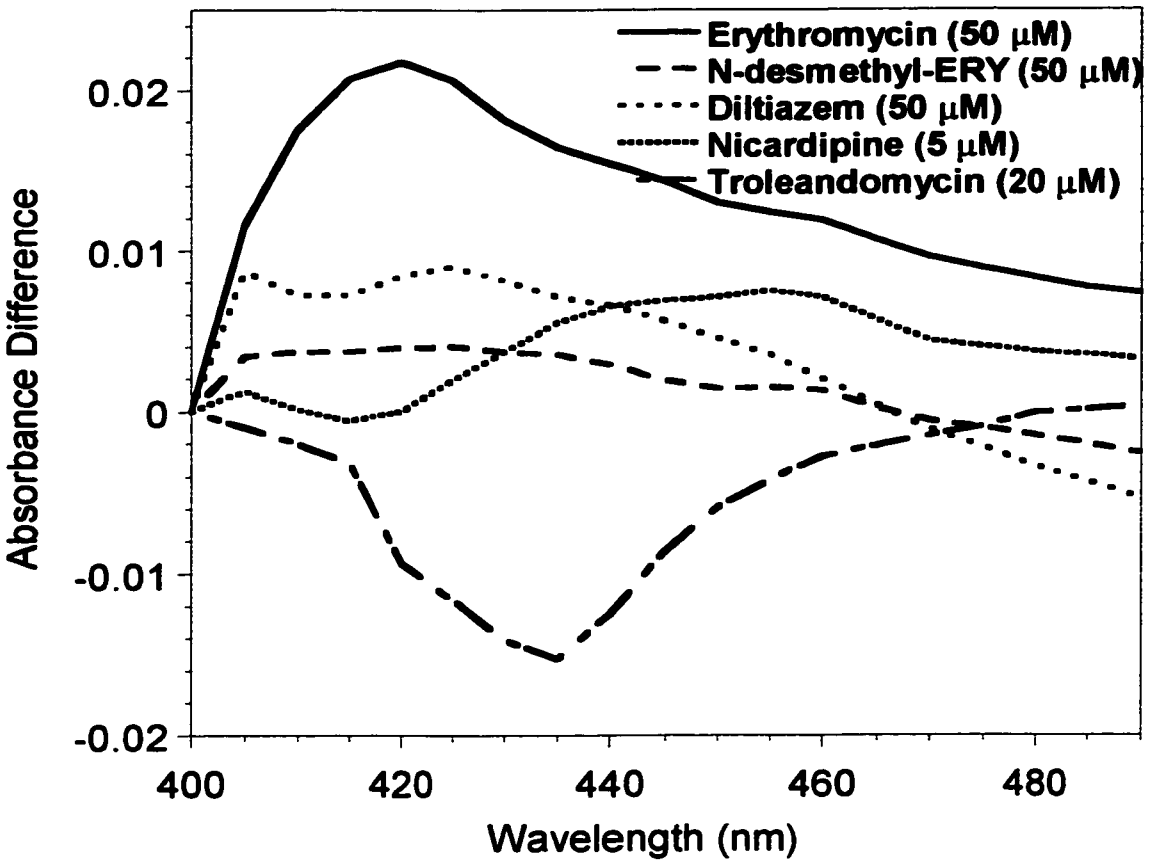

Figure 4.3B. Metabolite-intermediate complex (MIC) formation by erythromycin (50 μM), *N*-desmethyl erythromycin (50 μM), diltiazem (50 μM), troleandomycin (20 μM) and nicardipine (10 μM) in cDNA-expressed CYP3A4 **(A)** and CYP3A5 **(B).** Sample cuvettes contained expressed enzyme, inhibitor, buffer and NADPH, whereas reference cuvettes contained expressed enzyme, buffer, NADPH and evaporated inhibitor vehicle (acetone). Absorbance was monitored from 0-40 minutes; t = 40 minute scans are shown. All cuvettes were supplemented with cytochrome b_5 at a 3:1 cytochrome b_5:CYP3A molar ratio.

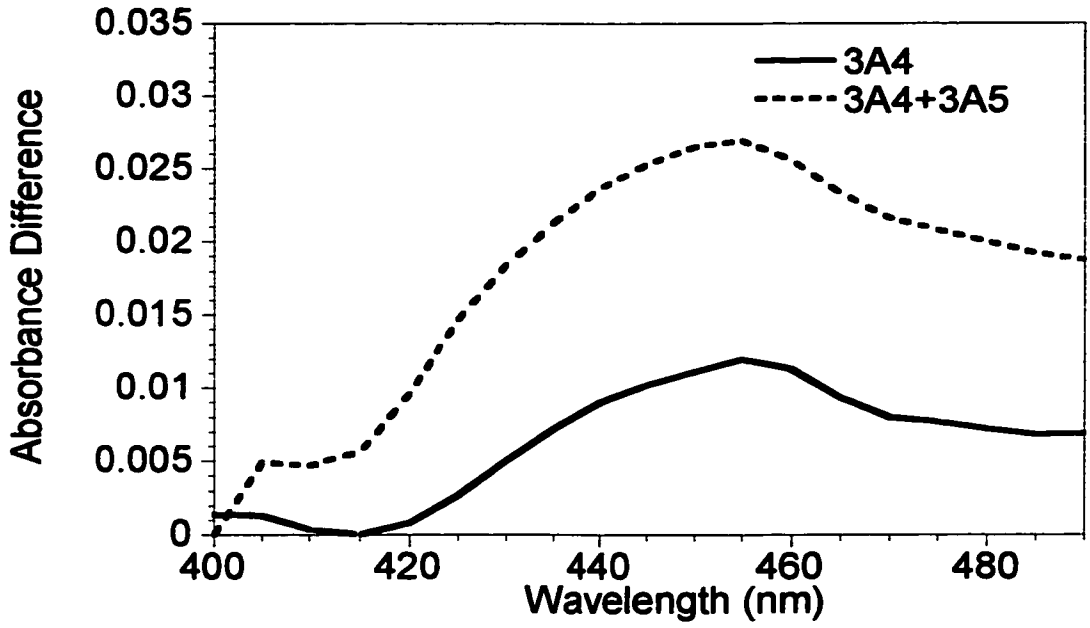

Figure 4.4. MI-complex formation in cDNA-expressed CYP3A4 and CYP3A5 + b_5 co-incubated with 50 μM erythromycin. MI-complex was monitored q. 5 min for 40 minutes. The t = 40 min scans are shown. Each curve is the mean of three experiments. CYP3A4: ΔAbs = 0.0071; CYP3A4 + CYP3A5: ΔAbs = 0.0086.

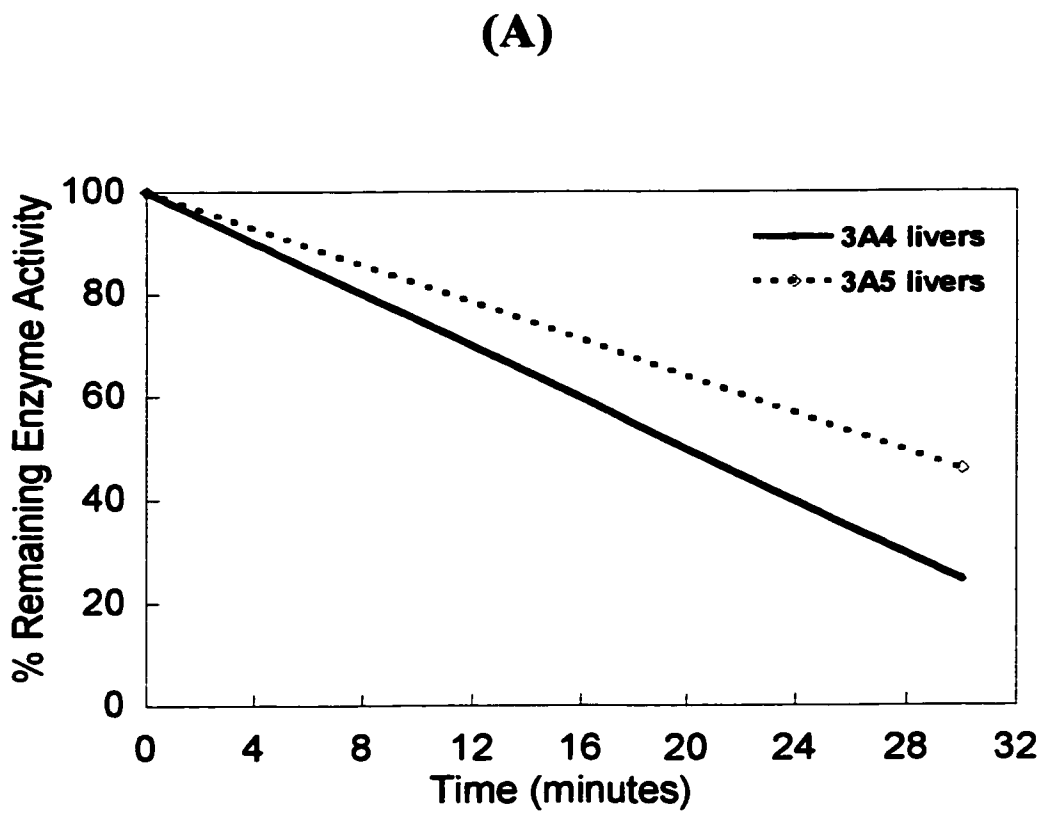

Figure 4.5. Comparison in loss of NADPH-dependent activity with (A) 50 μM erythromycin and (B) 20 μM TAO between CYP3A4 and CYP3A5-containing liver microsomes. Each line represents the mean activity loss for 4 human liver microsomal samples containing either no detectable CYP3A5 or at least 50% CYP3A5 (of total CYP3A).

(B)

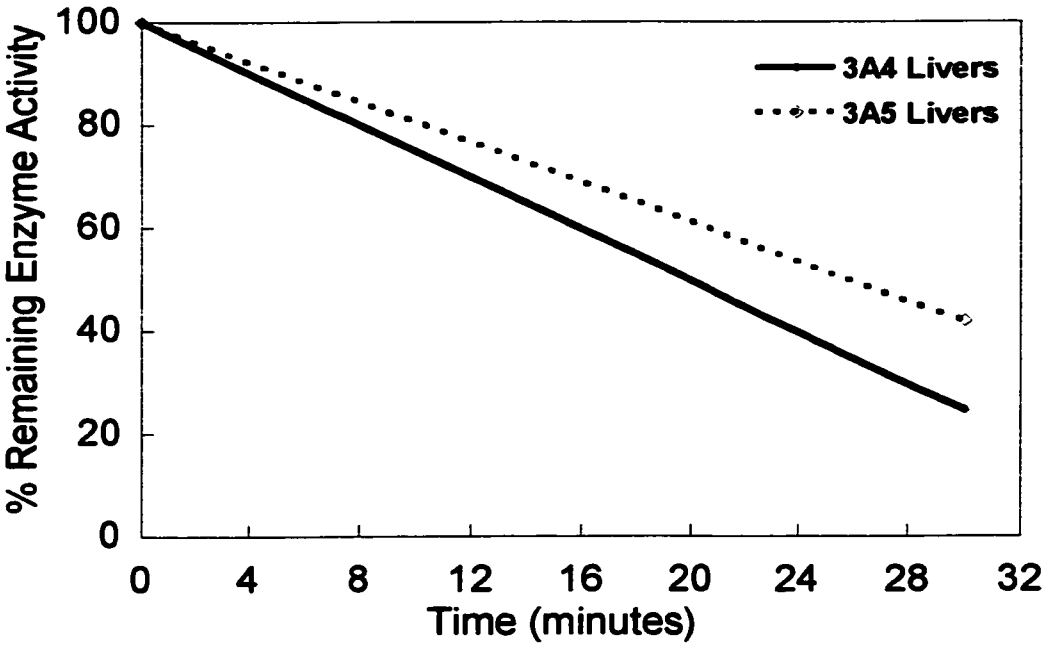

Figure 4.5. Comparison in loss of NADPH-dependent activity with (A) 50 μM erythromycin and (B) 20 μM TAO between CYP3A4 and CYP3A5-containing liver microsomes. Each line represents the mean activity loss for 4 human liver microsomal samples containing either no detectable CYP3A5 or at least 50% CYP3A5 (of total CYP3A).

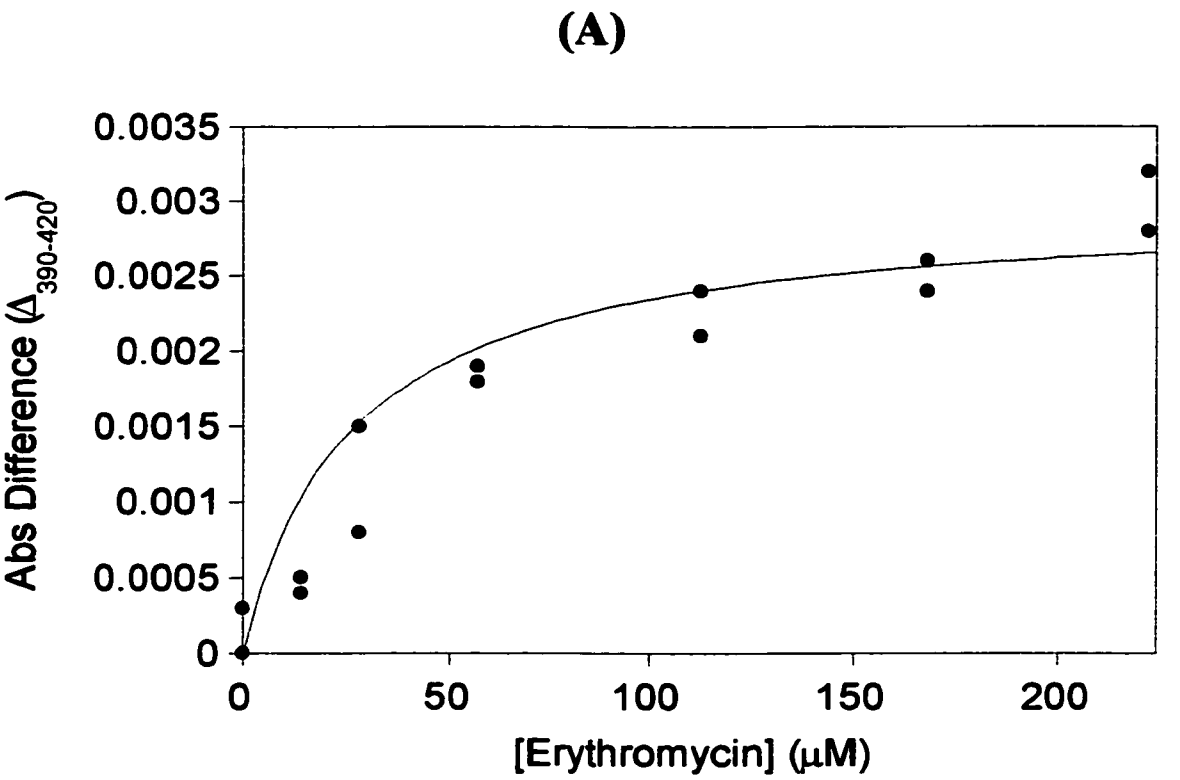

Figure 4.6. Michaelis-Menten Model fits for erythromycin (A) and *N*-desmethyl erythromycin (B) in cDNA-expressed CYP3A4 + b_5. Erythromycin: K_S = 26.7 μM ± 5.5; *N*-desmethyl erythromycin: K_S = 70.5 μM ± 17.4.

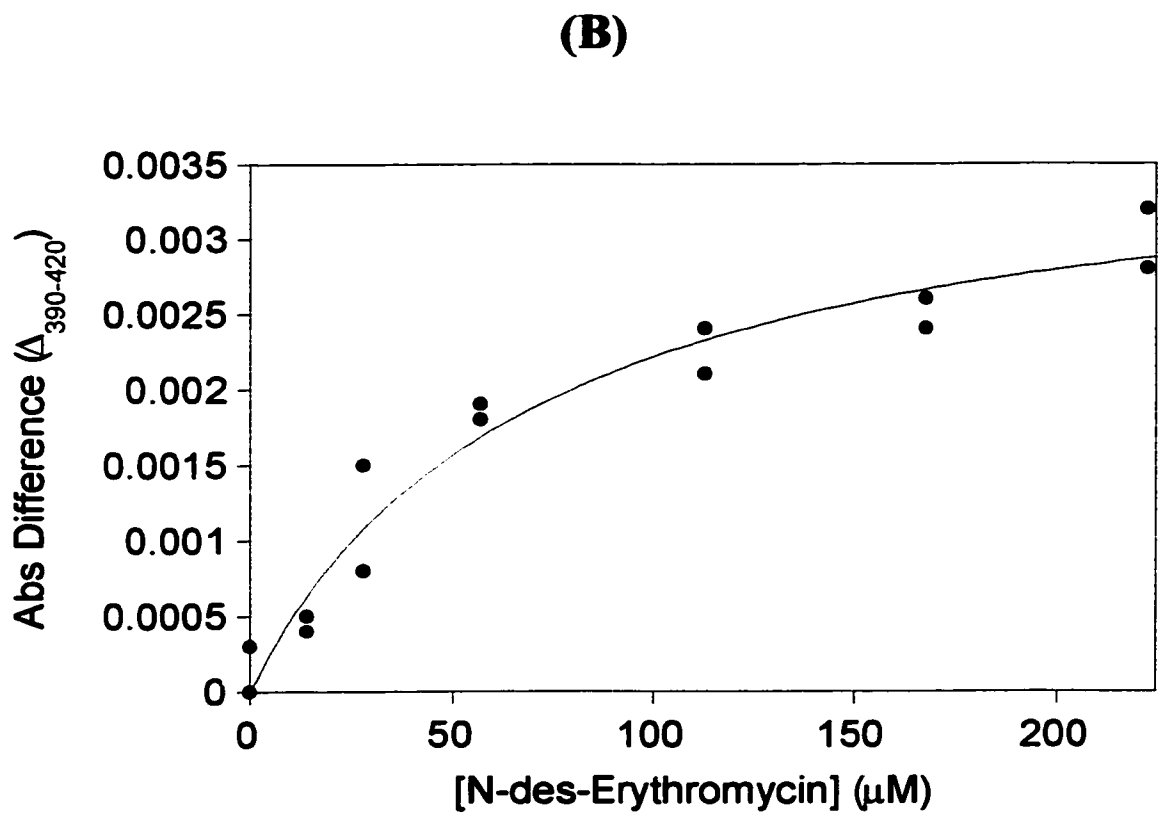

Figure 4.6. Michaelis-Menten Model fits for erythromycin (A) and *N*-desmethyl erythromycin (B) in cDNA-expressed CYP3A4 + b_5. Erythromycin: K_S = 26.7 μM ± 5.5; *N*-desmethyl erythromycin: K_S = 70.5 μM ± 17.4.

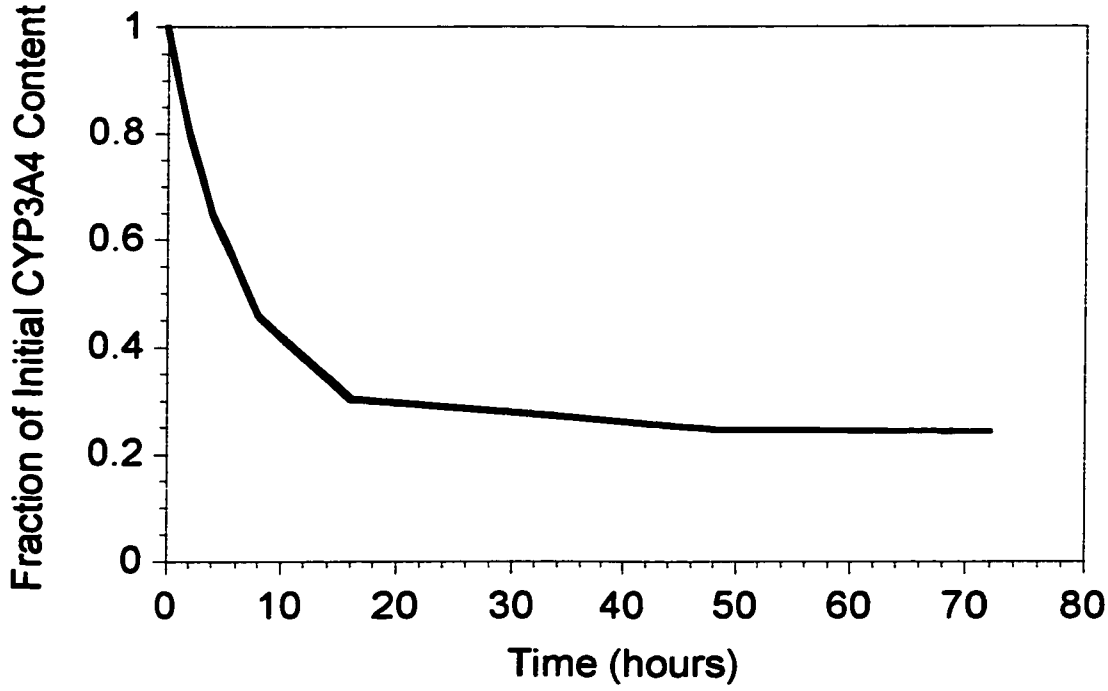

Figure 4.7. Simulation of the effect of steady-state erythromycin on hepatic CYP3A4 levels according to equation 4.3. This simulation assumes a steady-state unbound erythromycin concentration of 0.66 μM, $K_{I(app)}$ = 10.9 μM, k_{inact} = 0.0455 min^{-1}, k_{syn} = k_{deg} = 0.000825 min^{-1}. The value for λ was calculated using equation 4.2; λ = 0.0026 min^{-1}.

Table 4.1. IC_{50} values in various microsomal preparations

Inhibitor	*3A4 HL Mics*	*3A5 HL Mics*	*cDNA 3A4 + b_5*	*cDNA 3A5 + b_5*
Ketoconazole	22.3 nM ± 1.4*	53.6 nM ± 7.1	24.9 nM ± 3.8$^{\times}$	145 nM ± 24
Erythromycin	15.6 μM ± 1.7*	22.7 μM ± 1.9	33.4 μM ± 1.0$^{\times}$	64.2 μM ± 6.0
Diltiazem	125 μM ± 14	109 μM ± 5.3	62.3 μM ± 12	117 μM ± 96
Nicardipine	363 nM ± 21*	482 nM ± 43	24.5 nM ± 4.3	33.0 nM ± 6.3

All results based on midazolam 1'-hydroxylation at 4 μM midazolam concentration, and were performed in triplicate. Values are mean ± s.d. for both human liver microsome preparations, and mean ± s.e. for the model fit in the expressed microsomes. * = $p<0.05$ between 3A4 and 3A5 HL microsomes. $^{\times}$ = observed difference between cDNA 3A4 and cDNA 3A5 microsomes; n = 1, therefore no statistical tests were performed.

Table 4.2. $K_{I(app)}$ values in various microsomal preparations obtained from inactivation kinetics experiments

Inhibitor	*3A4 HL Mics*	*3A5 HL Mics*	*cDNA 3A4 + b_5*	*cDNA 3A5 + b_5*
Erythromycin	10.9 μM ± 4.0	10.1 μM ± 6.4 (2)	7.47 μM ± 3.0	7.14 μM ± 0.7
N-des-Ery	7.51 μM ± 5.4	12.8 μM ± 9.2 (1)	2.79 μM ± 0.3*	7.98 μM ± 1.3
Diltiazem	18.1 μM ± 7.6	ND	1.23 μM ± 0.04*	8.70 μM ± 7.9
Nicardipine	1.29 μM ± 0.6	ND	0.59 μM ± 0.4	0.39 μM ± 0.4

All results based on midazolam 1'-hydroxylation at 8 μM midazolam concentration as the marker for enzyme loss. Experiments were carried out with at least five inhibitor concentrations, and from pre-incubation times varying from 1 – 25 minutes. Human liver microsome values (n = 3) are given as the mean ± s.d. Numbers in parentheses were assigned if less than three livers could be statistically fit to the inactivation model. Values are mean ± s.e. for the model fit in the expressed microsomes. * = observed difference between cDNA 3A4 and cDNA 3A5 microsomes; n = 1, therefore no statistical tests were performed. ND = not determined due to inability for any of the microsomal samples to fit to the inactivation model.

Table 4.3. k_{inact} values in various microsomal preparations

Inhibitor	*3A4 HL Mics*	*3A5 HL Mics*	*cDNA 3A4 + b_5*	*cDNA 3A5 + b_5*
Erythromycin	0.046 ± 0.010*	0.015 ± 0.002 (2)	0.042 ± 0.007[x]	0.011 ± 0.0003
N-des-Erythro	0.052 ± 0.006*	0.014 ± 0.004 (1)	0.062 ± 0.002[x]	0.012 ± 0.0006
Diltiazem	0.015 ± 0.007	ND	0.030 ± 0.0002[x]	0.007 ± 0.001
Nicardipine	0.060 ± 0.01	ND	0.082 ± 0.02[x]	0.023 ± 0.005

All units in reciprocal time (min^{-1}). All results based on midazolam 1'-hydroxylation at 8 μM midazolam concentration as the marker for enzyme loss. Experiments were carried out with at least five inhibitor concentrations, and from pre-incubation times varying from 1 – 25 minutes. Human liver microsome values (n = 3) are given as the mean ± s.d. Numbers in parentheses were assigned if less than three livers could be statistically fit to the inactivation model. Values are mean ± s.e. for the model fit in the expressed microsomes. [x] = observed difference between cDNA 3A4 and cDNA 3A5 microsomes; n = 1, therefore no statistical tests were performed. ND = not determined due to inability for any of the microsomal samples to fit to the inactivation model.

Table 4.4. K_S values in cDNA-expressed and human liver microsomes.

Substrate	*cDNA-3A4 + b_5*	*Human Liver Microsomes*
Erythromycin	26.7 ± 5.5	49.4 ± 12.9
N-desmethyl erythromycin	70.5 ± 17	17.1 ± 8.7

Values are expressed as mean (μM) ± s.d. of triplicate measurements.

Table 4.5. Comparison between affinity measurements for erythromycin, diltiazem and nicardipine in cDNA expressed microsomes.

		IC_{50} (μM)	$K_{I(app)}$(μM)	K_S (μM)
Erythromycin	cDNA 3A4	33	7.5	26
	cDNA 3A5	64	7.1	ND
Diltiazem	cDNA 3A4	62	1.23	ND
	cDNA 3A5	117	8.7	ND
Nicardipine	cDNA 3A4	0.024	0.59	ND
	cDNA 3A5	0.033	0.39	ND

ND = not determined

CHAPTER 5

EFFECT OF CIRRHOSIS OF THE LIVER ON INTESTINAL CYTOCHROME P450 3A4-DEPENDENT DRUG METABOLISM

5.1 Introduction to Chapter 5

The clearance of many drugs that undergo metabolic elimination can be substantially altered by liver disease (McLean and Morgan, 1991). The mechanism for changes in metabolic clearance is presumed to involve irreversible changes in hepatic structure and cellular function, as reviewed under Chapter 1. In recent years there has been a considerable amount of effort to characterize the effect of liver disease on drug elimination in the liver (George et al, 1995), pancreas (Horvath et al, 1986) and kidney (Wood et al, 1988). Cirrhosis of the liver is generally characterized by a hardening and complete restructuring of the hepatic cellular framework and a loss of functional cellular mass. In addition, there can be alterations in the expression of drug metabolizing enzymes in the remaining functional "regenerated" hepatocytes. These changes have dramatic consequences on oxidative drug metabolism in that organ. Cirrhosis also affects normal homeostatic functions of the liver, such as storage of sugar, neutralization of other systemic toxins, and synthesis of plasma proteins. When the liver ceases to perform these aforementioned functions, it puts tremendous stress on the rest of the body, and can precipitate other organ failures.

The liver is responsible for the low oral bioavailability of many well-absorbed drugs. This is due to the large size of the liver, its high concentration of drug metabolizing enzymes and its location distal to the site of absorption. However, for several drugs that are cleared by cytochrome P450 3A (CYP3A)-dependent metabolism, the small intestine can contribute to first-pass metabolism (Thummel et al,

1996; Watkins et al, 1996; Kolars et al, 1992; Kolars et al, 1994), and the effect of liver disease on oral availability can be quite variable between individuals that have a comparably defined stage of liver disease (McLean and Morgan, 1991; George et al, 1995). For example, morphine (Tegeder et al, 1999) and torsemide (Schwartz et al, 1993) show wide variability in bioavailability in cirrhotic populations, even though both compounds are primarily eliminated by different enzymes (UGT and CYP2C9, respectively). These inter-individual differences may be the result of discordant and variable expression of drug metabolizing enzymes in the liver and intestine of patients with liver cirrhosis.

Although the effects of cirrhosis are traditionally deleterious, it may be worthwhile to ponder the possibility that cirrhosis affects the synthesis or degradation of metabolic enzymes in other organs. In particular, alterations in splanchnic blood flow and regulatory hormone or cytokine concentrations may affect enzyme expression in the gastrointestinal tract. Perhaps the body will compensate for a certain loss of metabolic function, as it does with target receptors (Stephanis et al, 1998). Thus, increased expression of drug metabolizing enzymes in the small intestine may be a compensatory response to the loss of drug metabolizing activity in the liver.

Analysis of the small intestine's contribution to first-pass metabolism or systemic clearance in liver disease has not been explored. The focus of this work was to determine the metabolic role of the small intestine in patients with cirrhosis. To accomplish this, duodenal biopsies were taken from cirrhotic and non-cirrhotic patients. Since CYP3A is the major drug-metabolizing enzyme subfamily in the small

intestine, we assessed CYP3A-dependent enzyme activity, as well as villin-normalized CYP3A4 and CYP3A5 contents in the two groups.

5.2 Materials and Methods

5.2.1 Chemicals

Midazolam, 1'-hydroxy midazolam, 4-hydroxy midazolam and $^{15}N_3$ – midazolam were kindly provided by Roche Laboratories (Nutley, NJ). $^{15}N_3$ –labeled 1'-OH and 4-OH midazolam were generated enzymatically from $^{15}N_3$-midazolam as described (Paine et al, 1997a). Acetonitrile and ethyl acetate were purchased from Fisher Scientific (Santa Clara, CA). *N*-methyl-*N*-(*t*-butyl-dimethylsilyl) trifluoroacetamide (MTBSTFA) was obtained from Pierce Chemical (Rockford, IL). Phenylmethylsulfonyl fluoride (PMSF), benzamidine, NADPH, aprotinin and β-glucuronidase were purchased from Sigma Chemical Co. (St. Louis, MO). Nitrocellulose was purchased from Schliecher and Schuell (Keene, NH). Alkaline phosphatase development reagents (5-bromo-4-chloro-3-indoyl phosphate and nitroblue tetrazolium) were purchased from Kirkegaard and Perry (Gaithersburg, MD). All other reagents were of the highest grade commercially available.

5.2.2 Biopsy Collection

Our study design involved the collection of five duodenal pinch biopsies from 20 mild to moderate cirrhotic volunteers (a score of B or C on the Child's test) that

underwent clinical endoscopy related to their condition. All biopsies were conducted at Harborview Medical Center (Seattle, WA) and were approved by the University of Washington and Harborview Institutional Review Board. Five control duodenal biopsies were taken from 14 non-cirrhotic patients undergoing endoscopy, and were matched for age, gender and ethnicity. Three biopsy samples were homogenized in 1 ml of solution D (0.05 M Tris-HCl, 20% glycerol and 2 mM EDTA) (Bonkovsky et al, 1985) with added protease inhibitors (aprotinin, benzamidine and 0.1 mM PMSF) and stored at –80 °C until analyzed for metabolic activity, whereas the other two biopsies were subjected to histological testing for suspected esophageal or gastric disease (i.e. esophageal reflux disease). Biopsies from all "control" subjects showed no histological evidence of duodenal disease.

5.2.3 Biopsy Analyses

Protein assays by the method of Lowry et al (1951) were performed in duplicate on all cirrhotic and control biopsies. Western immunoblot analysis was also performed to quantitate the level of CYP3A present in each of the biopsies according to the method described in Paine et al (1997b). Each biopsy sample was analyzed for CYP3A and the actin-binding protein villin. Villin is a protein expressed in fully differentiated enterocytes and is present uniformly down the length of the small intestinal mucosa. By using villin content as a marker, we are able to control for the differing sizes and

depth of the pinch biopsy samples. CYP3A4 content (pmol/mg protein) was normalized according to the following relationship:

$$CYP3A_{normalized} = CYP3A_{calculated} \times \frac{\text{Villin IOD}_{unknown}}{\text{Villin IOD}_{\text{"reference"}}} \quad [5.1]$$

where IOD refers to the integrated optical density of the specific band. A mucosal biopsy sample from the UW Tissue Bank was run concurrently with all samples to provide a villin "reference" value. The villin ratio was calculated for all biopsies, and was applied to both CYP3A4 and CYP3A5 samples. CYP3A5 was detected in 2 of the 20 cirrhotic subjects and in 4 of the 14 control subjects, but the levels were lower than those found for CYP3A4.

Incubations were conducted in solutions containing 100 mM potassium phosphate buffer at pH = 7.4 (0.5 ml). All incubations were performed in duplicate. Midazolam (4 μM final concentration), buffer and homogenate (100 μg protein) were incubated for 5 minutes at 37 °C prior to the addition of NADPH (1 mM final concentration), which commenced the incubation. After four minutes, reactions were terminated with the addition of 1 ml of 100 mM Na_2CO_3, pH ~11. After the reactions were quenched, 100 μl of internal standard ($^{15}N_3$ –labeled 1'-OH and 4-OH midazolam) was added to all tubes, followed by extraction with 5 ml of ethyl acetate. Standard curves were prepared with known amounts of 1'-OH midazolam and 4-OH midazolam, and were treated identically to incubation samples. The 1'-OH midazolam metabolite was measured by gas chromatography-negative chemical ionization mass

spectrometry as described previously (Paine et al, 1996). The ions monitored for 1'-OH midazolam were *m/z* = 455 and 460 for the *t*-butyl-dimethylsilyl derivitized compound and the ^{37}Cl signal for the $^{15}N_3$-labeled metabolite, respectively. The ions monitored for 4-OH midazolam were *m/z* = 323 and 328, representing a loss of water from the metabolite, and its ^{37}Cl signal for the $^{15}N_3$-labeled metabolite, respectively.

5.3 Results

CYP3A4 content and activity were compared to controls in a panel of 20 subjects exhibiting mild to moderate cirrhosis. The cirrhotic cohort ranged in age from 35-75 years (median = 48.5), and the subjects were from various ethnic backgrounds (Table 5.1). Control subjects were matched on the bases of age, gender and ethnicity. Control patients ranged from 40-59 years old (median = 48.5) (Table 5.2).

Western immunoblot analysis with CYP3A4 polyclonal and CYP3A5 isoform-specific antibodies (Figure 5.1) did not reveal a statistically significant difference in CYP3A4 content between the cirrhotic and control subjects (Figure 5.2). Cirrhotic CYP3A4 concentrations varied approximately 18-fold, from 7.41 to 146 pmol/mg protein, whereas control values ranged from 24.7 to 63.7 pmol/mg protein. CYP3A5 was detected in 10% of cirrhotics and 21% of controls, but no difference was observed between study populations in the levels of CYP3A5 content.

CYP3A activity, as measured by midazolam 1'- and 4-hydroxylation, was slightly increased in biopsy homogenates prepared from cirrhotic subjects compared to controls, although this difference was not statistically significant (Figure 5.3). Biopsy

incubations with 4 μM midazolam revealed 8 to 15-fold variability in reaction velocity for both control and cirrhotic subjects, respectively. Cirrhotic enzyme activity ranged from 87.6 to 1400 pmol formed/min/mg protein (mean = 286), whereas control activity varied from 73.6 to 581 pmol formed/min/mg protein (mean = 238).

Although no difference in CYP3A4 content or reaction velocity existed between cirrhotic and control groups, the metabolic ratio of 1'- to 4-hydroxy midazolam formation was statistically different between cirrhotic and control individuals (Table 5.3). The 1'- to 4-hydroxy midazolam metabolic ratio in cirrhotic subjects was 5.86 ± 0.9, and 4.15 ± 2.5 in control subjects ($p < 0.05$). Considering that CYP3A5 preferentially hydroxylates midazolam at the 1'-position (Gorski et al, 1994; Paine et al, 1997a), it is interesting that the cirrhotic group had a significantly higher 1'-OH/4-OH midazolam ratio, since there were fewer cirrhotic subjects expressing CYP3A5. Some other mechanism(s) separate from CYP3A5 expression, is/are responsible for this finding.

5.4 Discussion

Previous data have suggested that there can be up to a 30-fold difference in gut CYP3A expression (Paine et al, 1997b). Hepatic expression is also widely variable (Thummel et al, 1994). However, these data were generated from tissue procured from organ donors and under conditions that may compromise constitutive enzyme expression. Findings from the cirrhotic subjects in this report concur with intestinal

tissue bank results. Variability in the cirrhotic cohort was approximately 18-fold (7.4 – 146 pmol CYP3A4/mg homogenate protein) compared to 18-fold (1 – 18 pmol CYP3A4/mg homogenate protein) for our duodenal bank. Although cirrhotic variability was similar to previous findings, the intestinal biopsy results shown here demonstrate that the variability in control subjects does not appear to be as great. Once the gut biopsies were normalized for villin content the range of CYP3A4 content was between 24.7 and 63.7 pmol 3A4/mg protein, yielding only a 2-3 fold difference. Previous results by Lown et al (1994) concur with the control results presented here, and suggest that in otherwise healthy individuals, the variability in duodenal CYP3A content is probably only 4-fold, with an occasional outlier at a high or low extreme.

Although the variability was similar for the cirrhotic group and the UW intestinal tissue bank, a large discrepancy existed in the amount of CYP3A4 present in each group. The cirrhotic CYP3A4 levels were approximately 8-fold higher than the villin-normalized values from intestinal scraping homogenates. This observation is not localized to the cirrhotic samples. Control duodenal biopsy CYP3A4 levels were also higher than in the tissue bank (4-fold), suggesting that the tissue sampling method and not the disease state is responsible for higher CYP3A4 levels. The tissue bank samples obtained from organ donors had the entire duodenal epithelium scraped and collected, whereas pinch biopsy samples only involve the most proximal tips of the villi, where the highest expression of CYP3A4 is located. Perhaps the pinch biopsies represent a more concentrated pool of CYP3A4 than intestinal scrapings. The scrapings contain not only the proximal villi, but also contain the distal villi, crypt cells and possibly

basement membrane fractions as well, functionally diluting the concentration of CYP3A4 in the sample.

The presence of cirrhosis introduces many additional sources of potential variability in CYP3A expression. Cirrhosis has differential effects on the regulation of some P450 enzymes. Many cytokines mediate the fibrotic healing of injured hepatic tissue that occurs in the early stages of cirrhosis. Interleukin-1β (IL-1β) and interleukin 6 (IL-6) are present in high levels ascitic fluid from cirrhotic patients (Sanchez-Rodriguez et al, 2000), and can inactivate hepatic P450 enzymes (Bleau et al, 2000). It is possible that due to the hyper dynamic changes in splanchnic blood flow common in cirrhosis, a result of portal hypertension and excessive retention of sodium, higher levels of these inactivating cytokines can reach the small intestine and alter CYP3A regulation as well. These effects may explain the low level of CYP3A expression in some subjects.

A more direct regulatory mechanism involves the altered composition and production of bile in the cirrhotic liver. Since the enterocytes in the small intestine have direct continuous contact with bile, a compositional change in the bile may affect CYP3A regulation. As liver disease progresses towards cirrhosis, the amount of hepatocytes available to produce sufficient levels of bile acids decreases. Moreover, the cellular framework responsible for canalicular secretion into the bile ducts also diminishes during the progression of fibrotic nodule formation.

Although there was no significant difference in CYP3A4 content or midazolam hydroxylase activity, a significant difference was observed in the 1'-OH/4-OH

metabolic ratio. Other investigators have determined that livers that express CYP3A5 will exhibit a higher midazolam metabolic ratio (Gorski et al, 1994; Paine et al, 1997b). CYP3A5 levels were observed by Western immunoblot, but due to the low levels of CYP3A5 present (using relative IOD measurements) and the relatively lower percentage of livers expressing CYP3A5 in the cirrhotic cohort, the presence of CYP3A5 does not seem the likely reason for our finding. It is more likely that the difference in metabolic regiospecificity observed is due to other factors, such as endogenous co-activators, co-enzymes or membrane lipid composition that can also influence the midazolam product ratio *in vivo*.

Hepatic and intestinal CYP3A levels do not appear concordant *in vivo* (Thummel et al, 1996; Paine et al, 1997b; Gorski et al, 1998), thus it is likely that the CYP3A4 levels are differentially regulated in both organs. Recent studies show that regulation of hepatic CYP3A4 is mediated via the Pregnane X and Retinoid X receptor dimerization (Lehmann et al, 1998; Xie et al, 2001). In contrast, CYP3A4 regulation in the small intestine is likely mediated through the Vitamin D receptor (VDR) (Thummel et al, in press; Schmiedlin-Ren et al, 1997) in addition to PXR:RXR. VDR is found at higher levels in the intestine compared to the liver (Stumpf, 1995; Berger et al, 1998), and 1α,25-dihydroxy Vitamin D_3, a ligand for VDR, is known to induce CYP3A4 in intestinal cell culture (Schmiedlin-Ren et al, 1997; Fisher et al, 1999; Thummel et al, in press).

A common complication in patients with biliary cirrhosis is increased bone loss, and a higher incidence of osteoporosis (Hodgson et al, 1993; Stellon et al, 1987).

Since 1α,25-dihydroxy Vitamin D_3 is responsible for the calcium absorption, calcium and phosphate homeostasis as well as bone mineralization, it is possible that individuals with cirrhosis of the liver may have defective VDR function as a result of altered 1α,25-dihydroxy Vitamin D_3 availability or inactivating VDR polymorphisms. Indeed, recent reports (Springer et al, 2000; Guardiola et al, 2000; Resnick et al, 2000) concur that mutations in the VDR gene can result in an increased level of bone loss in some cirrhotic individuals. Alternately, a change in total or unbound 1α,25-dihydroxy Vitamin D_3 levels in plasma may lead to up or down-regulation in intestinal CYP3A4 transcription and altered steady-state enzyme levels. Total 1α,25-dihydroxy Vitamin D_3 levels are reduced by half in cirrhosis (Bikle et al, 1984). However, the unbound fraction is actually increased 2.5-fold as a consequence of reduced (~2-fold) levels of circulating Vitamin D binding protein (DBP). Predicting the effect of these changes on gut VDR signaling is difficult, since it is not clear whether unbound 1α,25-dihydroxy Vitamin D_3 or DBP-bound hormone is taken up by the enterocyte. Nonetheless, increased inter-individual variability in CYP3A4 content could be the result of differences in VDR signaling.

Recently, an *in vivo* study was performed (Gorski et al, 2001) using simultaneous administration of intravenous midazolam (MDZ) and oral $^{15}N_3$-midazolam (MDZ*) to characterize the role of the small intestine in first-pass extraction in patients with liver disease. By comparing the oral (intestinal and hepatic) and intravenous (hepatic) data, the small-intestinal component of first-pass metabolism in this population could be better estimated. These investigators saw a significant 50%

decline in the intravenous clearance of midazolam in cirrhotic volunteers, but saw only a 33% decrease in oral clearance although the oral result was not significant due to considerable variability. More intriguing was the observation that the apparent intestinal bioavailability (F_G) was unchanged (25% decrease, N.S.). These *in vivo* clinical data are fully consistent with our *in vitro* biochemical findings (i.e. a similar mean intestinal CYP3A4 expression level between groups, but more interindividual variability in the cirrhotic subjects).

5.5 Summary

Intestinal biopsies were acquired from 20 individuals with liver cirrhosis and from 14 non-cirrhotic control subjects who underwent endoscopy. The biopsies were homogenized and analyzed for CYP3A4 content and catalytic activity. No statistically significant difference was observed in either immunodetectable CYP3A4 content or in midazolam hydroxylase activity, although greater inter-individual variability for the cirrhotic group was noted. These data provide a mechanistic basis for the partial preservation of the first-pass metabolic extraction of moderate to high clearance CYP3A substrates, such as midazolam. The data also suggest that the response to disease in any individual will be variable as a result of potentially opposing regulation signals that increase or decrease the levels of enzyme expression.

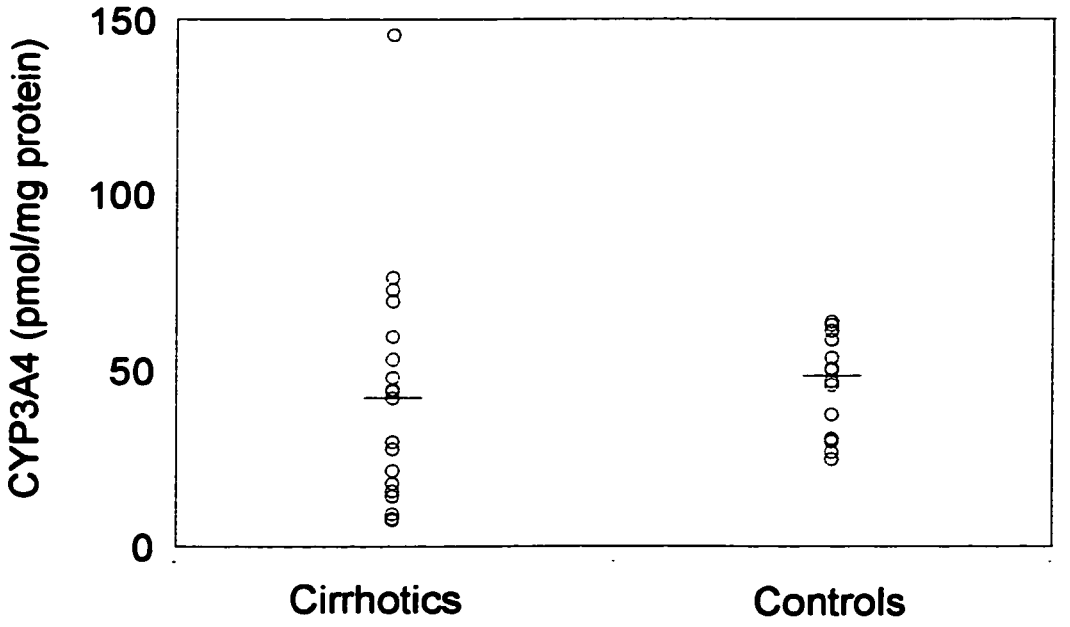

Figure 5.1. CYP3A4 levels in Cirrhotic and Control groups as measured by Western Immunoblot. The blue line denotes the median value.

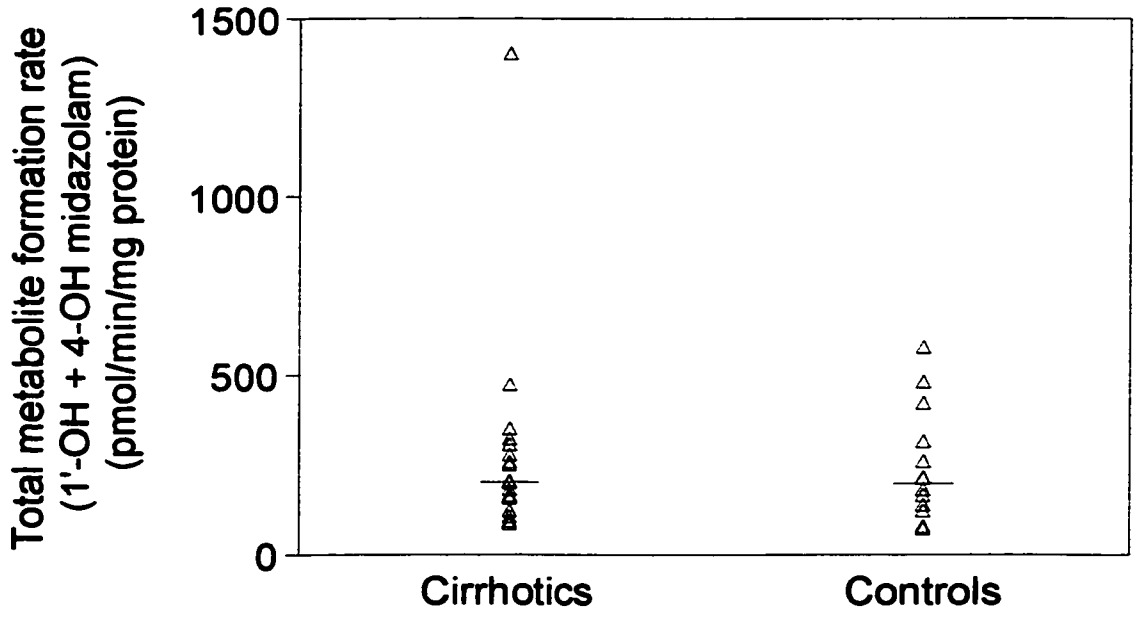

Figure 5.2A. Comparison of total midazolam reaction velocity between cirrhotic and control subjects. The bar denotes the median velocity.

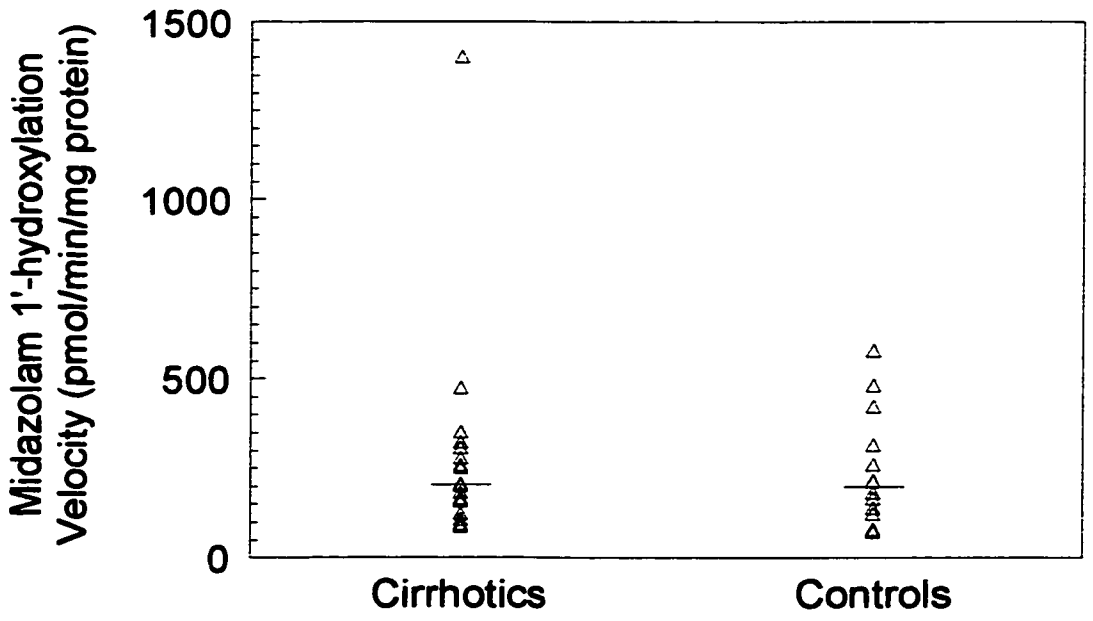

Figure 5.2B. Comparison of 1'-hydroxy midazolam reaction velocity between cirrhotic and control subjects. The bar denotes the median velocity.

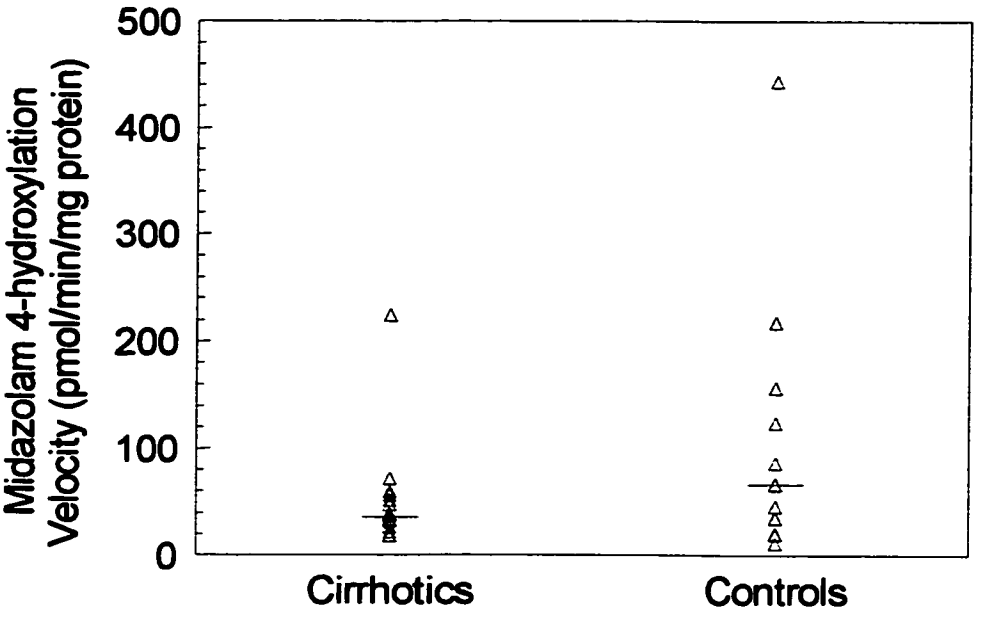

Figure 5.2C. Comparison of 4-hydroxy midazolam reaction velocity between cirrhotic and control subjects. The bar denotes the median velocity.

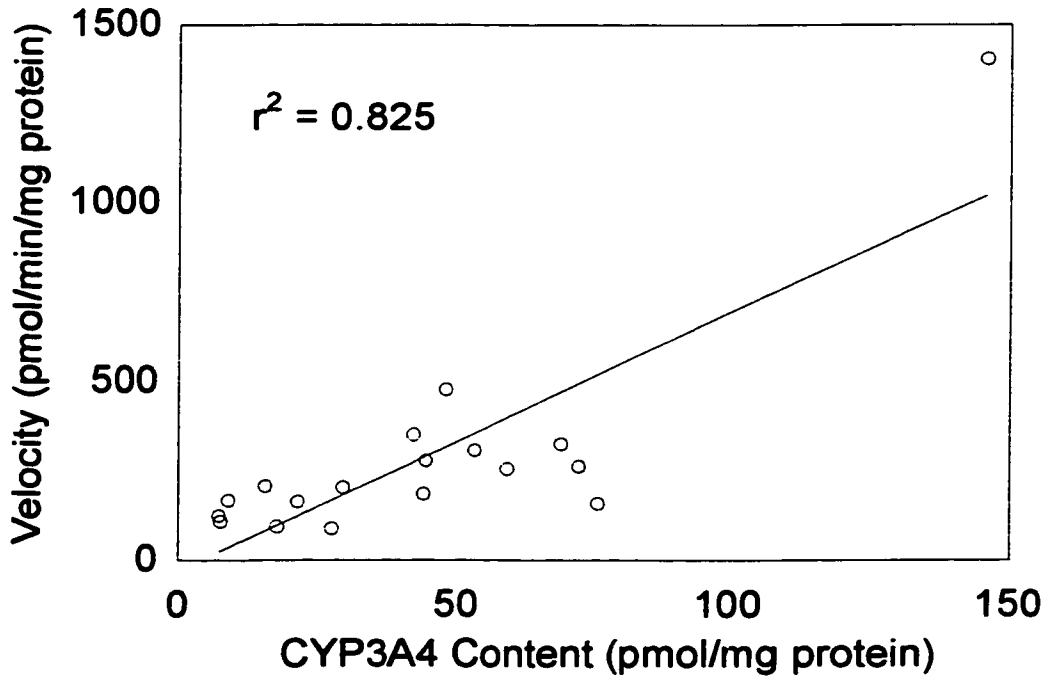

Figure 5.3. Correlation between CYP3A4 content and total midazolam reaction velocity in the cirrhotic cohort. The line represents the best linear fit.

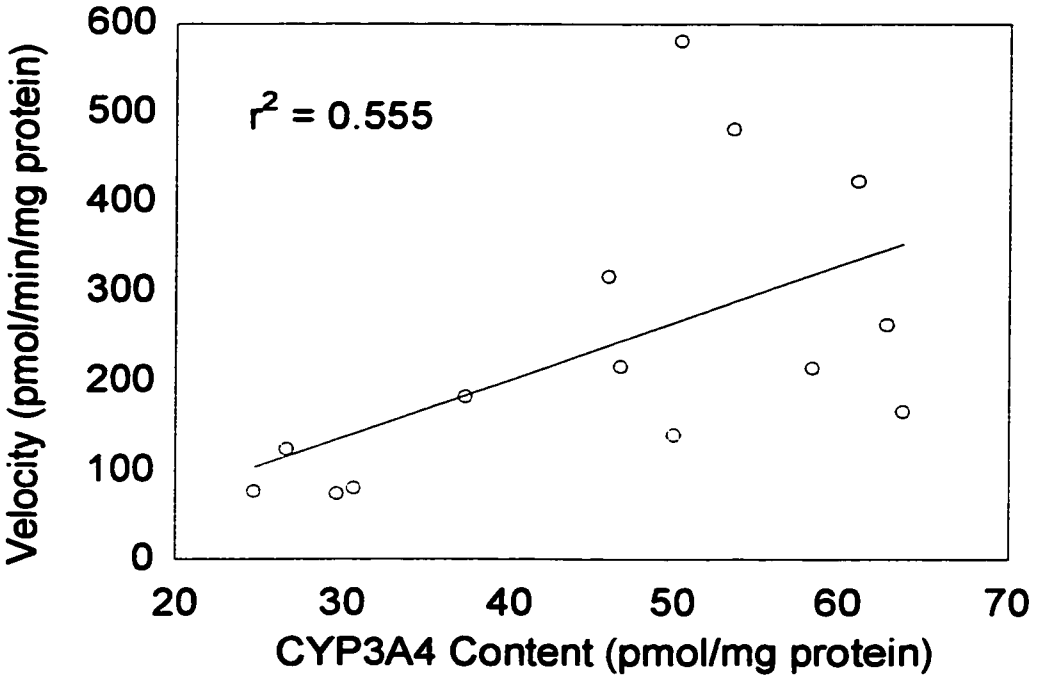

Figure 5.4. Correlation between CYP3A4 content and total midazolam reaction velocity in the control cohort. The line represents the best linear fit.

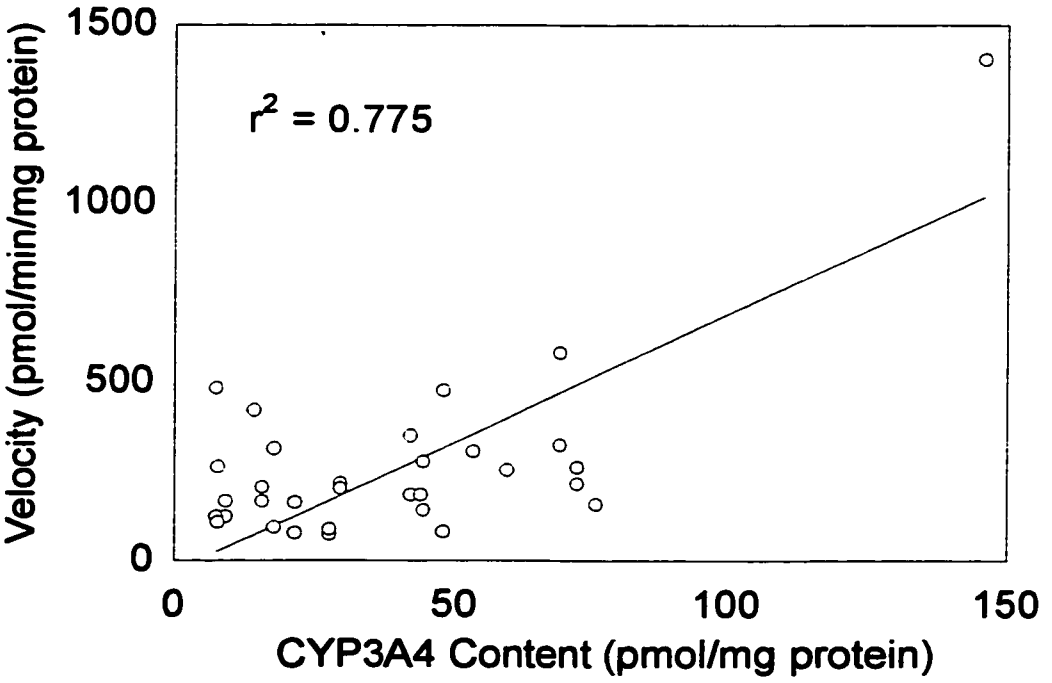

Figure 5.4A. Correlation between CYP3A4 content and total midazolam reaction velocity in the all samples. Blue circles denote control subjects, and red circles denote the cirrhotic subjects. The line represents the best linear fit.

Table 5.1. Cirrhotic Patient Demographics

Subject	*Age*	*Gender*	*Race*	*Diagnosis*
Cirrhotic 1	53	M	Caucasian	ALD
Cirrhotic 2	49	M	Caucasian	ALD/HCV
Cirrhotic 3	45	F	Caucasian	ALD/HCV
Cirrhotic 4	42	F	African-Amer.	HCV
Cirrhotic 5	54	M	Caucasian	ALD
Cirrhotic 6	44	M	Caucasian	ALD/HCV
Cirrhotic 7	54	M	Hispanic	ALD
Cirrhotic 8	58	F	Asian	HCV
Cirrhotic 9	52	F	Native Amer.	ALD/HCV
Cirrhotic 10	57	M	Caucasian	ALD
Cirrhotic 11	50	M	Caucasian	ALD
Cirrhotic 12	44	F	Caucasian	ALD/HCV
Cirrhotic 13	35	F	Caucasian	ALD
Cirrhotic 14	44	M	African-Amer.	ALD/HCV
Cirrhotic 15	65	M	Caucasian	ALD
Cirrhotic 16	44	M	Caucasian	ALD/HCV
Cirrhotic 17	47	M	Native Amer.	ALD
Cirrhotic 18	46	F	Caucasian	ALD/HCV
Cirrhotic 19	54	F	Caucasian	HCV
Cirrhotic 20	48	F	Caucasian	ALD/HCV

ALD, alcoholic liver disease present; HCV, Hepatitis C Virus present

Table 5.2. Control Patient Demographics

Subject	*Age*	*Gender*	*Race*	*Diagnosis*
Control 1	59	F	Caucasian	GERD
Control 2	53	F	Asian	GERD
Control 3	40	M	Hispanic	Low BP
Control 4	42	M	Caucasian	GERD
Control 5	56	M	Caucasian	GERD
Control 6	51	M	Caucasian	Diarrhea
Control 7	47	F	Caucasian	Barrett's
Control 8	57	M	Caucasian	GERD
Control 9	45	F	Caucasian	Inflammation
Control 10	45	M	Caucasian	Ulcer
Control 11	44	F	African-Amer.	GERD
Control 12	41	F	Caucasian	Bleeding
Control 13	52	M	Caucasian	Inflammation
Control 14	50	F	Caucasian	GERD

GERD, Gastroesophageal Reflux Disease; Low BP, decreased blood pressure; Barrett's, possible Barrett's esophagus

Table 5.3. Cirrhotic and control CYP3A4 content and activity values.

Cirrhotics			*Controls*		
CYP3A4 (pmol/mg)	*Velocity (pmol/min/mg)*	*1'-/4-OH Ratio*	*CYP3A4 (pmol/mg)*	*Velocity (pmol/min/mg)*	*1'-/4-OH Ratio*
42.4 ± 33.7	286 ± 297	5.86 ± 0.90	45.8 ± 13.8	238 ± 159	4.15 ± 2.50

All values are presented as mean ± s.d. The 1'-OH/4-OH midazolam ratio was calculated from reaction velocities.

CHAPTER 6

SUMMARY AND CONCLUSIONS

6.1 Summary and Conclusions

CYP3A4 and CYP3A5 comprise the majority of cytochromes P450 in both the liver and small intestine. Although the two enzymes share 84% amino acid sequence homology, the substrate specificity, affinity for substrates and regiospecificity in the metabolism of identical compounds can differ greatly. Since CYP3A4 and CYP3A5 metabolize over half of clinical medications cleared by biotransformation processes (Harris et al, 1995), the detailed metabolic differences between the two isoforms is a clinically relevant question.

There is high interindividual variability in the expression and activity of both CYP3A4 and CYP3A5 (~40-fold). Since CYP3A5 is a polymorphically expressed enzyme, the variability can be compounded in individuals that express considerable levels of both enzymes. Moreover, both enzymes are expressed in the small intestine and liver, which adds an additional level of variability compared to other P450 enzymes due to the addition of another clearance organ and discordant mechanisms of regulation (CYP3A4). Recently, the genetic polymorphisms responsible for the expression of CYP3A5 were uncovered (Kuehl et al, 2001). This information provides another tool for the elucidation of DNA sequence differences, and the ability to prospectively determine individuals in the population expressing at least one *CYP3A5*1* allele.

The overall goal of the investigations described in this dissertation was to better understand the disposition of midazolam when it is administered to humans, and to use midazolam as a tool in order to examine differences in metabolic specificity and

inhibitory potency between CYP3A4 and CYP3A5, and the effect of liver disease on intestinal CYP3A function. First, the biliary component of midazolam was assessed from biliary and fecal analysis after midazolam administration. Second, the interindividual variability and CYP3A5 impact on the midazolam 1'-OH/4-OH product ratio was determined. This allowed for the comparison between two enzymes that share a common substrate. Third, CYP3A4 and CYP3A5 were compared for their susceptibility to inhibition by compounds clinically relevant in CYP3A-dependent drug-drug interactions. These studies examined the possibility that the magnitude of single dose and steady-state drug-drug interactions will depend on the presence of CYP3A5 in liver and intestine. Fourth, the activity and content of intestinal CYP3A enzymes were compared in patients with cirrhosis of the liver. Patients with cirrhosis have a decreased hepatic drug-metabolizing capability, and therefore, examination of any alterations in intestinal CYP3A4/5 function would have important clinical implications.

Midazolam is a benzodiazepine sedative-hypnotic agent that has wide clinical use. It is well absorbed and is primarily metabolized to 1'-OH midazolam and 4-OH midazolam by CYP3A4 and CYP3A5. Recovery of the major metabolite, 1'-OH midazolam, in urine varies widely in the population (mean = 71%, range = 55-95) (Thummel et al, 1996). These observations could be explained by different degrees of metabolite formation, or possibly by different clearance mechanisms for the metabolite, such as biliary excretion. To address the issue of a biliary clearance pathway for midazolam, we (A) determined if midazolam or its metabolites were secreted into the

bile, and (B) addressed the issue of entero-hepatic recycling by assaying for midazolam or its metabolites in human feces. If fecal elimination was present, then secretion of midazolam into bile would constitute a true clearance mechanism. If, however, no midazolam metabolites were detected in feces, the bile would serve as a parallel reservoir to the plasma and behave as an additional distributive volume. In order to quantitatively detect midazolam metabolites in human feces, a solid phase extraction method was developed to remove matrix interferences and maintain a high level of instrument sensitivity.

Collection of bile from two patients undergoing liver transplant confirmed levels of 1'-OH midazolam glucuronide in the bile far greater than found in plasma, and comparable to concentrations found in urine. Analysis of human feces from two healthy volunteers receiving 1 mg midazolam intravenously, revealed that the feces was devoid of midazolam or its metabolic products. These findings suggest that 1'-OH midazolam glucuronide is secreted into bile, but that a large percentage of the excreted dose is reabsorbed (post-hydrolysis) upon biliary presentation to the lumen of the small intestine.

Once it was determined that the clearance of 1'-OH midazolam was almost exclusively via the kidney, we used midazolam as a probe to discern whether interindividual regiospecific metabolic differences in the oxidation of midazolam could explain the variable urinary 1'-OH midazolam recovery. Previous investigators revealed the preference of CYP3A5 to form 1'-OH midazolam compared to the 4-OH

product (Gorski et al, 1994; Paine et al, 1997). However, neither study was able to accurately address the regioselectivity due to small sample sizes.

To address the interindividual differences in the formation of 1'-OH midazolam and 4-OH midazolam, and the impact of CYP3A5 on the metabolic ratio, we examined the 1'-OH/4-OH metabolic ratios in a panel of 60 human liver microsomes. To address any concentration dependence that may exist due to cooperativity often observed in CYP3A-dependent oxidations (Ueng et al, 1997), three midazolam concentrations were used to approximate plasma (0.5 μM), enterocyte (40 μM) and intermediate (8 μM) levels. Concentration dependent metabolic ratios were observed in the microsomal panel. As the concentration of midazolam increased, the 1'-OH/4-OH ratio decreased. Midazolam 1'-hydroxylation became saturated at lower concentrations of substrate. As midazolam levels increased, so did the effectiveness of CYP3A4 and CYP3A5 to form 4-OH midazolam. This presumably is the result of multiple binding conformations within either enzyme active site.

CYP3A5 also had a significant impact on the 1'-OH/4-OH ratio, as livers expressing both CYP3A5 and CYP3A4 had higher metabolic ratios that were statistically significant. Thus, individuals who carry the *CYP3A5*1* allele are more likely to exhibit higher urinary 1'-OH midazolam recoveries.

Due to the large number of compounds that are metabolized by CYP3A4 and CYP3A5, there is a higher probability of drug-drug interactions than with other drug-metabolizing enzymes. Although extensive drug interaction databases exist, it is difficult to predict the degree of a drug-drug interaction, especially when the activity in

the biotransformation process is so variable. We suspect that some of this variability is due to metabolic clearance of CYP3A substrates by two different enzymes: CYP3A4 and CYP3A5. To address this, we examined the reversible as well as time-dependent inhibition of CYP3A4 and CYP3A5 microsomes and cDNA-expressed isoforms with a series of clinically relevant inhibitors of CYP3A (erythromycin, ketoconazole, diltiazem and nicardipine).

IC_{50} values were calculated in microsomes from 20 livers that contained no detectable CYP3A5, and from 15 livers that contained varying amount of CYP3A5 in addition to CYP3A4. Erythromycin and ketoconazole exhibited higher affinities toward CYP3A4 compared to CYP3A5, whereas the effect was more modest with diltiazem and nicardipine.

Time-dependent experiments revealed that CYP3A5 is inactivated at a slower rate than CYP3A4, and less of the enzyme becomes inactivated for 3 of the inhibitors tested (ketoconazole does not inhibit in a time-dependent manner). MI-complex formation was minimal for CYP3A5-containing microsomes and for the recombinant form as well. However, when CYP3A5 was co-incubated with CYP3A4, a more intense MI-complex was formed suggesting that CYP3A4 can influence the inactivation of CYP3A5. These data suggest that individuals expressing high levels of CYP3A5 may be relatively resistant to the inhibitory effects of erythromycin. However, if sufficient CYP3A4 is co-expressed, CYP3A4 may accelerate the inactivation of CYP3A5.

The previous studies involved different metabolic capabilities between CYP3A isoforms in healthy tissues. The next hypothesis we examined involved CYP3A expression in the cirrhotic disease state. Cirrhosis reduces the oxidative drug metabolizing capability of the liver, but limited data exist regarding the ability of the small intestine to metabolize drugs in patients with cirrhosis. If the liver has impaired function in cirrhosis, the small intestine's role becomes that much more important. We conducted a study with 20 patients exhibiting mild to moderate cirrhosis and collected pinch biopsies of the duodenum. The biopsies were homogenized and assayed for metabolic activity towards midazolam, and for CYP3A4 and CYP3A5 content. Control subjects (n = 14) were matched for age, gender and ethnicity. A comparison of data between the cirrhotic and control group showed no difference in intestinal CYP3A4 content or activity, although the cirrhotic group results were highly variable compared to controls. A similar range of variability was seen with intestines isolated intra-operatively from organ donors. Together, this suggests that intestinal CYP3A4 is susceptible to both up- and down-regulation by endogenous factors whose levels (circulatory or local) are perturbed by pathophysiological states. Greater interindividual variability in the oral clearance of high extraction CYP3A substrates is expected in patients with cirrhosis and other chronic diseases in comparison with healthy subjects.

Another interesting finding was that a higher 1'-OH/4-OH product ratio was observed in the cirrhotic group ($p < 0.05$). CYP3A5 levels were too low to be a factor, so other mechanisms are likely responsible for this finding. In summary, cirrhosis has

a deleterious effect on hepatic oxidative drug metabolism; however, these data suggest that mean intestinal activity is spared.

In conclusion, CYP3A5 appears to behave differently than CYP3A4 in both metabolic regioselectivity and in response to enzyme inhibitors, although both enzymes catalyze the metabolism of many drugs. Hopefully, knowledge of CYP3A5 expression and total CYP3A activity will allow for drug dosing regimens that are safer and without adverse effects. *A priori* knowledge of drug metabolizing activity may improve the likelihood of designing safer drug regimens.

LIST OF REFERENCES

Ahonen, J., Olkkola, K.T., Salmenpera, M., Hynynen, M. & Neuvonen, P.J. (1996). Effect of diltiazem on midazolam and alfentanil disposition in patients undergoing coronary artery bypass grafting. *Anesthesiology*, **85,** 1246-52.

Aoyama, T., Yamano, S., Waxman, D.J., Lapenson, D.P., Meyer, U.A., Fischer, V., Tyndale, R., Inaba, T., Kalow, W., Gelboin, H.V. & et al. (1989). Cytochrome P-450 hPCN3, a novel cytochrome P-450 IIIA gene product that is differentially expressed in adult human liver. cDNA and deduced amino acid sequence and distinct specificities of cDNA-expressed hPCN1 and hPCN3 for the metabolism of steroid hormones and cyclosporine. *J Biol Chem*, **264,** 10388-95.

Artursson, P. (1991). Cell cultures as models for drug absorption across the intestinal mucosa. *Crit Rev Ther Drug Carrier Syst*, **8,** 305-30.

Baarnhielm, C., Dahlback, H. & Skanberg, I. (1986). In vivo pharmacokinetics of felodipine predicted from in vitro studies in rat, dog and man. *Acta Pharmacol Toxicol (Copenh)*, **59,** 113-22.

Back, D.J. & Tjia, J.F. (1991). Comparative effects of the antimycotic drugs ketoconazole, fluconazole, itraconazole and terbinafine on the metabolism of cyclosporin by human liver microsomes. *Br J Clin Pharmacol*, **32,** 624-6.

Bailey, D.G., Spence, J.D., Munoz, C. & Arnold, J.M. (1991). Interaction of citrus juices with felodipine and nifedipine. *Lancet*, **337,** 268-9.

Ball, S.E., Scatina, J., Kao, J., Ferron, G.M., Fruncillo, R., Mayer, P., Weinryb, I., Guida, M., Hopkins, P.J., Warner, N. & Hall, J. (1999). Population distribution and effects on drug metabolism of a genetic variant in the 5' promoter region of CYP3A4. *Clin Pharmacol Ther*, **66,** 288-94.

Basaran, N., Doebler, R.W., Goldston, H. & Holloway, P.W. (1999). Effect of lipid unsaturation on the binding of native and a mutant form of cytochrome b5 to membranes. *Biochemistry*, **38,** 15245-52.

Bass, L., Robinson, P. & Bracken, A.J. (1978). Hepatic elimination of flowing substrates: the distributed model. *J Theor Biol*, **72,** 161-84.

Bauer, T.M., Ritz, R., Haberthur, C., Ha, H.R., Hunkeler, W., Sleight, A.J., Scollo-Lavizzari, G. & Haefeli, W.E. (1995). Prolonged sedation due to accumulation of conjugated metabolites of midazolam. *Lancet*, **346,** 145-7.

Baune, B., Flinois, J.P., Furlan, V., Gimenez, F., Taburet, A.M., Becquemont, L. & Farinotti, R. (1999). Halofantrine metabolism in microsomes in man: major role of CYP 3A4 and CYP 3A5. *J Pharm Pharmacol*, **51,** 419-26.

Bensoussan, C., Delaforge, M. & Mansuy, D. (1995). Particular ability of cytochromes P450 3A to form inhibitory P450-iron-metabolite complexes upon metabolic oxidation of aminodrugs. *Biochem Pharmacol*, **49,** 591-602.

Berger, U., Wilson, P., McClelland, R.A., Colston, K., Haussler, M.R., Pike, J.W. & Coombes, R.C. (1988). Immunocytochemical detection of 1,25-dihydroxyvitamin D receptors in normal human tissues. *J Clin Endocrinol Metab*, **67,** 607-13.

Bikle, D.D., Gee, E., Halloran, B. & Haddad, J.G. (1984). Free 1,25-dihydroxyvitamin D levels in serum from normal subjects, pregnant subjects, and subjects with liver disease. *J Clin Invest*, **74,** 1966-71.

Bleau, A.M., Levitchi, M.C., Maurice, H. & du Souich, P. (2000). Cytochrome P450 inactivation by serum from humans with a viral infection and serum from rabbits with a turpentine-induced inflammation: the role of cytokines. *Br J Pharmacol*, **130,** 1777-84.

Bonkovsky, H.L., Hauri, H.P., Marti, U., Gasser, R. & Meyer, U.A. (1985). Cytochrome P450 of small intestinal epithelial cells. Immunochemical characterization of the increase in cytochrome P450 caused by phenobarbital. *Gastroenterology*, **88,** 458-67.

Colburn, W.A. (1979). A pharmacokinetic model to differentiate preabsorptive, gut epithelial, and hepatic first-pass metabolism. *J Pharmacokinet Biopharm*, **7,** 407-15.

de Waziers, I., Cugnenc, P.H., Yang, C.S., Leroux, J.P. & Beaune, P.H. (1990). Cytochrome P 450 isoenzymes, epoxide hydrolase and glutathione transferases in rat and human hepatic and extrahepatic tissues. *J Pharmacol Exp Ther*, **253,** 387-94.

Domanski, T.L., Finta, C., Halpert, J.R. & Zaphiropoulos, P.G. (2001). cDNA cloning and initial characterization of CYP3A43, a novel human cytochrome P450. *Mol Pharmacol*, **59,** 386-92.

Dundee, J.W., Halliday, N.J., Harper, K.W. & Brogden, R.N. (1984). Midazolam. A review of its pharmacological properties and therapeutic use. *Drugs*, **28,** 519-43.

Eiselt, R., Domanski, T.L., Zibat, A., Mueller, R., Presecan-Siedel, E., Hustert, E., Zanger, U.M., Brockmoller, J., Klenk, H.P., Meyer, U.A., Khan, K.K., He, Y.A., Halpert, J.R. & Wojnowski, L. (2001). Identification and functional characterization of eight CYP3A4 protein variants. *Pharmacogenetics*, **11,** 447-58.

Fabre G, R.R., Placidi M, Combalbert J, Covo J, Cano JP, Coulange C, Ducros M, Rampal M. (1988). Characterization of midazolam metabolism using human hepatic microsomal fractions and hepatocytes in suspension obtained by perfusing whole human livers. *Biochem Pharmacol*, **37,** 4389-97.

Fisher, J.M., Wrighton, S.A., Calamia, J.C., Shen, D.D., Kunze, K.L. & Thummel, K.E. (1999). Midazolam metabolism by modified Caco-2 monolayers: effects of extracellular protein binding. *J Pharmacol Exp Ther*, **289,** 1143-50.

Fleishaker, J.C., Pearson, P.G., Wienkers, L.C., Pearson, L.K. & Peters, G.R. (1996). Biotransformation of tirilazad in human: 2. Effect of ketoconazole on tirilazad clearance and oral bioavailability. *J Pharmacol Exp Ther*, **277,** 991-8.

Freiberg, L.A. (1973). N-demethylation of 3-amino macrolides. USA.

Gallagher, E.P., Kunze, K.L., Stapleton, P.L. & Eaton, D.L. (1996). The kinetics of aflatoxin B1 oxidation by human cDNA-expressed and human liver microsomal cytochromes P450 1A2 and 3A4. *Toxicol Appl Pharmacol*, **141,** 595-606.

Gascon, M.P. & Dayer, P. (1991). In vitro forecasting of drugs which may interfere with the biotransformation of midazolam. *Eur J Clin Pharmacol*, **41,** 573-8.

Gellner, K., Eiselt, R., Hustert, E., Arnold, H., Koch, I., Haberl, M., Deglmann, C.J., Burk, O., Buntefuss, D., Escher, S., Bishop, C., Koebe, H.G., Brinkmann, U., Klenk, H.P., Kleine, K., Meyer, U.A. & Wojnowski, L. (2001). Genomic organization of the human CYP3A locus: identification of a new, inducible CYP3A gene. *Pharmacogenetics*, **11,** 111-21.

George, J., Murray, M., Byth, K. & Farrell, G.C. (1995). Differential alterations of cytochrome P450 proteins in livers from patients with severe chronic liver disease. *Hepatology*, **21,** 120-8.

Gerecke, M. (1983). Chemical structure and properties of midazolam compared with other benzodiazepines. *Br J Clin Pharmacol*, **16,** 11S-16S.

Gervot , L., Carriere, V., Costet, P., Cugnene, P.-H., Berger, A., Beaune, P.H. & de Waziers, I. (1996). CYP3A5 is the major cytochrome P450 expressed in human colon and colonic cell lines. *Environ Tox Pharmacol*, **2,** 381-388.

Gibaldi, M. & Perrier, D. (1982). *Pharmacokinetics*. New York, NY Basel, Switzerland: Marcel Dekker, Inc.

Gibbs, M.A., Thummel, K.E., Shen, D.D. & Kunze, K.L. (1999). Inhibition of cytochrome P-450 3A (CYP3A) in human intestinal and liver microsomes: comparison of Ki values and impact of CYP3A5 expression. *Drug Metab Dispos*, **27,** 180-7.

Gillam, E.M., Guo, Z., Ueng, Y.F., Yamazaki, H., Cock, I., Reilly, P.E., Hooper, W.D. & Guengerich, F.P. (1995). Expression of cytochrome P450 3A5 in Escherichia coli: effects of 5' modification, purification, spectral characterization, reconstitution conditions, and catalytic activities. *Arch Biochem Biophys*, **317,** 374-84.

Gomez, D.Y., Wacher, V.J., Tomlanovich, S.J., Hebert, M.F. & Benet, L.Z. (1995). The effects of ketoconazole on the intestinal metabolism and bioavailability of cyclosporine. *Clin Pharmacol Ther*, **58,** 15-9.

Goodman, L.S., Gilman, A., Hardman, J.G., Gilman, A.G., Limbird, L.E., Molinoff, P.B. & Ruddon, R.W. (2001). *Goodman & Gilman's the pharmacological basis of therapeutics*. New York: McGraw-Hill Health Professions Division.

Gorski, J.C., Hall, S.D., Jones, D.R., VandenBranden, M. & Wrighton, S.A. (1994). Regioselective biotransformation of midazolam by members of the human cytochrome P450 3A (CYP3A) subfamily. *Biochem Pharmacol*, **47,** 1643-53.

Gorski, J.C., Jones, D.R., Haehner-Daniels, B.D., Hamman, M.A., O'Mara, E.M., Jr. & Hall, S.D. (1998). The contribution of intestinal and hepatic CYP3A to the interaction between midazolam and clarithromycin. *Clin Pharmacol Ther*, **64,** 133-43.

Gorski, J.C., Chalasani, N., Patel, N., Galinsky, R.E., Craven, R. & Hall, S.D. (2001). Hepatic and Intestinal CYP3A Activity in Cirrhotics wit hTransjugular Intrahepatic Shunts (TIPS). In *2001 Annual Meeting of the American Society for Clinical Pharmacology and Therapeutics*. Orlando, FL: Mosby.

Gray, M.R. & Tam, Y.K. (1987). The series-compartment model for hepatic elimination. *Drug Metab Dispos*, **15,** 27-31.

Greenblatt, D.J., von Moltke, L.L., Harmatz, J.S., Counihan, M., Graf, J.A., Durol, A.L., Mertzanis, P., Duan, S.X., Wright, C.E. & Shader, R.I. (1998). Inhibition of triazolam clearance by macrolide antimicrobial agents: in vitro correlates and dynamic consequences. *Clin Pharmacol Ther*, **64,** 278-85.

Greenblatt, D.J., von Moltke, L.L., Harmatz, J.S., Mertzanis, P., Graf, J.A., Durol, A.L., Counihan, M., Roth-Schechter, B. & Shader, R.I. (1998). Kinetic and dynamic interaction study of zolpidem with ketoconazole, itraconazole, and fluconazole. *Clin Pharmacol Ther*, **64,** 661-71.

Greenblatt, D.J., Wright, C.E., von Moltke, L.L., Harmatz, J.S., Ehrenberg, B.L., Harrel, L.M., Corbett, K., Counihan, M., Tobias, S. & Shader, R.I. (1998). Ketoconazole inhibition of triazolam and alprazolam clearance: differential kinetic and dynamic consequences. *Clin Pharmacol Ther*, **64,** 237-47.

Guardiola, J., Xiol, X. & Nolla, J.M. (2000). Influence of vitamin D receptor gene polymorphism on bone mineral density in primary biliary cirrhosis. *Gastroenterology*, **119,** 599-600.

Guengerich, F.P. & Turvy, C.G. (1991). Comparison of levels of several human microsomal cytochrome P-450 enzymes and epoxide hydrolase in normal and disease states using immunochemical analysis of surgical liver samples. *J Pharmacol Exp Ther*, **256,** 1189-94.

Haehner, B.D., Gorski, J.C., Vandenbranden, M., Wrighton, S.A., Janardan, S.K., Watkins, P.B. & Hall, S.D. (1996). Bimodal distribution of renal cytochrome P450 3A activity in humans. *Mol Pharmacol*, **50,** 52-9.

Harris, R.Z., Benet, L.Z. & Schwartz, J.B. (1995). Gender effects in pharmacokinetics and pharmacodynamics. *Drugs*, **50,** 222-39.

Heinig, R., Adelmann, H.G. & Ahr, G. (1999). The effect of ketoconazole on the pharmacokinetics, pharmacodynamics and safety of nisoldipine. *Eur J Clin Pharmacol*, **55,** 57-60.

Heizmann, P. & Ziegler, W.H. (1981). Excretion and metabolism of 14C-midazolam in humans following oral dosing. *Arzneimittelforschung*, **31,** 2220-3.

Hellstern, A., Hildebrand, M., Humpel, M., Hellenbrecht, D., Saller, R. & Madetzki, C. (1990). Minimal biliary excretion and enterohepatic recirculation of lormetazepam in man as investigated by a new nasobiliary drainage technique. *Int J Clin Pharmacol Ther Toxicol*, **28,** 256-61.

Hildebrandt, A. & Estabrook, R.W. (1971). Evidence for the participation of cytochrome b 5 in hepatic microsomal mixed-function oxidation reactions. *Arch Biochem Biophys*, **143,** 66-79.

Ho, K.J., Ho, L.H. & Kruger, O.R. (1979). Characterization and determination of the activity of biliary beta-glucuronidase in rats. *J Lab Clin Med*, **93,** 916-25.

Hodgson, S.F., Dickson, E.R., Eastell, R., Eriksen, E.F., Bryant, S.C. & Riggs, B.L. (1993). Rates of cancellous bone remodeling and turnover in osteopenia associated with primary biliary cirrhosis. *Bone*, **14,** 819-27.

Honig, P.K., Wortham, D.C., Zamani, K., Conner, D.P., Mullin, J.C. & Cantilena, L.R. (1993). Terfenadine-ketoconazole interaction. Pharmacokinetic and electrocardiographic consequences. *Jama*, **269,** 1513-8.

Horvath, T., Par, A., Past, T., Bero, T., Tapsonyi, Z. & Kadas, I. (1986). Disorders of biotransformation during the progression of alcoholic liver disease. *Acta Med Hung*, **43,** 351-7.

Ilett, K.F., Tee, L.B., Reeves, P.T. & Minchin, R.F. (1990). Metabolism of drugs and other xenobiotics in the gut lumen and wall. *Pharmacol Ther*, **46,** 67-93.

Janardan, S.K., Lown, K.S., Schmiedlin-Ren, P., Thummel, K.E. & Watkins, P.B. (1996). Selective expression of CYP3A5 and not CYP3A4 in human blood. *Pharmacogenetics*, **6,** 379-85.

Jones, D.R., Gorski, J.C., Hamman, M.A., Mayhew, B.S., Rider, S. & Hall, S.D. (1999). Diltiazem inhibition of cytochrome P-450 3A activity is due to metabolite intermediate complex formation. *J Pharmacol Exp Ther*, **290,** 1116-25.

Jounaidi, Y., Hyrailles, V., Gervot, L. & Maurel, P. (1996). Detection of CYP3A5 allelic variant: a candidate for the polymorphic expression of the protein? *Biochem Biophys Res Commun*, **221,** 466-70.

Kanamitsu, S., Ito, K., Green, C.E., Tyson, C.A., Shimada, N. & Sugiyama, Y. (2000). Prediction of in vivo interaction between triazolam and erythromycin based on in vitro studies using human liver microsomes and recombinant human CYP3A4. *Pharm Res*, **17,** 419-26.

Katoh, M., Nakajima, M., Shimada, N., Yamazaki, H. & Yokoi, T. (2000). Inhibition of human cytochrome P450 enzymes by 1,4-dihydropyridine calcium antagonists: prediction of in vivo drug-drug interactions. *Eur J Clin Pharmacol*, **55,** 843-52.

Keppler, D., Konig, J. & Buchler, M. (1997). The canalicular multidrug resistance protein, cMRP/MRP2, a novel conjugate export pump expressed in the apical membrane of hepatocytes. *Adv Enzyme Regul*, **37,** 321-33.

Keyes, S.R., Alfano, J.A., Jansson, I. & Cinti, D.L. (1979). Rat liver microsomal elongation of fatty acids. Possible involvement of cytochrome b5. *J Biol Chem*, **254,** 7778-84.

Kivisto, K.T., Bookjans, G., Fromm, M.F., Griese, E.U., Munzel, P. & Kroemer, H.K. (1996). Expression of CYP3A4, CYP3A5 and CYP3A7 in human duodenal tissue. *Br J Clin Pharmacol*, **42,** 387-9.

Klippert, P.J. & Noordhoek, J. (1983). Influence of administration route and blood sampling site on the area under the curve. Assessment of gut wall, liver, and lung metabolism from a physiological model. *Drug Metab Dispos*, **11,** 62-6.

Kolars, J.C., Schmiedlin-Ren, P., Schuetz, J.D., Fang, C. & Watkins, P.B. (1992). Identification of rifampin-inducible P450IIIA4 (CYP3A4) in human small bowel enterocytes. *J Clin Invest*, **90,** 1871-8.

Kolars, J.C., Lown, K.S., Schmiedlin-Ren, P., Ghosh, M., Fang, C., Wrighton, S.A., Merion, R.M. & Watkins, P.B. (1994). CYP3A gene expression in human gut epithelium. *Pharmacogenetics*, **4,** 247-59.

Koritz, G.D., Bourne, D.W., Hunt, J.P., Prasad, V.I., Bevill, R.F. & Gautam, S.R. (1981). Pharmacokinetics of theophylline in swine: a potential model for human drug bioavailability studies. *J Vet Pharmacol Ther*, **4,** 233-9.

Korzekwa, K.R., Krishnamachary, N., Shou, M., Ogai, A., Parise, R.A., Rettie, A.E., Gonzalez, F.J. & Tracy, T.S. (1998). Evaluation of atypical cytochrome P450 kinetics with two-substrate models: evidence that multiple substrates can simultaneously bind to cytochrome P450 active sites. *Biochemistry*, **37,** 4137-47.

Kronbach, T., Mathys, D., Umeno, M., Gonzalez, F.J. & Meyer, U.A. (1989). Oxidation of midazolam and triazolam by human liver cytochrome P450IIIA4. *Mol Pharmacol*, **36,** 89-96.

Kuehl, P., Zhang, J., Lin, Y., Lamba, J., Assem, M., Schuetz, J., Watkins, P.B., Daly, A., Wrighton, S.A., Hall, S.D., Maurel, P., Relling, M., Brimer, C., Yasuda, K., Venkataramanan, R., Strom, S., Thummel, K., Boguski, M.S. & Schuetz, E. (2001). Sequence diversity in CYP3A promoters and characterization of the genetic basis of polymorphic CYP3A5 expression. *Nat Genet*, **27,** 383-391.

Lamba, J.T., Lin, Y.S., Thummel, K.E., Daly, A., Watkins, P.B., Strom, S., Zhang, J. & Schuetz, E.G. (2001). Common Allelic Variants of Cytochrome P4503A4 and thier Prevalence in Different Populations. *Pharmacogenetics*, **In press**.

Lampen, A., Christians, U., Guengerich, F.P., Watkins, P.B., Kolars, J.C., Bader, A., Gonschior, A.K., Dralle, H., Hackbarth, I. & Sewing, K.F. (1995). Metabolism of the immunosuppressant tacrolimus in the small intestine: cytochrome P450, drug interactions, and interindividual variability. *Drug Metab Dispos*, **23,** 1315-24.

Lampen, A., Christians, U., Gonschior, A.K., Bader, A., Hackbarth, I., von Engelhardt, W. & Sewing, K.F. (1996). Metabolism of the macrolide immunosuppressant, tacrolimus, by the pig gut mucosa in the Ussing chamber. *Br J Pharmacol*, **117,** 1730-4.

Lee, A.J., Kosh, J.W., Conney, A.H. & Zhu, B.T. (2001). Characterization of the NADPH-dependent metabolism of 17beta-estradiol to multiple metabolites by human liver microsomes and selectively expressed human cytochrome P450 3A4 and 3A5. *J Pharmacol Exp Ther*, **298,** 420-32.

Lehmann, J.M., McKee, D.D., Watson, M.A., Willson, T.M., Moore, J.T. & Kliewer, S.A. (1998). The human orphan nuclear receptor PXR is activated by compounds that regulate CYP3A4 gene expression and cause drug interactions. *J Clin Invest*, **102,** 1016-23.

Lin, Y.S., Lockwood, G., Graham, M., Brian, W., Loi, C., Dobrinska, D.R., Shen, D.D., Watkins, P.B., Wilkinson, G.R., Kharasch, E.D. & Thummel, K.E. (2001). In Vivo Phenotyping for CYP3A by a Single-Point Determination of Midazolam Plasma Concentration. *Pharmacogenetics*, **In Press**.

Lown, K.S., Kolars, J.C., Thummel, K.E., Barnett, J.L., Kunze, K.L., Wrighton, S.A. & Watkins, P.B. (1994). Interpatient heterogeneity in expression of CYP3A4 and CYP3A5 in small bowel. Lack of prediction by the erythromycin breath test. *Drug Metab Dispos*, **22,** 947-55.

Lown, K.S., Bailey, D.G., Fontana, R.J., Janardan, S.K., Adair, C.H., Fortlage, L.A., Brown, M.B., Guo, W. & Watkins, P.B. (1997). Grapefruit juice increases felodipine oral availability in humans by decreasing intestinal CYP3A protein expression. *J Clin Invest*, **99,** 2545-53.

Lowry, O.H., Rosebrough, N.J., Farr, A.L. & Randal, l.R.J. (1951). Protein measurement with the Folin phenol reagent. *J Biol Chem*, **193,** 265-75.

Ma, B., Prueksaritanont, T. & Lin, J.H. (2000). Drug interactions with calcium channel blockers: possible involvement of metabolite-intermediate complexation with CYP3A. *Drug Metab Dispos*, **28,** 125-30.

Madon, J., Hagenbuch, B., Landmann, L., Meier, P.J. & Stieger, B. (2000). Transport function and hepatocellular localization of mrp6 in rat liver. *Mol Pharmacol*, **57,** 634-41.

McLean, A.J. & Morgan, D.J. (1991). Clinical pharmacokinetics in patients with liver disease. *Clin Pharmacokinet*, **21,** 42-69.

Mirghani, R.A., Hellgren, U., Westerberg, P.A., Ericsson, O., Bertilsson, L. & Gustafsson, L.L. (1999). The roles of cytochrome P450 3A4 and 1A2 in the 3-hydroxylation of quinine in vivo. *Clin Pharmacol Ther*, **66,** 454-60.

Mistry, M. & Houston, J.B. (1987). Glucuronidation in vitro and in vivo. Comparison of intestinal and hepatic conjugation of morphine, naloxone, and buprenorphine. *Drug Metab Dispos*, **15,** 710-7.

Montellano, P.R.O.d. (1995). *Cytochrome P450: Structure, Mechanism and Biochemistry*. New York, NY: Plenum Press.

Ochs, H.R., Greenblatt, D.J., Eichelkraut, W., Bakker, C., Gobel, R. & Hahn, N. (1987). Hepatic vs. gastrointestinal presystemic extraction of oral midazolam and flurazepam. *J Pharmacol Exp Ther*, **243,** 852-6.

Olkkola, K.T., Aranko, K., Luurila, H., Hiller, A., Saarnivaara, L., Himberg, J.J. & Neuvonen, P.J. (1993). A potentially hazardous interaction between erythromycin and midazolam. *Clin Pharmacol Ther*, **53,** 298-305.

Olkkola, K.T., Backman, J.T. & Neuvonen, P.J. (1994). Midazolam should be avoided in patients receiving the systemic antimycotics ketoconazole or itraconazole. *Clin Pharmacol Ther*, **55,** 481-5.

Omura, T. & Sato, R. (1964). The carbon monoxide-binding pigment of liver microsomes. I. Evidence for its hemoprotein nature. *J Biol Chem*, **239,** 2370-2378.

Paine, M.F., Shen, D.D., Kunze, K.L., Perkins, J.D., Marsh, C.L., McVicar, J.P., Barr, D.M., Gillies, B.S. & Thummel, K.E. (1996). First-pass metabolism of midazolam by the human intestine. *Clin Pharmacol Ther*, **60,** 14-24.

Paine, M.F. (1997a). Intestinal Versus Hepatic CYP3A-Dependent First-Pass Metabolism. In *Pharmaceutics*. pp. 207. Seattle: University of Washington.

Paine, M.F., Khalighi, M., Fisher, J.M., Shen, D.D., Kunze, K.L., Marsh, C.L., Perkins, J.D. & Thummel, K.E. (1997b). Characterization of interintestinal and intraintestinal variations in human CYP3A-dependent metabolism. *J Pharmacol Exp Ther*, **283,** 1552-62.

Pappo, A. & Apostolescu, I. (1967). [Enzyme activity of bile]. *Stud Cercet Med Interna*, **8,** 205-9.

Pentikainen, P.J., Valisalmi, L., Himberg, J.J. & Crevoisier, C. (1989). Pharmacokinetics of midazolam following intravenous and oral administration in patients with chronic liver disease and in healthy subjects. *J Clin Pharmacol*, **29,** 272-7.

Periti, P., Mazzei, T., Mini, E. & Novelli, A. (1992). Pharmacokinetic drug interactions of macrolides. *Clin Pharmacokinet*, **23,** 106-31.

Perret, A. & Pompon, D. (1998). Electron shuttle between membrane-bound cytochrome P450 3A4 and b5 rules uncoupling mechanisms. *Biochemistry*, **37,** 11412-24.

Pershing, L.K. & Franklin, M.R. (1982). Cytochrome P-450 metabolic-intermediate complex formation and induction by macrolide antibiotics; a new class of agents. *Xenobiotica*, **12,** 687-99.

Pichard, L., Fabre, I., Fabre, G., Domergue, J., Saint Aubert, B., Mourad, G. & Maurel, P. (1990). Cyclosporin A drug interactions. Screening for inducers and inhibitors of cytochrome P-450 (cyclosporin A oxidase) in primary cultures of human hepatocytes and in liver microsomes. *Drug Metab Dispos*, **18,** 595-606.

Podoll, T.D. (1996). Defining the use of midazolam as a probe of CYP3A4 activity : sensitive quantitation of the metabolites and characterization of mechanism-based inactivation. In *Medicinal Chemistry*. Seattle, WA: University of Washington.

Pond, S.M. & Tozer, T.N. (1984). First-pass elimination. Basic concepts and clinical consequences. *Clin Pharmacokinet*, **9,** 1-25.

Porter, W.R., Branchflower, R.V. & Trager, W.F. (1977). A kinetic method for the determination of the multiple forms of microsomal cytochrome P-450. *Biochem Pharmacol*, **26,** 549-50.

Regardh, C.G., Edgar, B., Olsson, R., Kendall, M., Collste, P. & Shansky, C. (1989). Pharmacokinetics of felodipine in patients with liver disease. *Eur J Clin Pharmacol*, **36,** 473-9.

Remmel, R.P. & Elmer, G.W. (1981). The effect of broad-spectrum antibiotics on warfarin excretion and metabolism in the rat. *Res Commun Chem Pathol Pharmacol*, **34,** 503-14.

Resnick, R.H. & Chopra, S. (2000). Vitamin D receptor gene analysis in primary biliary cirrhosis. *Gastroenterology*, **119,** 1805.

Roberts, M.S. & Rowland, M. (1985). Hepatic elimination--dispersion model. *J Pharm Sci*, **74,** 585-7.

Rowland, M., Benet, L.Z. & Graham, G.G. (1973). Clearance concepts in pharmacokinetics. *J Pharmacokinet Biopharm*, **1,** 123-36.

Sata, F., Sapone, A., Elizondo, G., Stocker, P., Miller, V.P., Zheng, W., Raunio, H., Crespi, C.L. & Gonzalez, F.J. (2000). CYP3A4 allelic variants with amino acid substitutions in exons 7 and 12: evidence for an allelic variant with altered catalytic activity. *Clin Pharmacol Ther*, **67,** 48-56.

Schenkman, J.B. & Jansson, I. (1999). Interactions between cytochrome P450 and cytochrome b5. *Drug Metab Rev*, **31,** 351-64.

Schmider, J., Brockmoller, J., Arold, G., Bauer, S. & Roots, I. (1999). Simultaneous assessment of CYP3A4 and CYP1A2 activity in vivo with alprazolam and caffeine. *Pharmacogenetics*, **9,** 725-34.

Schmiedlin-Ren, P., Thummel, K.E., Fisher, J.M., Paine, M.F., Lown, K.S. & Watkins, P.B. (1997). Expression of enzymatically active CYP3A4 by Caco-2 cells grown on extracellular matrix-coated permeable supports in the presence of 1alpha,25-dihydroxyvitamin D3. *Mol Pharmacol*, **51,** 741-54.

Schrag, M.L. & Wienkers, L.C. (2001). Covalent alteration of the CYP3A4 active site: evidence for multiple substrate binding domains. *Arch Biochem Biophys*, **391,** 49-55.

Schuetz, J.D., Kauma, S. & Guzelian, P.S. (1993). Identification of the fetal liver cytochrome CYP3A7 in human endometrium and placenta. *J Clin Invest*, **92,** 1018-24.

Schwartz, S., Brater, D.C., Pound, D., Green, P.K., Kramer, W.G. & Rudy, D. (1993). Bioavailability, pharmacokinetics, and pharmacodynamics of torsemide in patients with cirrhosis. *Clin Pharmacol Ther*, **54,** 90-7.

Segel, I.H. (1975). *Enzyme Kinetics: Behavior and Analysis of Rapid Equilibrium and Steady-State Enzyme Systems*: Wiley and Sons.

Shimada, T., Yamazaki, H., Mimura, M., Inui, Y. & Guengerich, F.P. (1994). Interindividual variations in human liver cytochrome P-450 enzymes involved in the oxidation of drugs, carcinogens and toxic chemicals: studies with liver microsomes of 30 Japanese and 30 Caucasians. *J Pharmacol Exp Ther*, **270,** 414-23.

Shimakata, T., Mihara, K. & Sato, R. (1972). Reconstitution of hepatic microsomal stearoyl-coenzyme A desaturase system from solubilized components. *J Biochem (Tokyo)*, **72,** 1163-74.

Shou, M., Grogan, J., Mancewicz, J.A., Krausz, K.W., Gonzalez, F.J., Gelboin, H.V. & Korzekwa, K.R. (1994). Activation of CYP3A4: evidence for the simultaneous binding of two substrates in a cytochrome P450 active site. *Biochemistry*, **33,** 6450-5.

Shou, M., Mei, Q., Ettore, M.W., Jr., Dai, R., Baillie, T.A. & Rushmore, T.H. (1999). Sigmoidal kinetic model for two co-operative substrate-binding sites in a cytochrome P450 3A4 active site: an example of the metabolism of diazepam and its derivatives. *Biochem J*, **340,** 845-53.

Silverman, R.B. (1988). *Mechanism-Based Enzyme Inactivation: Chemistry and Enzymology*. Boca Raton, FL: CRC Press.

Sisenwine, S.F., Tio, C.O., Hadley, F.V., Liu, A.L., Kimmel, H.B. & Ruelius, H.W. (1982). Species-related differences in the stereoselective glucuronidation of oxazepam. *Drug Metab Dispos*, **10,** 605-8.

Springer, J.E., Cole, D.E., Rubin, L.A., Cauch-Dudek, K., Harewood, L., Evrovski, J., Peltekova, V.D. & Heathcote, E.J. (2000). Vitamin D-receptor genotypes as independent genetic predictors of decreased bone mineral density in primary biliary cirrhosis. *Gastroenterology*, **118,** 145-51.

Stefanis, N.C., Bresnick, J.N., Kerwin, R.W., Schofield, W.N. & McAllister, G. (1998). Elevation of D4 dopamine receptor mRNA in postmortem schizophrenic brain. *Brain Res Mol Brain Res*, **53,** 112-9.

Stellon, A.J., Webb, A., Compston, J. & Williams, R. (1987). Low bone turnover state in primary biliary cirrhosis. *Hepatology*, **7,** 137-42.

Stumpf, W.E. (1995). Vitamin D sites and mechanisms of action: a histochemical perspective. Reflections on the utility of autoradiography and cytopharmacology for drug targeting. *Histochem Cell Biol*, **104,** 417-27.

Sutton, D., Butler, A.M., Nadin, L. & Murray, M. (1997). Role of CYP3A4 in human hepatic diltiazem N-demethylation: inhibition of CYP3A4 activity by oxidized diltiazem metabolites. *J Pharmacol Exp Ther*, **282,** 294-300.

Tam, Y.K. (1993). Individual variation in first-pass metabolism. *Clin Pharmacokinet*, **25,** 300-28.

Tang, W. & Stearns, R.A. (2001). Heterotropic cooperativity of cytochrome P450 3A4 and potential drug-drug interactions. *Curr Drug Metab*, **2,** 185-98.

Tateishi, T., Watanabe, M., Moriya, H., Yamaguchi, S., Sato, T. & Kobayashi, S. (1999). No ethnic difference between Caucasian and Japanese hepatic samples in the expression frequency of CYP3A5 and CYP3A7 proteins. *Biochem Pharmacol*, **57,** 935-9.

Tayeb, M.T., Clark, C., Ameyaw, M.M., Haites, N.E., Evans, D.A., Tariq, M., Mobarek, A., Ofori-Adjei, D. & McLeod, H.L. (2000). CYP3A4 promoter variant in Saudi, Ghanaian and Scottish Caucasian populations. *Pharmacogenetics*, **10,** 753-6.

Tegeder, I., Lotsch, J. & Geisslinger, G. (1999). Pharmacokinetics of opioids in liver disease. *Clin Pharmacokinet*, **37,** 17-40.

Thummel, K.E., Shen, D.D., Podoll, T.D., Kunze, K.L., Trager, W.F., Hartwell, P.S., Raisys, V.A., Marsh, C.L., McVicar, J.P., Barr, D.M. & et al. (1994). Use of midazolam as a human cytochrome P450 3A probe: I. In vitro-in vivo correlations in liver transplant patients. *J Pharmacol Exp Ther*, **271,** 549-56.

Thummel, K.E., O'Shea, D., Paine, M.F., Shen, D.D., Kunze, K.L., Perkins, J.D. & Wilkinson, G.R. (1996). Oral first-pass elimination of midazolam involves both gastrointestinal and hepatic CYP3A-mediated metabolism. *Clin Pharmacol Ther*, **59,** 491-502.

Thummel, K.E. & Wilkinson, G.R. (1998). In vitro and in vivo drug interactions involving human CYP3A. *Annu Rev Pharmacol Toxicol*, **38,** 389-430.

Thummel, K.E. (2001). Transcriptional Control of Intestinal CYP3A4 by 1α-25-Dihydroxy Vitamin D_3. *Molecular Pharmacology*, **In Press**.

Tse, F.L., Ballard, F. & Jaffe, J.M. (1983). Biliary excretion of [14C]temazepam and its metabolites in the rat. *J Pharm Sci*, **72,** 311-2.

Ueng, Y.F., Kuwabara, T., Chun, Y.J. & Guengerich, F.P. (1997). Cooperativity in oxidations catalyzed by cytochrome P450 3A4. *Biochemistry*, **36,** 370-81.

Varhe, A., Olkkola, K.T. & Neuvonen, P.J. (1996). Diltiazem enhances the effects of triazolam by inhibiting its metabolism. *Clin Pharmacol Ther*, **59,** 369-75.

Venkatakrishnan, K., von Moltke, L.L. & Greenblatt, D.J. (2001). Application of the relative activity factor approach in scaling from heterologously expressed cytochromes p450 to human liver microsomes: studies on amitriptyline as a model substrate. *J Pharmacol Exp Ther*, **297,** 326-37.

Wandel, C., Witte, J.S., Hall, J.M., Stein, C.M., Wood, A.J. & Wilkinson, G.R. (2000). CYP3A activity in African American and European American men: population differences and functional effect of the CYP3A4*1B5'-promoter region polymorphism. *Clin Pharmacol Ther*, **68,** 82-91.

Watkins, P.B., Wrighton, S.A., Schuetz, E.G., Molowa, D.T. & Guzelian, P.S. (1987). Identification of glucocorticoid-inducible cytochromes P-450 in the intestinal mucosa of rats and man. *J Clin Invest*, **80,** 1029-36.

Westlind, A., Malmebo, S., Johansson, I., Otter, C., Andersson, T.B., Ingelman-Sundberg, M. & Oscarson, M. (2001). Cloning and tissue distribution of a novel human cytochrome p450 of the CYP3A subfamily, CYP3A43. *Biochem Biophys Res Commun*, **281,** 1349-55.

Winkler, K., Bass, L., Keiding, S. & Tygstrup, N. (1979). The physiologic basis for clearance measurements in hepatology. *Scand J Gastroenterol*, **14,** 439-48.

Woo, G.K., Williams, T.H., Kolis, S.J., Warinsky, D., Sasso, G.J. & Schwartz, M.A. (1981). Biotransformation of [14C]midazolam in the rat in vitro and in vivo. *Xenobiotica*, **11,** 373-84.

Wood, L.J., Massie, D., McLean, A.J. & Dudley, F.J. (1988). Renal sodium retention in cirrhosis: tubular site and relation to hepatic dysfunction. *Hepatology*, **8,** 831-6.

Woodcock, B.G., Rietbrock, I., Vohringer, H.F. & Rietbrock, N. (1981). Verapamil disposition in liver disease and intensive-care patients: kinetics, clearance, and apparent blood flow relationships. *Clin Pharmacol Ther*, **29,** 27-34.

Wrighton, S.A., Ring, B.J., Watkins, P.B. & VandenBranden, M. (1989). Identification of a polymorphically expressed member of the human cytochrome P-450III family. *Mol Pharmacol*, **36,** 97-105.

Wrighton, S.A. & Vandenbranden, M. (1989). Isolation and characterization of human fetal liver cytochrome P450HLp2: a third member of the P450III gene family. *Arch Biochem Biophys*, **268,** 144-51.

Wrighton, S.A., Brian, W.R., Sari, M.A., Iwasaki, M., Guengerich, F.P., Raucy, J.L., Molowa, D.T. & Vandenbranden, M. (1990). Studies on the expression and metabolic capabilities of human liver cytochrome P450IIIA5 (HLp3). *Mol Pharmacol*, **38,** 207-13.

Wrighton, S.A. & Stevens, J.C. (1992). The human hepatic cytochromes P450 involved in drug metabolism. *Crit Rev Toxicol*, **22,** 1-21.

Wrighton, S.A. & Ring, B.J. (1994). Inhibition of human CYP3A catalyzed 1'-hydroxy midazolam formation by ketoconazole, nifedipine, erythromycin, cimetidine, and nizatidine. *Pharm Res*, **11,** 921-4.

Xie, W., Radominska-Pandya, A., Shi, Y., Simon, C.M., Nelson, M.C., Ong, E.S., Waxman, D.J. & Evans, R.M. (2001). An essential role for nuclear receptors SXR/PXR in detoxification of cholestatic bile acids. *Proc Natl Acad Sci U S A*, **98,** 3375-3380.

Yamakoshi, Y., Kishimoto, T., Sugimura, K. & Kawashima, H. (1999). Human prostate CYP3A5: identification of a unique 5'-untranslated sequence and characterization of purified recombinant protein. *Biochem Biophys Res Commun*, **260,** 676-81.

Yamazaki, H. & Shimada, T. (1997). Progesterone and testosterone hydroxylation by cytochromes P450 2C19, 2C9, and 3A4 in human liver microsomes. *Arch Biochem Biophys*, **346,** 161-9.

Yamazaki, H., Nakajima, M., Nakamura, M., Asahi, S., Shimada, N., Gillam, E.M., Guengerich, F.P., Shimada, T. & Yokoi, T. (1999). Enhancement of cytochrome P-450 3A4 catalytic activities by cytochrome b(5) in bacterial membranes. *Drug Metab Dispos*, **27,** 999-1004.

Zeng, H., Liu, G., Rea, P.A. & Kruh, G.D. (2000). Transport of amphipathic anions by human multidrug resistance protein 3. *Cancer Res*, **60,** 4779-84.

Zhang, Q.Y., Dunbar, D., Ostrowska, A., Zeisloft, S., Yang, J. & Kaminsky, L.S. (1999). Characterization of human small intestinal cytochromes P-450. *Drug Metab Dispos*, **27,** 804-9.

Zhu, X.X., Brizard, F., Piche, J., Yim, C.T. & Brown, G.R. (2000). Bile Salt Anion Sorption by Polymeric Resins: Comparison of a Functionalized Polyacrylamide Resin with Cholestyramine. *J Colloid Interface Sci*, **15,** 282-288.

VITA

Donavon Jay McConn II was born on September 13, 1970 in Phoenix, Arizona. He was raised in Martinez, California with his brother Eric, and graduated from Alhambra High School in 1987. After high school, he attended the University of California at Davis and received his Bachelor of Science degree in Biological Sciences in 1991. After a few odd jobs, including washing laboratory glassware and amateur mechanic work, he was a Senior Chemist for American Environmental Network for 4 years prior to his admission to the University of Washington Pharmaceutics program in September of 1995. While at the University of Washington, he received an Achievement Rewards for College Scientists (ARCS) fellowship, National Institute of Health Training Grant Appointment, and a fellowship from the Pfizer Corporation. Under the support and guidance of Dr. Ken Thummel, he received his Ph.D. in September of 2001. After graduation, he and his wife Nicole relocated to Research Triangle Park, North Carolina, where he accepted a Senior Scientist position at GlaxoSmithKline Pharmaceuticals.